

UNCLASSIFIED

AD NUMBER

AD837645

NEW LIMITATION CHANGE

TO

**Approved for public release, distribution
unlimited**

FROM

**Distribution authorized to U.S. Gov't.
agencies and their contractors; Critical
Technology; AUG 1968. Other requests shall
be referred to Air Force Weapons Lab.,
AFSC, Kirtland AFB, NM.**

AUTHORITY

AFWL ltr, 30 Nov 1971

THIS PAGE IS UNCLASSIFIED

AFWL-TR-68-61

AFWL-TR-
68-61

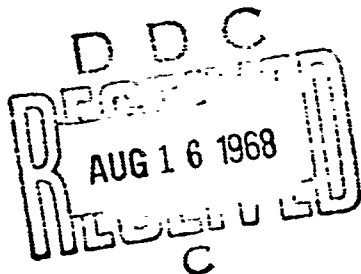
AN INTEGRATED SIX-DEGREE-OF-FREEDOM
TRAJECTORY AND AERODYNAMIC HEATING
AND ABLATION COMPUTER PROGRAM

(STRAB-6)

W. J. Moulds

TECHNICAL REPORT NO. AFWL-TR-68-61

August 1968



AIR FORCE WEAPONS LABORATORY
Air Force Systems Command
Kirtland Air Force Base
New Mexico

This document is subject to special export controls and each transmittal to foreign governments or foreign nationals may be made only with prior approval of AFWL (WLDE) , Kirtland AFB, NM, 87117.

151

**Best
Available
Copy**

AFWL-TR-68-61

AN INTEGRATED SIX-DEGREE-OF-FREEDOM TRAJECTORY AND
AERODYNAMIC HEATING AND ABLATION COMPUTER PROGRAM

(STRAB-6)

W. J. Moulds

TECHNICAL REPORT NO. AFWL-TR-68-61

This document is subject to special export controls and each transmittal to foreign governments or foreign nationals may be made only with prior approval of AFWL (WLDE), Kirtland AFB, NM, 87117. Distribution is limited because of the technology discussed in the report.

FOREWORD

This research was performed under Program Element 6.24.05.06.F, Project 5791, Task 579122.

Inclusive dates of research were July 1966 through November 1967. This report was submitted by the Air Force Weapons Laboratory Project Officer, Mr. W. J. Moulds (WLDE), on 13 May 1968.

The author wishes to express his appreciation and thanks to Lt Colonel P. D. Cronquist and Mr. C. E. O'Haver for suggesting and encouraging the accomplishment of this work. Special thanks are due to Captain J. D. Young and Lt R. H. Aungier for their assistance and answers to the numerous questions by the author. Last, but not least, the author wishes to acknowledge the assistance of Mr. J. L. Hitchcock, who did much of the programing of STRAB-6.

This technical report has been reviewed and is approved.



W. J. MOULDS
Project Officer


PARLEY D. CRONQUIST
Lt Colonel, USAF
Chief, Electronics Branch
GEORGE C. DARBY, JR
Colonel, USAF
Chief, Development Division

ABSTRACT

(Distribution Limitation Statement No. 2)

An integrated computer program (STRAB-6) for the complete analysis of a blunt, conical reentry vehicle as to its trajectory and aerothermal environment upon atmospheric reentry is presented. The trajectory portion of the program calculates the vehicle motions in six-degrees-of-freedom, while the thermal portion calculates the aerodynamic heating and ablation of the vehicle. The earth model is an oblate, rotating spheroid whose parameters and gravitational potential are described herein. The equations of motion, the method of integration, thermal model and input forms for the program are discussed. The thermal model examined in this report assumes thick skin solution where the skin is of any composite structure made of discrete layers of material whose properties may vary from layer to layer. Also, the heatshield is comprised of one, two, or more different ablative materials. STRAB-6 computes nose-blunting and includes this effect in the aerodynamics. STRAB-6 is written in FORTRAN IV for the CDC 6600 computer.

This page intentionally left blank.

CONTENTS

<u>Section</u>	<u>age</u>
I INTRODUCTION	1
II MAIN PROGRAM DESCRIPTION	3
General	3
Equations of Motion	5
Integration Technique	44
Aerodynamic Heating and Ablation	45
Aerodynamics	64
III SUBROUTINES	74
Atmospheric Properties	74
Hot-Air Properties	74
Ablator Thermal Properties	75
Ablation Gas Properties	75
Stability Derivatives	76
Subroutine Initial	76
Subroutine ATT&SSL	77
Subroutine DLON	77
IV PROGRAM OPERATION	78
Input Data Requirements	78
Output Data Requirements	79
Flow Diagrams	81
APPENDIXES	
I STRAB-6 Program Listing	91
II STRAB-6 Program Listing for Multiple Case Run	129
III Sample Case Output	133
REFERENCES	151
DISTRIBUTION	154

ILLUSTRATIONS

<u>Figure</u>		<u>Page</u>
1	Geocentric Earth Model	4
2	Inertial Reference Frame, R, and Earth Reference Frame, E	7
3	Geocentric, Geodetic, and Astronomical Latitudes	8
4	Geodetic to Geocentric	10
5	Horizontal Reference Frame	13
6	Inertial, Horizontal Body Axis Coordinate System	15
7	Gravitational Direction	24
8	Gravitational Transformation	27
9	System of Angular Displacement	30
10	Angular Velocities of Euler Angles	33
11	Moment of Momentum about 0	36
12	Components of Momentum	37
13	Schmidt Plot in an Infinitely Thick Wall	51
14	Model for Wall Temperature Profile and Ablation Recession Calculations	52
15	Ablative Process	54
16	Vehicle Nomenclature	60
17	Vehicle Nose-Shape Change	62
18	Aerodynamic Body Subject to Normal and Tangential Forces	67

SECTION I

INTRODUCTION

The effects of aerodynamic heating and ablation on the motions, aerodynamic forces, and trajectory deviations of a reentry vehicle have been the subject of many analyses in recent years. Previous trajectory and heating programs have been separate, requiring that each be run separately with data from one used as input to the other. Such a method sometimes requires numerous runs before the output data converge to reasonable answers, and is both expensive in computer costs and time consuming. This report presents a computer program (STRAB-6) for the complete analysis of a reentry vehicle as to its trajectory and aerothermal environment. STRAB-6 provides a six-degree-of-freedom trajectory analysis as well as aerodynamic heating and ablation analysis for conical vehicles reentering the atmosphere at hypersonic speeds.

STRAB-6 uses some of the features from other 6-D programs (Refs. 1, 2, 3, 4, 5, 6). The trajectory portion of the program computes the six-degree-of-freedom rigid body motions for an aerodynamically symmetric reentry vehicle encountering a model atmosphere. Slender-body aerodynamic theory was used and the required aerodynamic coefficients are provided by subroutine input (as a function vehicle shape, angle-of-attack, and either Mach number or altitude). The atmospheric model that is used is based on the 1962 ARDC atmosphere, and the geocentric model that is used is a rotating oblate spheroid.

The aerodynamic heating and ablation portion of the program (Ref. 7) (HEATAB), in its original form, computed point mass heating for a sharp-nosed conical vehicle. The basic heating equations of this original program (HEATAB) are described in reference 7. There have been numerous improvements to the original program to include: heating on a blunt-nosed vehicle, the case where a vehicle heatshield is comprised of two or more different ablators, and boundary layer edge conditions.

The equations of motion and of heat transfer are general in that they apply to most axially symmetric vehicles. Even though this program considers the body in general motion under combined angles of attack and sideslip, the vehicle is assumed to ablate symmetrically. The ablation weight loss, nose bluntness, and vehicle volume changes are considered in the calculations for

the viscous and inviscid drag coefficients (CD) and stability derivatives, as well as the vehicle mass moment of inertia properties. In addition, the aerodynamic coefficients are calculated for the complete range of angle-of-attack ($0 \leq \alpha \leq 360^\circ$) and sideslip ($0 \leq \beta \leq 360^\circ$).

The position vector is calculated in a rotating earth-centered coordinate system, while the angular positions are calculated in a reentry-centered coordinate system. Computations are carried out, using the Runge-Kutta method of numerical integration employing a fixed step size-mode.

This program is specific in that the equations have been applied to a blunt-nosed conical vehicle with the starting point at reentry conditions. With some modifications, the user could easily adapt the program to analyze a missile from launch by adding thrust subroutines and substituting launch conditions for reentry conditions.

SECTION II
MAIN PROGRAM DESCRIPTION

1. GENERAL

The computer program, STRAB-6, is a self-contained program in the sense that it can generate the required aerodynamic data, and calculate the mass and inertial properties due to ablation changes of a symmetrical vehicle without any additional preliminary calculations.

STRAB-6 calculates the resultant loads, motions, and trajectory of a rigid vehicle in general 6-D motion as well as boundary-layer properties and time-temperature distribution in a body. If a nonablating trajectory is desired, an option is provided to omit the heating and ablation portion of the program.

At the initiation of a reentry run, the vehicle is located in space with the desired reentry conditions (i.e., velocity, flight path angle, altitude, roll rate). Also, the user must input the latitude, longitude, and azimuth at which he wishes to start the trajectory. Other trajectory parameters the user may wish to input are angle-of-attack and angle-of-sideslip; otherwise, these values are zero for a nominal trajectory.

The aerodynamic drag coefficients (CD) are obtained from Newtonian slender-body theory for inviscid drag and modified Blasius flat plate theory for viscous drag. These coefficients are calculated in subroutines CDSF and CDPW and are limited to vehicle shapes of spherically blunted cones where the ratio of base radius to axial length is approximately equal to the cone half-angle. A discussion of these theories is in section II-5.

The atmospheric model used in the program is based on the 1962 ARDC model atmosphere, and it expresses the density, ambient temperature, pressure, and the speed of sound as functions of altitude. The geocentric model used is a rotating oblate spheroid, where the sea level radius, R_E , is (figure 1)

$$R_E = \frac{R_{EQ}}{\left(1 + \frac{R_E}{c} \sin^2 \phi\right)^{1/2}} \quad (1)$$

where

R_{EQ} = earth equatorial radius-ft

λ_c = geocentric latitude-degree

$$P_E = \frac{e_E^2}{1 - e_E^2} = 0.00673852 \text{ (Ref 8)} \quad (2)$$

e_E = eccentricity of earth = 0.0818133302

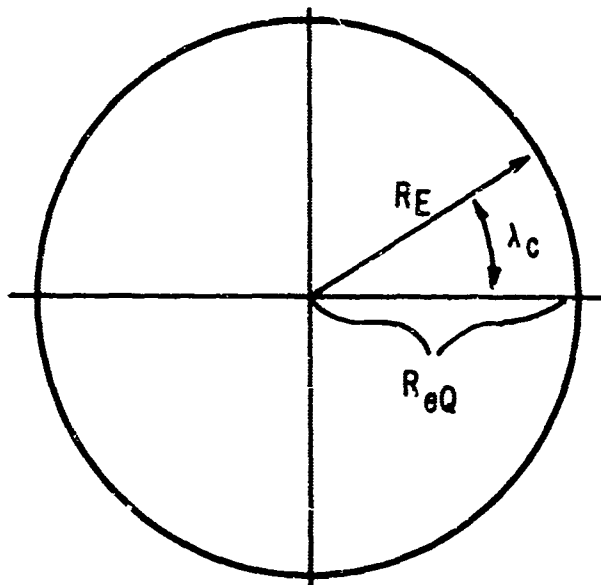


Figure 1. Geocentric Earth Model

The vehicle thermal model as presented in HEATAB has been modified to extend the calculations to include the total integrated ablation mass loss rate for a conical reentry vehicle. The body is divided into a number of segments, or stations along the cone, and the heating rate at each station is computed. In addition to the original input data required by HEATAB, the fore and aft radii, slant length, and transition Reynolds number of each body segment must be supplied. These input data are identified as: Data RS, Data RL, Data SOL, and Data RN. Computations of the skin temperature profile and ablation mass loss rate are identical to the method in HEATAB, except that these calculations are made for each X-station at each trajectory point.

As written, the STRAB-6 output will give, for each time interval, an output of trajectory conditions, body conditions, and aerodynamic parameters. The trajectory output conditions include time, altitude, velocity, and flight path angle. The body conditions for each X-station include weight loss rate per unit area, wall recession, and wall temperature profile. The aerodynamic parameters include CD, maximum aerodynamic load, angle-of-attack and sideslip, restoring forces and moments, and boundary layer edge conditions.

2. EQUATIONS OF MOTION

The equations of motion for an ascent or descent through the atmosphere can be written with various degrees of complexity. The equations differ in form depending upon the coordinate system, the number of degrees of freedom, the method of adjusting for the earth's rotation, and the integration scheme. In the evaluation of reentry vehicles for height-of-burst (HOB) errors, dispersion analysis, or circular error probable (CEP), the equations of motion must be written with six-degrees-of-freedom (6-D). This program employs a Runge-Kutta method of integration for a high degree of accuracy.

a. Coordinate Systems

The equations of motion can be written in vector notation using Newton's second law. A summation of the forces acting on the vehicle results in the equation

$$m \frac{\vec{d^2R}}{dt^2} = \sum \vec{F} - 2m\vec{\omega} \times \vec{v} - m\vec{\omega} \times (\vec{\omega} \times \vec{R})$$

Before this equation can be solved, however, it must be expressed in terms of a convenient coordinate system.

There are five principal coordinate systems or reference frames associated with orbital mechanics and trajectories. Various other reference frames can be used depending on the complexity of the problem to be solved. For this report, there are three reference frames: inertial reference frame, topocentric or horizontal reference frame, and earth reference frame. The following is a description of each and their interrelationships. All the reference frames are right-handed orthogonal coordinate systems.

(1) Inertial Reference Frame

The basic coordinate for the program is a nonrotating inertial reference frame fixed with its origin at the geocenter as shown in figure 2. Z_R points north along the axis of rotation of the earth and X_R and Y_R lie in the equatorial plane. X_R lies in the prime meridian plane at the start of a trajectory run (time, $t = 0$). The earth rotates with an angular velocity ω_E about Z_R ; hence the earth reference frame, E , differs from the inertial frame, R , by a rotation $\omega_E t$.

The vehicle center of gravity (CG) is located in the inertial R frame by the longitude, β , latitude, λ_c , and vehicle altitude, ALT. The distance from the geocenter to the vehicle CG, measured along the vector whose orientation is determined by the angles β and λ_c is

$$R = R_E + \text{ALT} \quad (3)$$

where R_E is defined by equation (1).

It may be worthwhile to digress briefly on the subject of latitude. There are three latitudes commonly used in astrodynamics; however, in this report we will be concerned only with geocentric and geodetic. Geocentric latitude, λ_c , is defined as the angle, measured at the earth's center, between the equatorial plane and a radius, R_E , to the point of interest on the earth's surface. The geodetic latitude, λ_g , is the angle between the equatorial plane and a normal to a reference spheroidal surface, Z_H , as shown in figure 3.

The reference spheroid is an oblate ellipsoid whose surface nearly approximates the sea-level surface of the earth. Such a spheroid is characterized by a "flattening" or "oblateness," f , where

$$f = (a - b)/a \quad (4)$$

and a is the semimajor, and b the semiminor axis of the ellipse of revolution forming the spheroid. The derivation of equation (1) can be easily obtained from the equation for an ellipse if a equals equatorial radius, R_{EQ} , and b equals polar radius, R_{Po} . Therefore,

$$\frac{x^2}{R_{EQ}^2} + \frac{z^2}{R_{Po}^2} = 1 \quad (5)$$

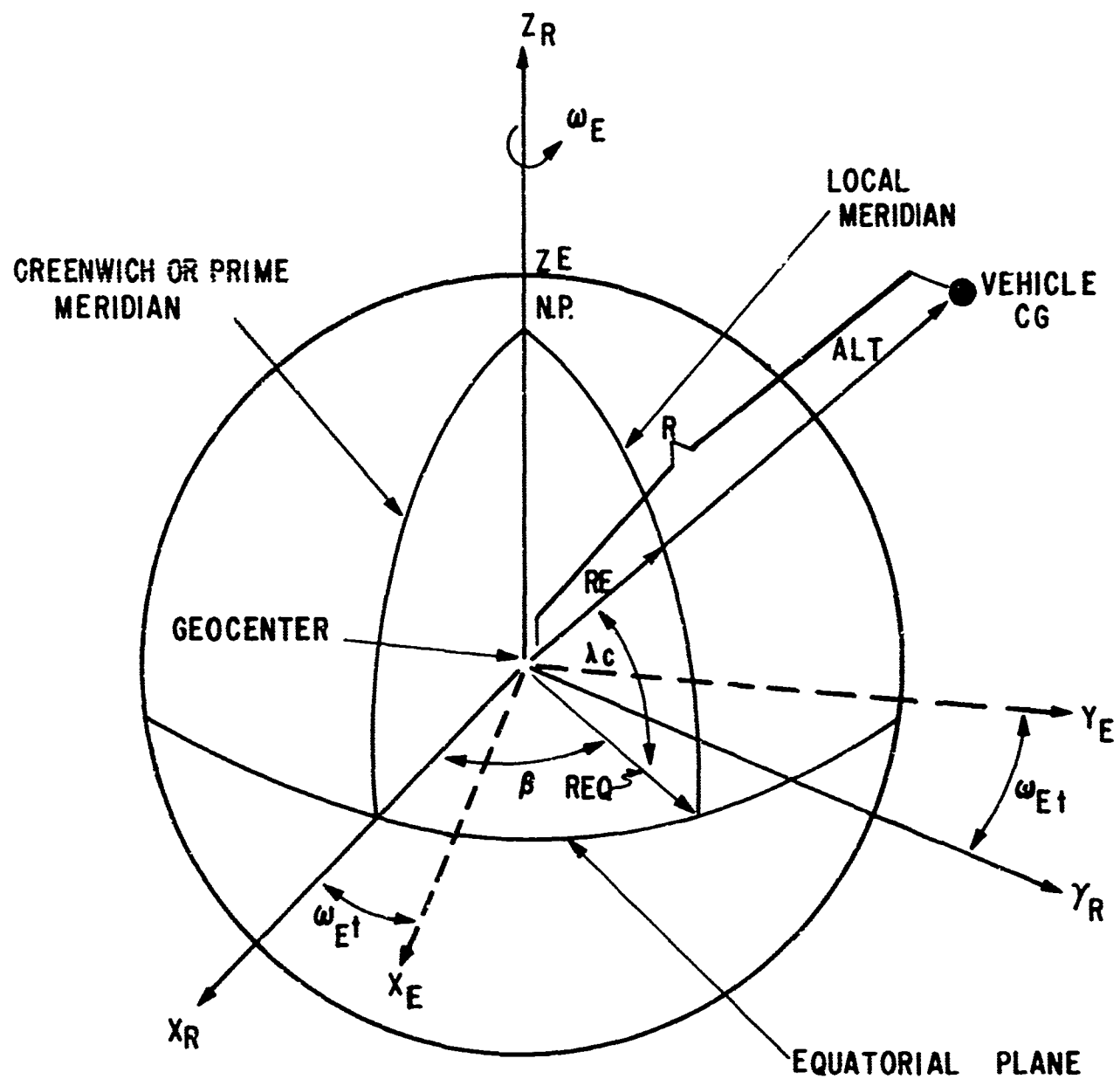


Figure 2. Inertial Reference Frame, R , and Earth Reference Frame, E

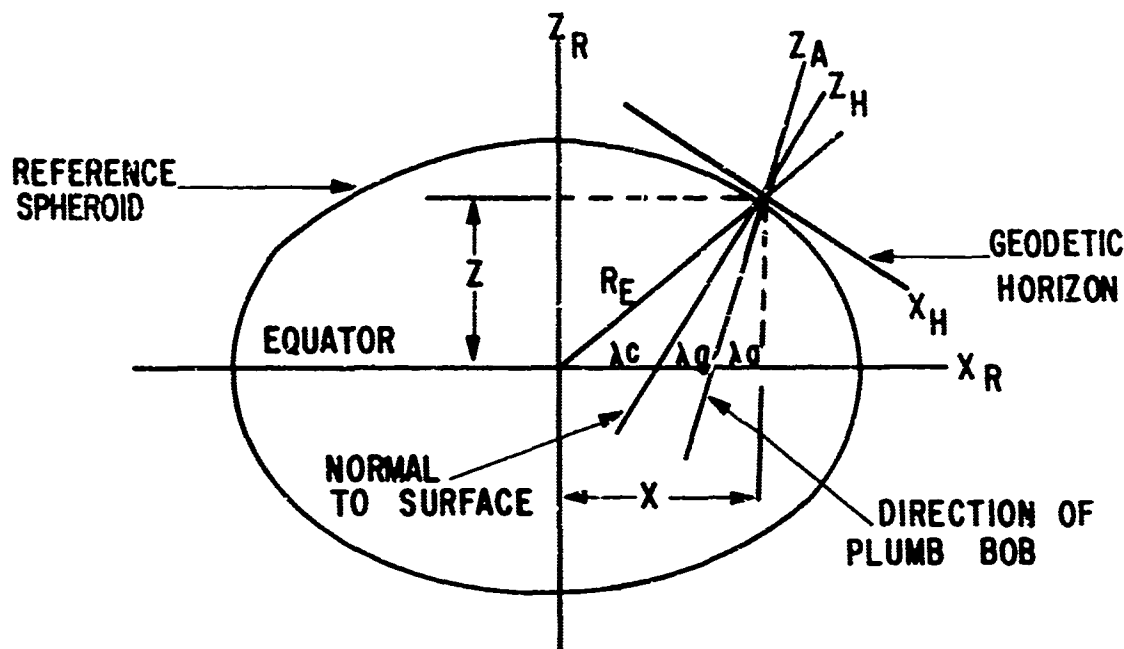


Figure 3. Geocentric, Geodetic, and Astronomical Latitudes (Ref. 9)

By multiplying R_{EQ}^2 and adding and subtracting z^2 on the left side,

$$x^2 + z^2 - z^2 + \frac{R_{EQ}^2 z^2}{R_{PO}^2} = R_{EQ}^2$$

But from figure 3

$$x^2 + z^2 = R_E^2$$

$$z = R_E \sin \lambda_c \quad (6)$$

Therefore,

$$R_E^2 + R_E^2 \sin^2 \lambda_c \left(\frac{R_{EQ}^2}{R_{PO}^2} - 1 \right) = R_{EQ}^2 \quad (7)$$

Solving for R_E

$$R_E = \frac{R_{EQ}}{\left[1 + \sin^2 \lambda_c \left(\frac{R_{EQ}^2}{R_{PO}^2} - 1 \right) \right]^{1/2}} \quad (8)$$

From reference 10

$$f = 1 - \sqrt{1 - e_E^2} \quad (9)$$

and from equation (4)

$$\frac{R_{EQ}}{R_{PO}} = \frac{1}{1 - f}$$

By squaring both sides and substituting equation (9) for f ,

$$\frac{R_{EQ}^2}{R_{PO}^2} = \frac{1}{1 - e_E^2} \quad (10)$$

Now, by adding -1 to both sides,

$$\frac{R_{EQ}^2}{R_{PO}^2} - 1 = \frac{1}{1 - e_E^2} - 1 = \frac{e_E^2}{1 - e_E^2}$$

From equation (2), it is shown that

$$P_E = \frac{R_{EQ}^2}{R_{PO}^2} - 1 \quad (11)$$

Equation (1) is now obtained by substituting equation (11) into equation (8).

$$R_E = \frac{R_{EQ}}{\left(1 + P_E \sin^2 \lambda_c \right)^{1/2}}$$

The sea-level radius of the earth can now be determined at any station by knowing the geocentric latitude, λ_c , of the station.

The astronomical latitude, λ_a , is defined as the angle between the local astronomical zenith, Z_a , or vertical (as determined by a plumb bob or, actually, by the direction of the local gravitational field) and the equatorial plane. Since astronomical latitude is based upon the local gravitational field and is also centrifugal-force affected, it differs from the geodetic latitude by a very small value and can be considered negligible. Therefore, this report will consider geodetic and astronomical latitudes identical and will be concerned only with the relationship between geodetic and geocentric.

To convert from geodetic latitude to geocentric latitude, the slope (θ) of the tangent (geodetic horizon, see figure 4) at the station on the earth's surface can be obtained by differentiating equation (5).

$$\frac{2x}{R_{EQ}^2} + \frac{2z}{R_{PO}^2} \frac{dz}{dx} = 0$$

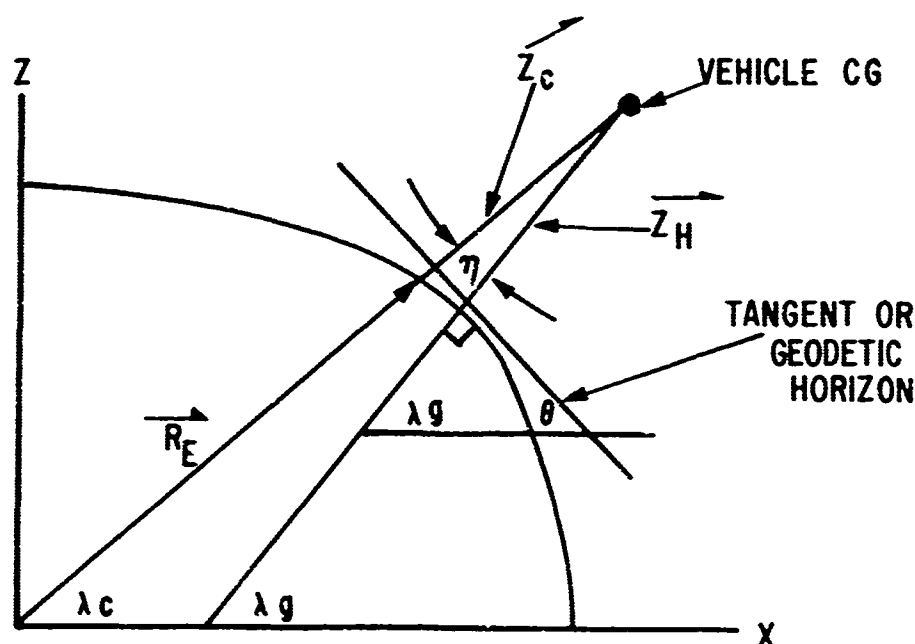


Figure 4. Geodetic to Geocentric

Therefore,

$$\tan \theta = \left| \frac{dz}{dx} \right| = \left| - \frac{R_{Po}^2}{R_{EQ}^2} \frac{x}{z} \right| \quad (12)$$

but

$$\tan \theta = \frac{1}{\tan \lambda_g}$$

$$\tan \lambda_c = \frac{z}{x}$$

By substituting these quantities into equation (12), the relationship between λ_g and λ_c is established.

$$\tan \lambda_g = \frac{R_{EQ}^2}{R_{Po}^2} \tan \lambda_c \quad (13a)$$

But by substituting equation (10) into equation (13a), λ_c can be determined from one constant. Therefore,

$$\lambda_c = \arctan \left[\left(1 - e_E^2 \right) \tan \lambda_g \right] \quad (13b)$$

$$\eta = \lambda_g - \lambda_c \quad (14)$$

With the foregoing relationships established, the second reference frame can now be defined.

(2) Topocentric or Horizontal Reference Frame

The second of these coordinate systems is commonly known as the topocentric, but has other names depending upon the user's application. Some of the names are horizon, launch, reentry, and trajectory system. This report refers to this coordinate system as the horizontal, H. The word topocentric

is derived from the Greek *topos*, meaning a place. In this reference frame, the origin is taken at the observer as shown in figure 5. The Y_H -axis is directed toward the east, the X_H -axis toward the south, and the Z_H -axis is directed toward the astronomical zenith. This system is rotated along with the earth's reference frame, and is, therefore, not inertial. The angle from the north direction measured clockwise (or east) in the X_H , Y_H plane is defined as azimuth, AZ.

With the horizontal reference frame now defined, it is now possible to complete three of the six-degrees-of-freedom.

b. Equation Development

Newton's second law for a rotating coordinate system is repeated here for convenience.

$$m \frac{\vec{d^2R}}{dt^2} = \sum \vec{F} - 2m\vec{\omega} \times \vec{v} - m\vec{\omega} \times (\vec{\omega} \times \vec{R})$$

or

$$\frac{\vec{d^2R}}{dt^2} = \frac{\sum \vec{F}}{m} - 2 \left(\vec{\omega}_E \times \frac{\vec{dR}}{dt} \right) - \vec{\omega}_E \times (\vec{\omega}_E \times \vec{R}) \quad (15)$$

where

$\frac{\vec{d^2R}}{dt^2}$ is the vector acceleration of the vehicle CG with respect to the inertial reference frame

\vec{F} is the total force vector on the reentry vehicle

$2 \left(\vec{\omega}_E \times \frac{\vec{dR}}{dt} \right)$ is the coriolis acceleration of the axis system due to the rotation of the earth

m is vehicle mass

$\vec{\omega}_E \times (\vec{\omega}_E \times \vec{R})$ is the centrifugal acceleration of the axis system due to the earth's rotation

$\omega_E = 0.7292 \times 10^{-5}$ radian/sec, earth rotational angular velocity

Since the horizontal reference system (X_H, Y_H, Z_H) will rotate with the earth, several vector cross-products will appear in the final equation for d^2R/dt^2 . Therefore, the rotation rate vector, $\vec{\omega}_E$, and general vector, \vec{R} , must be expressed in the same reference frame (X_H', Y_H', Z_H') for expansion.

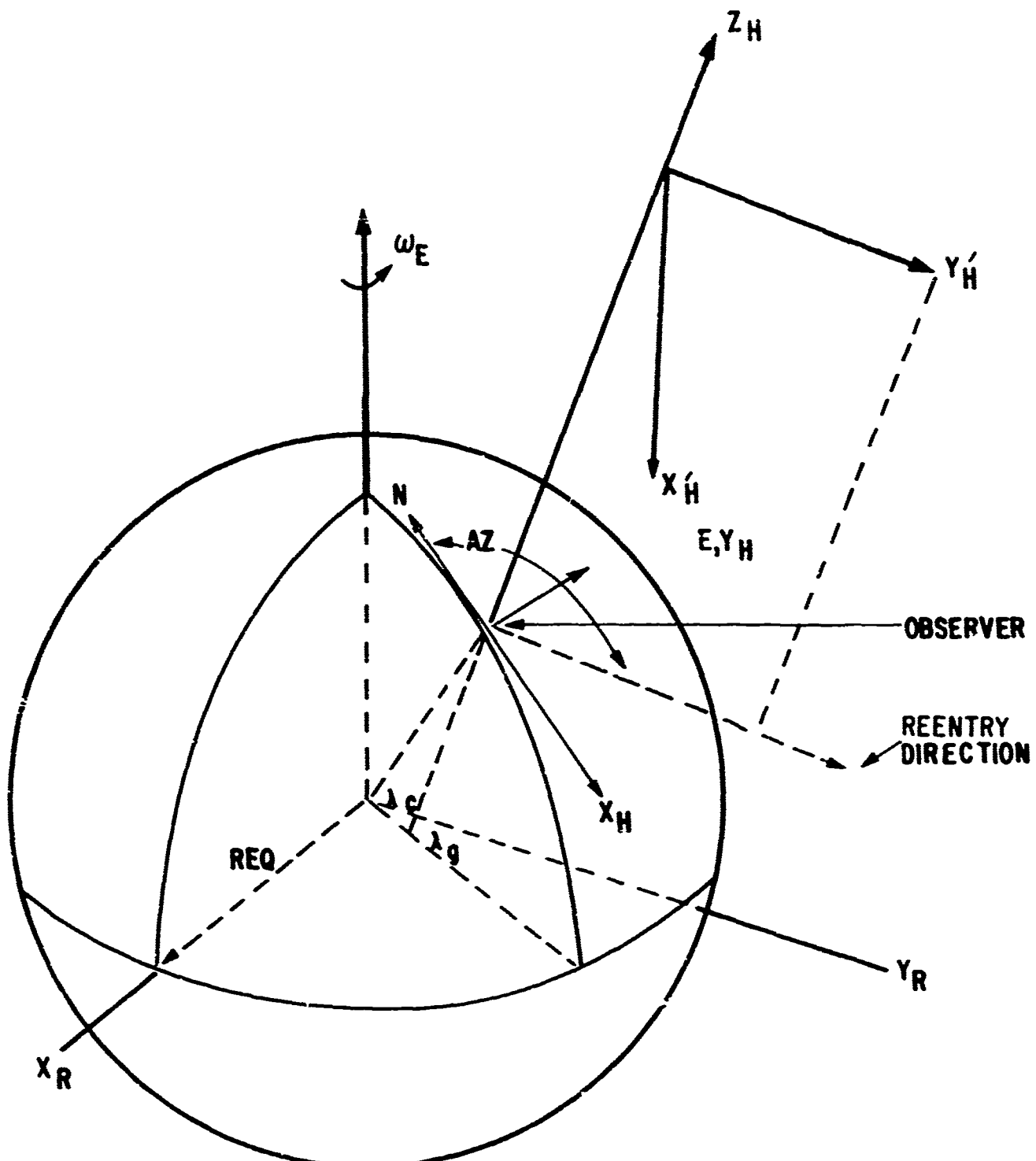


Figure 5. Horizontal Reference Frame

As shown in figure 5, pseudo-trajectory reference frame $(\vec{X}_H', \vec{Y}_H', \vec{Z}_H')$ has its origin at the initial position of the vehicle center of gravity. This frame is fixed in space (with respect to the horizontal (H) frame), with \vec{Z}_H' equal to the reentry altitude, and with \vec{X}_H' and \vec{Y}_H' rotated from \vec{X}_H , \vec{Y}_H about \vec{Z}_H some initial azimuth angle, AZ. The vehicle flight path is initially fixed in the $\vec{Y}_H' - \vec{Z}_H'$ plane directed downward some reentry angle, γ_e .

Therefore, the components of \vec{X}_H , \vec{Y}_H , \vec{Z}_H on \vec{X}_H' , \vec{Y}_H' , \vec{Z}_H' is

$$\vec{X}_H' = \cos AZ \cdot \vec{X}_H + \sin AZ \cdot \vec{Y}_H \quad (16a)$$

$$\vec{Y}_H' = \sin AZ \cdot \vec{X}_H - \cos AZ \cdot \vec{Y}_H \quad (16b)$$

$$\vec{Z}_H' = \vec{Z}_H \quad (16c)$$

As previously shown, the horizontal reference frame is not inertial, and therefore, rotates at the same rotation rate as the earth. So that $\vec{\omega}_E$ may be written

$$\vec{\omega}_E = \omega_E \sin \lambda_g \vec{Z}_H - \omega_E \cos \lambda_g \vec{Y}_H \quad (17)$$

Equation (17) may be rewritten after substituting equation (16b) into equation (17).

$$\begin{aligned} \vec{\omega}_E = \omega_E \sin \lambda_g \vec{Z}_H - \omega_E \cos \lambda_g \cdot \sin AZ \vec{X}_Y \\ + \omega_E \cos \lambda_g \cdot \cos AZ \vec{Y}_H \end{aligned} \quad (18)$$

Therefore, the components of the earth's rotation rate in the horizontal reference frame may be written

$$\omega_{EX_H} = -\omega_E \cos \lambda_g \cdot \sin AZ \quad (19a)$$

$$\omega_{EY_H} = \omega_E \cos \lambda_g \cdot \cos AZ \quad (19b)$$

$$\omega_{EZ_H} = -\omega_E \sin \lambda_g \quad (19c)$$

To determine the general vector, \vec{R} , and displacement accelerations, the vehicle CG must be considered displaced from the horizontal reference frame by the vector, \vec{R} , as shown in figure 6.

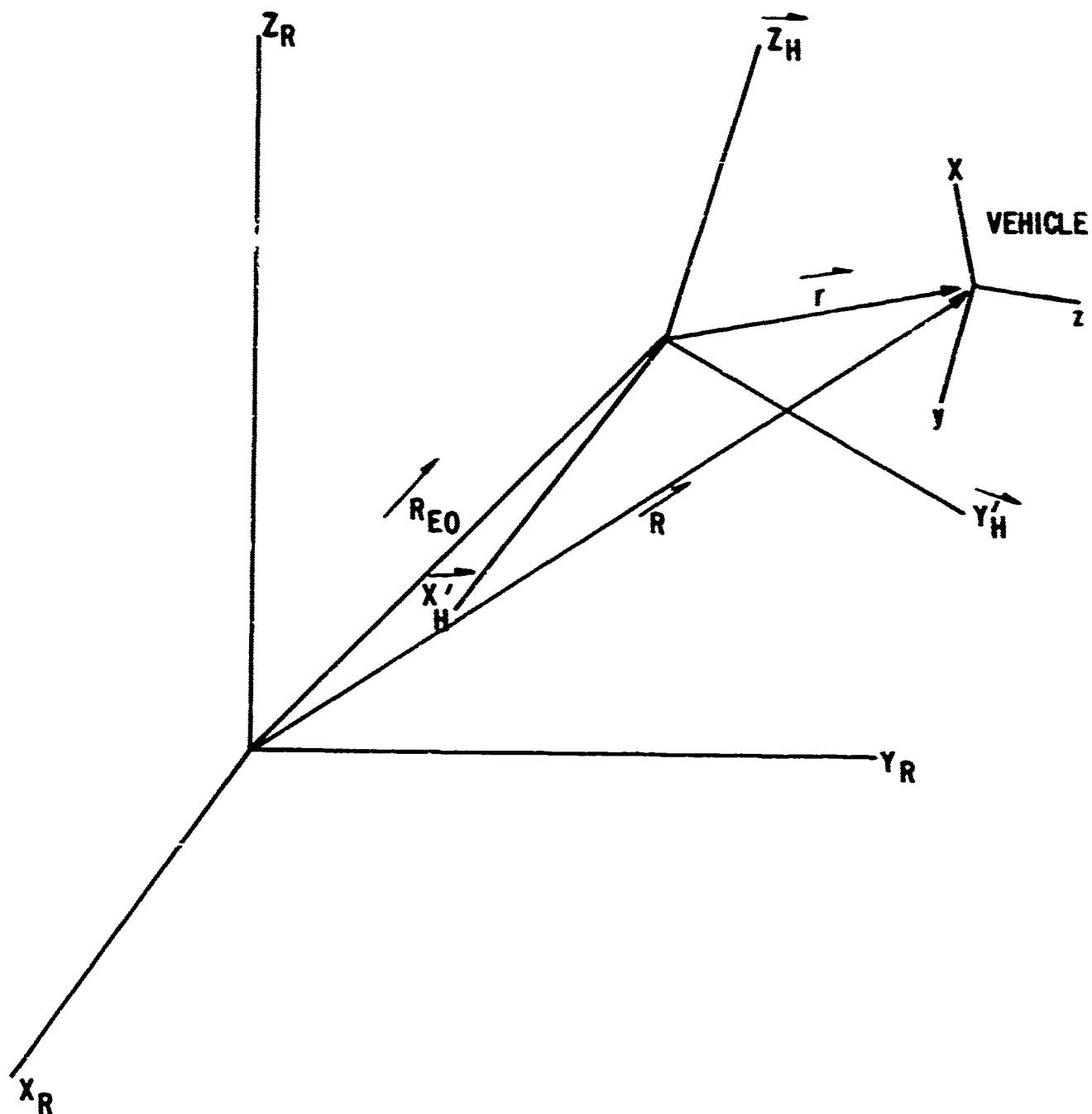


Figure 6. Inertial and Body Axis Coordinate Systems

From figure 6, the following relationship can be established:

$$\vec{R} = \vec{R}_{eo} + \vec{r} \quad (20)$$

\vec{r} can be written in terms of its components on the horizontal reference frame as

$$\vec{r} = X \vec{X}_H' + Y \vec{Y}_H' + Z \vec{Z}_H \quad (21)$$

where X, Y, Z are the scalar vehicle CG displacement on the horizontal reference frame. \vec{R} can now be written as

$$\vec{R} = X \vec{X}_H' + Y \vec{Y}_H' + Z \vec{Z}_H + \vec{R}_{eo} \quad (22)$$

Although \vec{R} can be written in any reference frame, its vector components must be in the same reference frame. Therefore, the equation

$$\vec{R}_{eo} = R_{eo} \vec{Z}_c \quad (23)$$

must be written in terms of the horizontal reference system.

From figure 4, the vector, \vec{Z}_c , in the geocentric reference frame can be written in the form

$$\vec{Z}_c = \vec{Z}_H \cos \eta + \vec{Y}_H \cos \eta$$

or by substituting in equations (16b) and (16c), the following is obtained:

$$\vec{Z}_c = \vec{Z}_H \cos \eta + \vec{X}_H' \sin AZ \sin \eta - \vec{Y}_H' \cos AZ \sin \eta \quad (24)$$

Equation (23) can now be rewritten as

$$\vec{R}_{eo} = R_{eo} \sin AZ \sin \eta \vec{X}_H' - R_{eo} \cos AZ \sin \eta \vec{Y}_H' + R_{eo} \cos \eta \vec{Z}_H \quad (25)$$

where components of \vec{R}_{eo} in horizontal reference frame are

$$R_{XH} = R_{eo} \sin AZ \sin \eta$$

$$R_{YH} = -R_{eo} \cos AZ \sin \eta$$

$$R_{ZH} = R_{eo} \cos \eta \quad (26)$$

By substituting and collecting terms, the equation for \vec{R} is

$$\vec{R} = (R_{xH} + x) \vec{x}_H' + (R_{yH} + y) \vec{y}_H' + (R_{zH} + z) \vec{z}_H \quad (27)$$

The vectors \vec{R} and $\vec{\omega}_E$ have now been expressed in the horizontal reference frame. The development of equation (15) can proceed further by taking the first derivative of R , with respect to time, in the following general form for an inertial coordinate system:

$$\left(\frac{d\vec{R}}{dt} \right) = \left[\frac{d\vec{R}}{dt} \right] + \vec{\omega} \times \vec{R}$$

where

$\left[\frac{d\vec{R}}{dt} \right]$ is the derivative relative to the rotating reference system

$\left(\frac{d\vec{R}}{dt} \right)$ is the vehicle CG velocity vector with respect to the inertial reference frame (R)

Therefore,

$$\begin{aligned} \frac{d\vec{R}}{dt} &= (\dot{R}_{xH} + \dot{x}) \vec{x}_H' + (\dot{R}_{yH} + \dot{y}) \vec{y}_H' + (\dot{R}_{zH} + \dot{z}) \vec{z}_H \\ &+ \vec{\omega}_E \times \left[(\dot{R}_{xH} + \dot{x}) \vec{x}_H' + (\dot{R}_{yH} + \dot{y}) \vec{y}_H' + (\dot{R}_{zH} + \dot{z}) \vec{z}_H \right] \quad (28) \end{aligned}$$

where a dot above the variable denotes first derivative with respect to time.

The last term may be expanded in the following matrix form:

$$\begin{aligned} \vec{\omega}_E \times \vec{R} &= \begin{vmatrix} \vec{x}_H' & \vec{y}_H' & \vec{z}_H' \\ \omega_{E_{xH}} & \omega_{E_{yH}} & \omega_{E_{zH}} \\ (R_{xH} + x) & (R_{yH} + y) & (R_{zH} + z) \end{vmatrix} \\ &= \left[\omega_{E_{yH}} (R_{zH} + z) - \omega_{E_{zH}} (R_{yH} + y) \right] \vec{x}_H' + \left[\omega_{E_{zH}} (R_{xH} + x) \right. \\ &\quad \left. - \omega_{E_{xH}} (R_{zH} + z) \right] \vec{y}_H' + \left[\omega_{E_{xH}} (R_{yH} + y) - \omega_{E_{yH}} (R_{xH} + x) \right] \vec{z}_H \end{aligned}$$

From this expanded form, the following equations can be established:

$$A = \omega_{E_{yH}} (R_{zH} + z) - \omega_{E_{zH}} (R_{yH} + y) \quad (29a)$$

$$B = \omega_{E_{zH}} (R_{xH} + x) - \omega_{E_{xH}} (R_{zH} + z) \quad (29b)$$

$$C = \omega_{E_{xH}} (R_{yH} + y) - \omega_{E_{yH}} (R_{xH} + x) \quad (29c)$$

Therefore, the velocity vector is

$$\frac{\vec{dR}}{dt} = (\dot{X} + A) \vec{X}_H^t + (\dot{Y} + B) \vec{Y}_H^t + (\dot{Z} + C) \vec{Z}_H \quad (30)$$

To obtain the acceleration, the second derivative of \vec{R} with respect to time is taken

$$\begin{aligned} \frac{\vec{d^2R}}{dt^2} &= (\ddot{X} + \dot{A}) \vec{X}_H^t + (\ddot{Y} + \dot{B}) \vec{Y}_H^t + (\ddot{Z} + \dot{C}) \vec{Z}_H \\ &+ \omega_{E_x} X \left[(\dot{X} + A) \vec{X}_H^t + (\dot{Y} + B) \vec{Y}_H^t + (\dot{Z} + C) \vec{Z}_H \right] \end{aligned} \quad (31)$$

where \dot{A} , \dot{B} , \dot{C} are the derivatives of equations (29a), (29b), and (29c),

$$\dot{A} = \omega_{E_{yH}} \dot{Z} - \omega_{E_{zH}} \dot{Y} \quad (32a)$$

$$\dot{B} = \omega_{E_{zH}} \dot{X} - \omega_{E_{xH}} \dot{Z} \quad (32b)$$

$$\dot{C} = \omega_{E_{xH}} \dot{Y} - \omega_{E_{yH}} \dot{X} \quad (32c)$$

and the last term is expanded to give

$$\begin{aligned}
 \vec{\omega}_E \times \frac{d\vec{R}}{dt} &= \begin{vmatrix} \vec{x}'_H & \vec{y}'_H & \vec{z}'_H \\ \omega_{E_{xH}} & \omega_{E_{yH}} & \omega_{E_{zH}} \\ (\dot{x} + A) & (\dot{y} + B) & (\dot{z} + C) \end{vmatrix} \\
 &= \left[\omega_{E_{yH}} (\dot{z} + C) - \omega_{E_{zH}} (\dot{y} + B) \right] \vec{x}'_H \\
 &+ \left[\omega_{E_{zH}} (\dot{x} + A) - \omega_{E_{xH}} (\dot{z} + C) \right] \vec{y}'_H \\
 &+ \left[\omega_{E_{xH}} (\dot{y} + B) - \omega_{E_{yH}} (\dot{x} + A) \right] \vec{z}'_H
 \end{aligned}$$

By substituting the above into equation (31), the following is obtained for the acceleration

$$\begin{aligned}
 \frac{d^2\vec{R}}{dt^2} &= \left[\ddot{x} + \omega_{E_{yH}} \dot{z} - \omega_{E_{zH}} \dot{y} + \omega_{E_{yH}} (\dot{z} + C) - \omega_{E_{zH}} (\dot{y} + B) \right] \vec{x}'_H \\
 &+ \left[\ddot{y} + \omega_{E_{zH}} \dot{x} - \omega_{E_{xH}} \dot{z} + \omega_{E_{zH}} (\dot{x} + A) - \omega_{E_{xH}} (\dot{z} + C) \right] \vec{y}'_H \\
 &+ \left[\ddot{z} + \omega_{E_{xH}} \dot{y} - \omega_{E_{yH}} \dot{x} + \omega_{E_{xH}} (\dot{y} + B) - \omega_{E_{yH}} (\dot{x} + A) \right] \vec{z}'_H \quad (33)
 \end{aligned}$$

By collecting terms and reducing equation (33), the final development of vehicle acceleration with respect to the horizontal reference frame is

$$\frac{d^2\vec{R}}{dt^2} = \left(\ddot{x} + 2\dot{A} + \omega_{E_{yH}} C - \omega_{E_{yH}} B \right) \vec{x}'_H$$

$$\begin{aligned}
 & + \left(\ddot{Y} + 2\dot{B} + \omega_{E_{zH}} A - \omega_{E_{xH}} C \right) \vec{Y}_H \\
 & + \left(\ddot{Z} + 2\dot{C} + \omega_{E_{xH}} B - \omega_{E_{yH}} A \right) \vec{Z}_H
 \end{aligned} \tag{34}$$

or in component form in the horizontal reference frame,

$$a_x = \ddot{X} + 2\dot{A} + \omega_{E_{yH}} C - \omega_{E_{zH}} B \tag{35a}$$

$$a_y = \ddot{Y} + 2\dot{B} + \omega_{E_{zH}} A - \omega_{E_{xH}} C \tag{35b}$$

$$a_z = \ddot{Z} + 2\dot{C} + \omega_{E_{xH}} B - \omega_{E_{yH}} A \tag{35c}$$

This completes the derivation of the acceleration equations, which includes coriolis and centripetal acceleration due to rotation of the coordinate system, and accelerations of the vehicle CG due to forces and moments.

To complete the equations of motion, it will be necessary to introduce the forces and moments acting on the vehicle. These forces and moments result mainly, for this program, from gravitational attraction, and from reaction of the air on the vehicle as a result of its motion. This is not to say other types of forces cannot be involved.

c. Earth Position Coordinates

Since the components of the gravitational force are dependent upon the position of the vehicle in the earth coordinate system, the instantaneous longitude and geocentric latitude can be obtained by the following method.

From equation (6) and reference 9, the geocentric latitude is

$$\lambda_c = \arcsin \frac{z_E}{R_{EQ}}$$

and the longitude is

$$\beta = \arctan \frac{Y_E}{X_E}$$

where X_E , Y_E , and Z_E are coordinates in the earth reference system.

This program expresses the vehicle position in the horizontal reference frame; therefore, the position must be transformed to the earth reference frame. This can be done through examination of figures 2, 5, and 6, and the following transformation matrixes.

The order of transformation will be from X'_H , Y'_H , Z'_H to X_H , Y_H , and Z_H , to X_E , Y_E , and Z_E .

Therefore,

$$X_H = X'_H \sin AZ - Y'_H \cos AZ$$

$$Y_H = X'_H \cos AZ + Y'_H \sin AZ$$

$$Z_H = Z'_H \quad (36a)$$

or in matrix form

$$\begin{bmatrix} X_H \\ Y_H \\ Z_H \end{bmatrix} = \begin{bmatrix} \sin AZ & (-\cos AZ) & 0 \\ \cos AZ & \sin AZ & 0 \\ 0 & 0 & 1 \end{bmatrix} \cdot \begin{bmatrix} X'_H \\ Y'_H \\ Z'_H \end{bmatrix} \quad (36b)$$

and

$$X_E = X_H \sin \lambda_g + Z_H \cos \lambda_g$$

$$Y_E = Y_H$$

$$Z_E = -X_H \cos \lambda_g + Z_H \sin \lambda_g \quad (37a)$$

from which the following matrix is formed:

$$\begin{bmatrix} X_e \\ Y_e \\ Z_e \end{bmatrix} = \begin{bmatrix} \sin \lambda_g & 0 & \cos \lambda_g \\ 0 & 1 & 0 \\ -\cos \lambda_g & 0 & \sin \lambda_g \end{bmatrix} \cdot \begin{bmatrix} X_H \\ Y_H \\ Z_H \end{bmatrix} \quad (37b)$$

By substituting equation (36b) into equation (37b)

$$\begin{bmatrix} X_e \\ Y_e \\ Z_e \end{bmatrix} = \begin{bmatrix} \sin \lambda_g & 0 & \cos \lambda_g \\ 0 & 1 & 0 \\ -\cos \lambda_g & 0 & \sin \lambda_g \end{bmatrix} \cdot \begin{bmatrix} \sin AZ & (-\cos AZ) & 0 \\ \cos AZ & \sin AZ & 0 \\ 0 & 0 & 1 \end{bmatrix} \cdot \begin{bmatrix} X'_H \\ Y'_H \\ Z'_H \end{bmatrix} \quad (38)$$

and expanding equation (38),

$$\begin{bmatrix} X_e \\ Y_e \\ Z_e \end{bmatrix} = \begin{bmatrix} (\sin \lambda_g \sin AZ) & (-\sin \lambda_g \cos AZ) & \cos \lambda_g \\ \cos AZ & \sin AZ & 0 \\ (-\cos \lambda_g \sin AZ) & (\cos \lambda_g \cos AZ) & \cos \lambda_g \end{bmatrix} \cdot \begin{bmatrix} X'_H \\ Y'_H \\ Z'_H \end{bmatrix} \quad (39)$$

From equation (39)

$$X_E = X'_H (\sin \lambda_g \sin AZ) - Y'_H (\sin \lambda_g \cos AZ) + Z'_H \cos \lambda_g \quad (40a)$$

$$Y_E = X'_H \cos AZ + Y'_H \sin AZ \quad (40b)$$

$$Z_E = -X'_H (\cos \lambda_g \sin AZ) + Y'_H (\cos \lambda_g \cos AZ) + Z'_H \sin \lambda_g \quad (40c)$$

where

$$X'_H = R_{xH} + X$$

$$Y'_H = R_{yH} + Y$$

$$Z'_H = R_{zH} + Z$$

R_{xH} , R_{yH} , and R_{zH} are defined by equation (26). Therefore, the instantaneous geocentric latitude can be obtained from

$$\lambda_c = \arcsin \left(\frac{z_E}{R} \right) \quad (41)$$

where

$$R = \left[(R_{xH} + x)^2 + (R_{yH} + y)^2 + (R_{zH} + z)^2 \right]^{1/2}$$

since the earth is assumed to be a body of revolution about the polar axis, the instantaneous longitude may be defined as

$$\theta = \arctan \left(\frac{y_E}{x_E} \right) \quad (42)$$

and will be considered positive when measured east from the prime meridian and negative when measured west.

d. Gravitational Equations

The potential function and equations used to obtain the gravitational forces to be included in the equations of motion are presented in this subsection. The gravitational potential of the earth is an expansion of spherical harmonics as a function of latitude and longitude. However, in this program, the earth is assumed to be a body of revolution so that the longitudinal effects may be ignored. Although some satellite data indicate that the earth's equator is elliptical where the major axis is somewhat larger than the minor axis, the difference though is very small compared to the equatorial radius.

The gravity components are determined by taking partial derivatives of the gravitational potential equation (Ref. 9).

$$\begin{aligned} \Phi(R, \lambda) = & \frac{-GM}{R} \left[1 + \frac{J}{3} \left(\frac{R_{EQ}}{R} \right)^2 \left(1 - 3 \sin^2 \lambda_c \right) \right. \\ & + \frac{H}{5} \left(\frac{R_{EQ}}{R} \right)^2 \left(3 \sin \lambda_c - 5 \sin^3 \lambda_c \right) \\ & \left. + \frac{K}{30} \left(\frac{R_{EQ}}{R} \right)^4 \left(3 - 30 \sin^2 \lambda_c + 35 \sin^4 \lambda_c \right) + \dots \right] \end{aligned} \quad (43)$$

where

$G M_0 = 1.4076427 \times 10^{16} \text{ ft}^3/\text{sec}^2$ gravitational constant of the earth

R = radial distance to body CG from earth's geocenter

R_{EQ} = earth's equatorial radius

λ_c = geocentric latitude

$J = 1623.41 \times 10^{-6}$, coefficient of the second harmonic

$H = 6.04 \times 10^{-6}$, coefficient of the third harmonic

$K = 6.37 \times 10^{-6}$, coefficient of the fourth harmonic

The gravitational potential field is usually defined by spherical harmonics. Each higher order term in equation (43) is due to a deviation of the potential from that of a true sphere. Therefore, the potential is expressed as a series of Legendre polynomials in the variable, λ_c . Many analyses (Refs. 9, 11, 12) consider only the second-, third-, and fourth-order terms. The first harmonic (R_{EQ}/k) is missing because of the choice of an equatorial coordinate system in which λ_c is measured relative to the center of the earth. The fifth harmonic is not sufficiently well known to justify its inclusion in this equation.

The gravitational acceleration of a vehicle along any line is the partial derivative of the potential function, ψ , along that line. See figure 7.

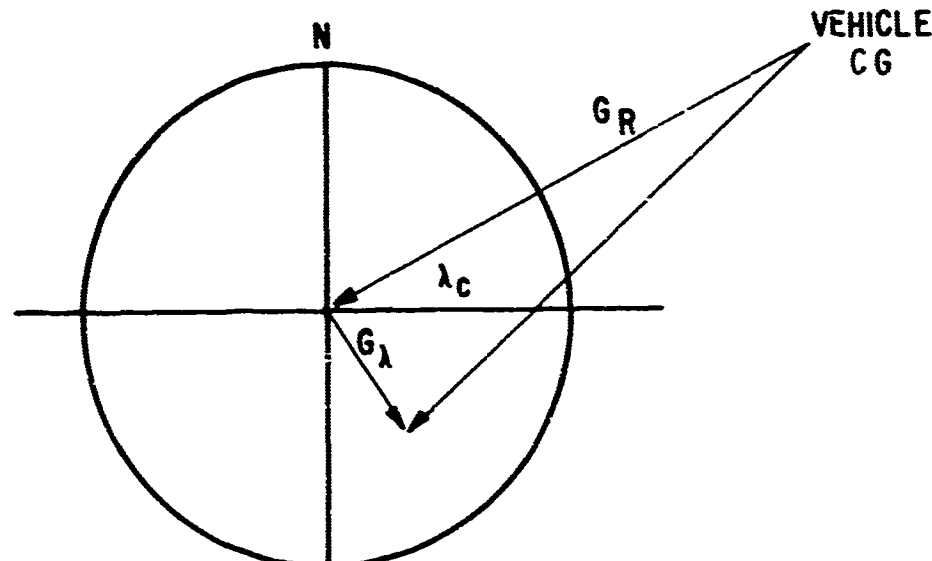


Figure 7. Gravitational Direction

\vec{g} is related to $\hat{v}(R, \lambda_c)$ by

$$\vec{g} = -\nabla \hat{v}(R, \lambda_c)$$

where $\nabla \hat{v}$ is the gradient vector of $\hat{v}(R, \lambda_c)$. From figure 7, the force along the radius, R , is

$$G_R = mg_R = -m \frac{\partial \hat{v}(R, \lambda_c)}{\partial R}$$

and in R, λ_c direction

$$G_{\lambda} = mg_{\lambda_c} = -\frac{m}{R} \frac{\partial \hat{v}(R, \lambda_c)}{\partial \lambda_c}$$

where m = mass of vehicle in slugs. From equation (43), G_R and G_{λ_c} are obtained.

$$G_R = -m \frac{\partial \hat{v}}{\partial R} = +m G_0 M_0 \left[-\frac{1}{R^2} - \frac{3J}{3} \left(\frac{R_{EQ}^2}{R^4} \right) \left(1 - 3 \sin^2 \lambda_c \right) \right. \\ \left. - \frac{4}{5} H \left(\frac{R_{EQ}^3}{R^5} \right) \left(3 \sin \lambda_c - 5 \sin^3 \lambda_c \right) \right. \\ \left. - \frac{5K}{30} \left(\frac{R_{EQ}^4}{R^6} \right) \left(3 - 30 \sin^2 \lambda_c + 35 \sin^4 \lambda_c \right) \right]$$

$$G_{\lambda_c} = -\frac{m}{R} \frac{\partial \hat{v}}{\partial \lambda_c} = \frac{+m G_0 M_0}{R^2} \left[\frac{J}{3} \left(\frac{R_{EQ}^2}{R^2} \right) \left(-6 \sin \lambda_c \cos \lambda_c \right) \right. \\ \left. + \frac{H}{5} \left(\frac{R_{EQ}^3}{R^3} \right) \left(3 \cos \lambda_c - 15 \sin^2 \lambda_c \cos \lambda_c \right) \right. \\ \left. + \frac{K}{30} \left(\frac{R_{EQ}^4}{R^4} \right) \left(-60 \sin \lambda_c \cos \lambda_c + 140 \sin^3 \lambda_c \cos \lambda_c \right) \right]$$

simplifying and dividing through by m ,

$$G_R = - \frac{G M_0}{R^2} \left[1 + J \left(\frac{R_{EQ}}{R} \right)^2 \left(1 - 3 \sin^2 \lambda_c \right) + \frac{4H}{5} \left(\frac{R_{EQ}}{R} \right)^3 \left(3 \sin \lambda_c - 5 \sin^3 \lambda_c \right) + \frac{K}{6} \left(\frac{R_{EQ}}{R} \right)^4 \left(3 - 30 \sin^2 \lambda_c + 35 \sin^4 \lambda_c \right) \right] \quad (44a)$$

$$G\lambda_c = - \frac{G M_0}{R^2} \left[-2 J \left(\frac{R_{EQ}}{R} \right)^2 \left(\sin \lambda_c \cos \lambda_c \right) + \frac{3H}{5} \left(\frac{R_{EQ}}{R} \right)^3 \left(\cos \lambda_c - 5 \sin^2 \lambda_c \cos \lambda_c \right) + \frac{2K}{3} \left(\frac{R_{EQ}}{R} \right)^4 \left(-3 \sin \lambda_c \cos \lambda_c + 7 \sin^3 \lambda_c \cos \lambda_c \right) \right] \quad (44b)$$

Since G_R is along the radius \vec{R} and $G\lambda_c$ is perpendicular to \vec{R} , they are in the inertial reference frame. For them to be included in the equations of motion, their components must be found with respect to the horizontal reference frame. This can be accomplished by the use of direction cosines and transformation matrices.

After examination of figure 8, the following series of equations can be written to transpose G_R and $G\lambda_c$ to the horizontal reference frame.

It is noted that G_R and $G\lambda$ are taken as positive in the direction shown in figures 7 and 8. Therefore, by definition

$$G_R = + \frac{\partial \hat{r}}{\partial R}$$

$$G\lambda = + \frac{1}{R} \frac{\partial \hat{\lambda}}{\partial R}$$

$$G\delta = 0 \quad (45)$$

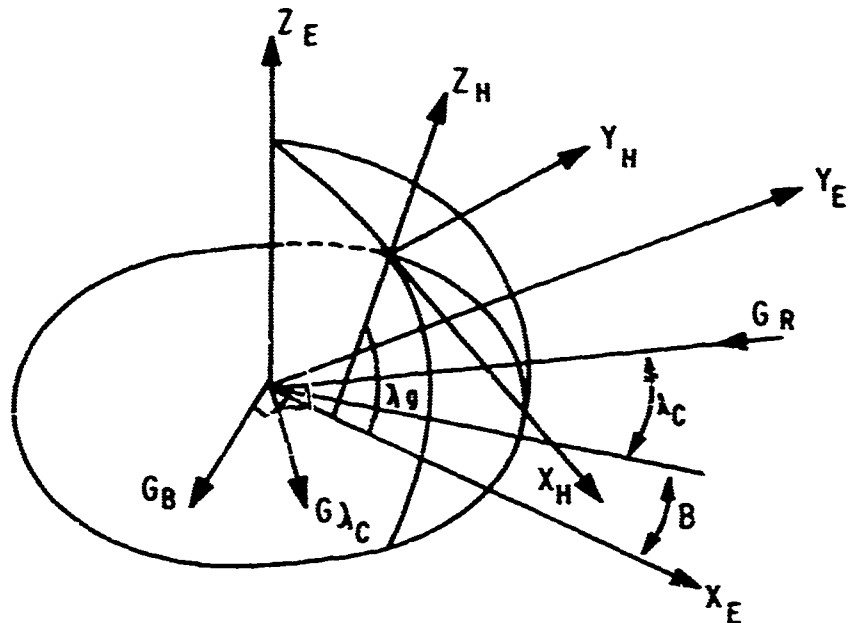


Figure 8. Gravitational Transformations

$$GX_E = -GR \left(\cos \lambda_c \cos \hat{s} \right) + GL \left(\sin \lambda_c \cos \hat{s} \right) + GS \sin \hat{s}$$

$$GY_E = -GR \left(\cos \lambda_c \sin \hat{s} \right) + GL \left(\sin \lambda_c \sin \hat{s} \right) - GS \cos \hat{s}$$

$$GZ_E = -GR \sin \lambda_c - GL \cos \lambda_c \quad (46)$$

$$GX_H = GX_E \sin \lambda_g - GZ_E \cos \lambda_g$$

$$GY_H = GY_E$$

$$GZ_H = GX_E \cos \lambda_g + GZ_E \sin \lambda_g \quad (47)$$

From equations (16a), (16b), and (16c), the following is obtained:

$$GX_H' = GX_H \sin AZ + GY_H \cos AZ$$

$$GY_H' = -GX_H \cos AZ + GY_H \sin AZ$$

$$GZ_H' = GZ_H \quad (48)$$

Equations (46) and (47) can be expressed in matrix form

$$\begin{bmatrix} GX_H \\ GY_H \\ GZ_H \end{bmatrix} = \begin{bmatrix} (-\sin \lambda_g \cos \lambda_c \cos \beta + \cos \lambda_g \sin \lambda_c) \\ (-\cos \lambda_c \sin \beta) \\ (-\cos \lambda_g \cos \lambda_c \cos \beta - \sin \lambda_g \sin \lambda_c) \end{bmatrix}$$

$$\begin{bmatrix} (\sin \lambda_g \sin \lambda_c \cos \beta + \cos \lambda_g \cos \lambda_c) & (\sin \lambda_g \sin \beta) \\ (\sin \lambda_c \sin \beta) & (-\cos \beta) \\ (\cos \lambda_g \sin \lambda_c \cos \beta - \sin \lambda_g \cos \lambda_c) & (\cos \lambda_g \sin \beta) \end{bmatrix} \cdot \begin{bmatrix} GR \\ G\lambda \\ GB \end{bmatrix} \quad (49)$$

This matrix may be written into the following equations for transformation:

$$\begin{aligned} G11 &= -\sin \lambda_g \cos \lambda_c \cos \beta + \cos \lambda_g \sin \lambda_c \\ G12 &= \sin \lambda_g \sin \lambda_c \cos \beta + \cos \lambda_g \cos \lambda_c \\ G21 &= -\cos \lambda_c \sin \beta \\ G22 &= \sin \lambda_c \sin \beta \\ G31 &= -\cos \lambda_g \cos \lambda_c \cos \beta - \sin \lambda_g \sin \lambda_c \\ G32 &= +\cos \lambda_g \sin \lambda_c \cos \beta - \sin \lambda_g \cos \lambda_c \end{aligned} \quad (50)$$

The final transformation is obtained by substituting equation (49) into equation (48).

$$\begin{aligned} GX'_H &= GR (G11 \cdot \sin AZ + G21 \cdot \cos AZ) \\ &\quad + G\lambda (G12 \cdot \sin AZ + G22 \cdot \cos AZ) \\ GY'_H &= GR (-G11 \cdot \cos AZ + G21 \cdot \sin AZ) \\ &\quad + G\lambda (-G12 \cdot \cos AZ + G22 \cdot \sin AZ) \\ GZ'_H &= GZ_H = GR (G31) + G\lambda (G32) \end{aligned} \quad (51)$$

The components of the gravitational forces are now expressed in the horizontal reference frame and may be included with equations (35) to complete the equations of motion.

Before the aerodynamic forces and moments can be resolved, a method must be established for the transformation of components from the body reference frame to the horizontal reference frame and the inverse.

e. Euler Angles

Up to this point, only the equations for the three-translational degrees-of-freedom have been derived. This establishes the vehicle CG with respect to a horizontal reference system. To analyze the body forces and moments as a result of its motion about the CG, the angular orientation of the vehicle must be known with respect to the horizontal reference system.

The Euler angles describing the angular motion are ϕ , θ , and ψ , and will be noted as pitch, yaw, and roll angles, respectively. These angles are to be differentiated from the angles of attack and sideslip. The angles of attack and sideslip have a kinematic definition based on the components of the free-stream velocity relative to the body axes of the vehicle. The angular displacements, ϕ , θ , and ψ , on the other hand, are used to measure the vehicle attitude with respect to a fixed set of axes (X, Y, and Z), and in no way require motion of the vehicle relative to the surrounding air for their definition.

Consider a vehicle moving with respect to the inertial axes X, Y, and Z which are also fixed in space. The following will describe one of several ways of specifying the angular orientation of a vehicle at any instant of time. This will be done by successively pitching, yawing, and rolling the X, Y, and Z axes until they coincide with the axes x, y, and z of the vehicle as shown in figure 9.

First, pitch the vehicle by an angular displacement ϕ around OX so that Z goes to Z_1 and Y goes to Y_1 (figure 9a). The relationship between the two coordinate systems is then given by the following transfer matrix:

$$\begin{bmatrix} X_1 \\ Y_1 \\ Z_1 \end{bmatrix} = \begin{bmatrix} 1 & 0 & 0 \\ 0 & \cos \phi & -\sin \phi \\ 0 & \sin \phi & \cos \phi \end{bmatrix} \cdot \begin{bmatrix} X \\ Y \\ Z \end{bmatrix} \quad (52)$$

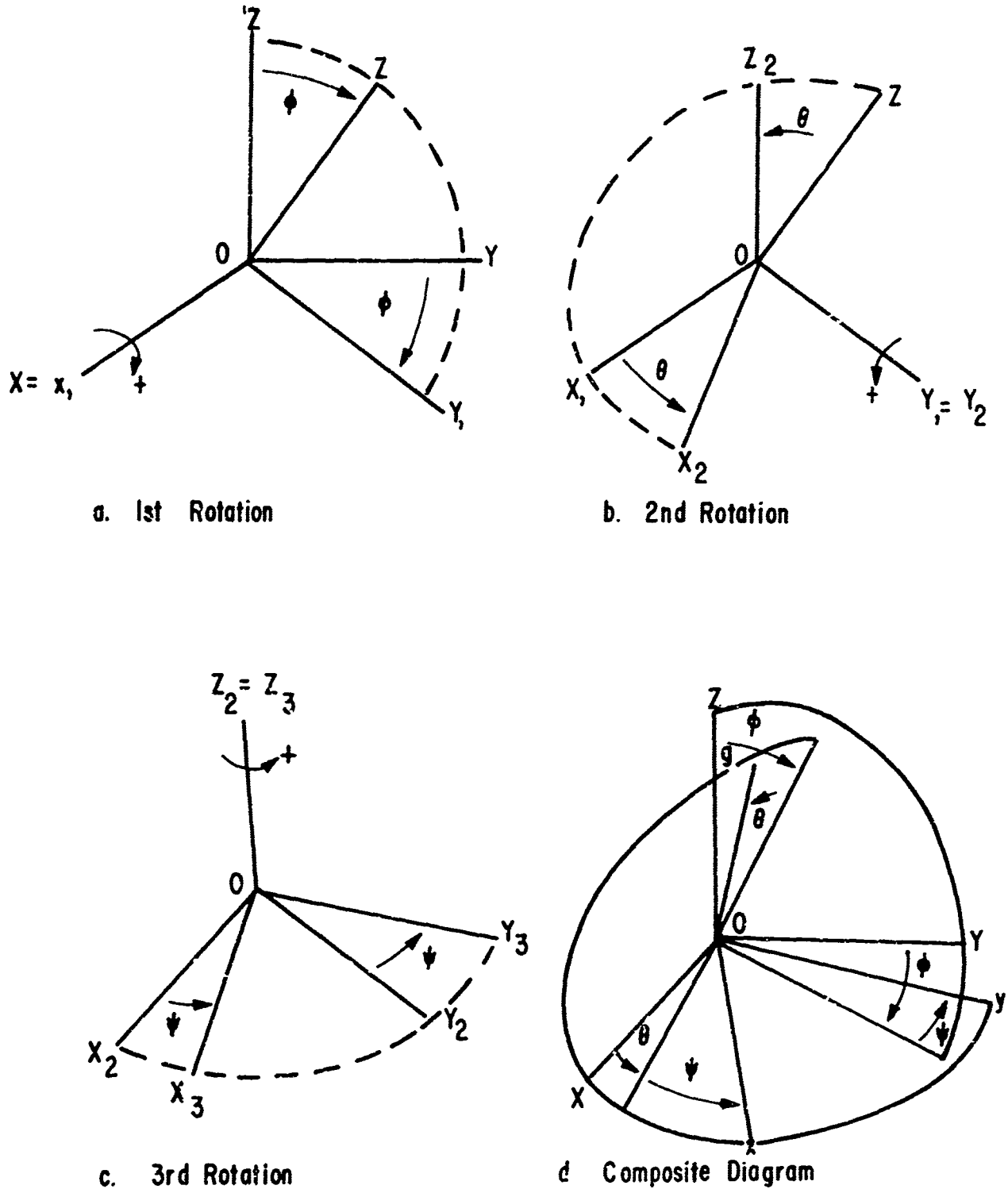


Figure 9. System of Angular Displacements

Next, yaw the vehicle by an angle θ about the OY_1 axes so that X_1 goes to X_2 and Z_1 to Z_2 (figure 9b). The new relationship is given by the transfer matrix

$$\begin{bmatrix} X_2 \\ Y_2 \\ Z_2 \end{bmatrix} = \begin{bmatrix} \cos \theta & 0 & -\sin \theta \\ 0 & 1 & 0 \\ \sin \theta & 0 & \cos \theta \end{bmatrix} \cdot \begin{bmatrix} X_1 \\ Y_1 \\ Z_1 \end{bmatrix} \quad (53)$$

Finally, roll the vehicle by angle ψ around the OZ_2 axis so that X_2 moves to X_3 , and Y_2 to Y_3 (figure 9c). The transfer matrix for this rotation is

$$\begin{bmatrix} x \\ y \\ z \end{bmatrix} = \begin{bmatrix} \cos \psi & \sin \psi & 0 \\ -\sin \psi & \cos \psi & 0 \\ 0 & 0 & 1 \end{bmatrix} \cdot \begin{bmatrix} X_2 \\ Y_2 \\ Z_2 \end{bmatrix} \quad (54)$$

where

$$x = X_3$$

$$y = Y_3$$

$$z = Z_3$$

The operations of pitch, yaw, and roll for this program must always be performed in this order since angular displacements do not follow the ordinary laws of vector addition, but, in fact, follow a noncommutative law. Under this system of rotations, the direction cosines of the finial vehicle axes x , y , and z to the fixed axis X , Y , and Z are obtained by substituting equation (52) into equations (53).

$$\begin{bmatrix} X_2 \\ Y_2 \\ Z_2 \end{bmatrix} = \begin{bmatrix} \cos \theta & (-\sin \theta \sin \psi) & (-\sin \theta \cos \psi) \\ 0 & \cos \psi & -\sin \psi \\ \sin \theta & (\sin \theta \cos \psi) & (\cos \theta \cos \psi) \end{bmatrix} \cdot \begin{bmatrix} x \\ y \\ z \end{bmatrix} \quad (55)$$

Then substitute equation (54) into equation (55)

$$\begin{bmatrix} x \\ y \\ z \end{bmatrix} = \begin{bmatrix} (\cos \psi \cos \theta) & (-\sin \theta \sin \phi \cos \psi + \sin \psi \cos \theta) \\ (-\sin \psi \cos \theta) & (\sin \theta \sin \phi \sin \psi + \cos \psi \cos \phi) \\ \sin \theta & (\cos \theta \sin \phi) \end{bmatrix}$$

$$\begin{bmatrix} (-\sin \theta \cos \phi \cos \psi - \sin \psi \sin \phi) \\ (\sin \psi \sin \theta \cos \phi - \sin \phi \cos \psi) \\ (\cos \theta \cos \phi) \end{bmatrix} \begin{bmatrix} x \\ y \\ z \end{bmatrix} \quad (56)$$

Therefore, equation (56) will transform components from the fixed axes or horizontal reference system to the vehicle or body reference system. To transform components from the vehicle axes to the horizontal references axes, the matrix of equation (56) must be inverted by interchanging rows and columns. The elements of equation (56) may be written for simplicity as follows, where subscripts indicate rows and columns.

$$\begin{aligned} A_{11} &= \cos \theta \cos \psi \\ A_{12} &= -\sin \theta \sin \phi \cos \psi + \sin \psi \cos \theta \\ A_{13} &= -\sin \theta \cos \phi \cos \psi - \sin \psi \sin \phi \\ A_{21} &= -\sin \psi \cos \theta \\ A_{22} &= \sin \theta \sin \phi \sin \psi + \cos \psi \cos \phi \\ A_{23} &= \sin \psi \sin \theta \cos \phi - \sin \phi \cos \psi \\ A_{31} &= \sin \theta \\ A_{32} &= \cos \theta \sin \phi \\ A_{33} &= \cos \theta \cos \phi \end{aligned} \quad (57)$$

f. Transformation of Angular Velocities

It is now necessary to express the angular velocities ω_x , ω_y , and ω_z with respect to the vehicle axes in terms of the Euler angles.

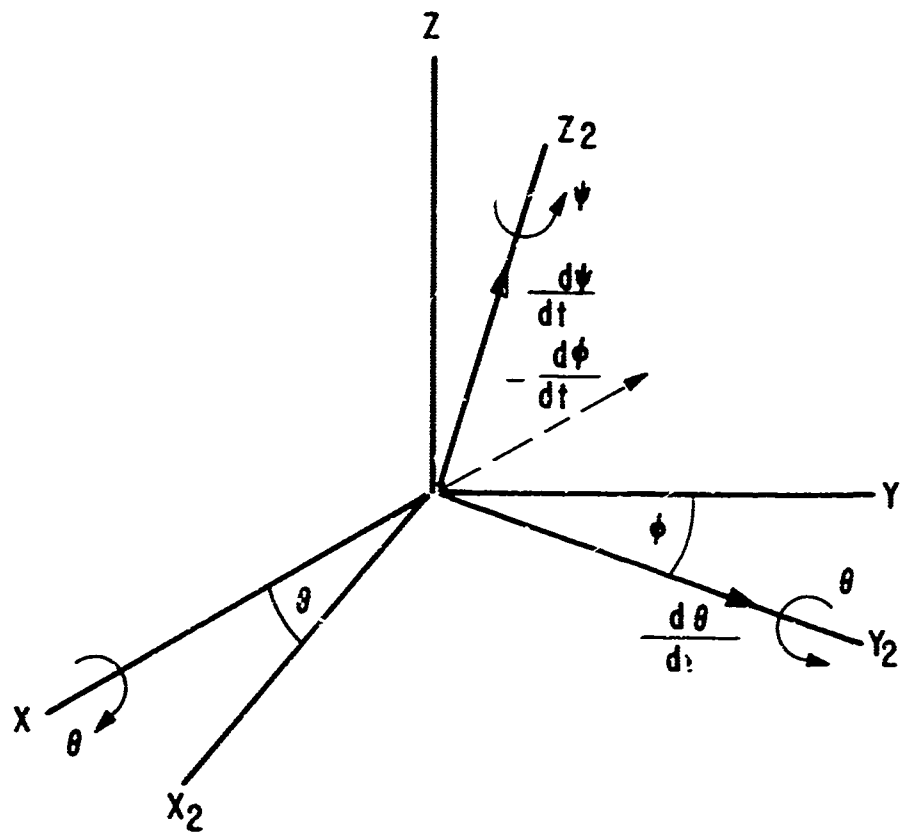


Figure 10. Angular Velocities of Euler Angles

The components of the angular velocities along the X_2 , Y_2 , and Z_2 axes to the vehicle axes x , y , and z shown in figure 10 are

$$\begin{aligned}\omega_x &= \frac{-d\phi}{dt} \cos \theta \cos \psi + \frac{d\psi}{dt} \sin \psi \\ \omega_y &= \frac{d\phi}{dt} \cos \theta \sin \psi + \frac{d\psi}{dt} \cos \psi \\ \omega_z &= \frac{-d\phi}{dt} \sin \theta + \frac{d\psi}{dt} \end{aligned}\quad (58)$$

The equations in section II-2e and equation (56) have been derived with respect to the inertial axes X , Y , and Z . If the axes system is allowed to rotate, the angular velocity of the earth ω_E must be included. Therefore, the inertial angular rates of the vehicle are

$$\begin{aligned}\Omega_x &= \omega_x + \omega_{E_{xH}} \\ \Omega_y &= \omega_y + \omega_{E_{yH}} \\ \Omega_z &= \omega_z + \omega_{E_{zH}}\end{aligned}\quad (59)$$

where $\omega_{E_{xH}}$, $\omega_{E_{yH}}$, and $\omega_{E_{zH}}$ are defined by equation (19). These are the components of the earth's rotation rate in the horizontal reference frame.

Since this program was written for a symmetrical cone with uniform weight distribution and further assumes symmetrical ablation, then the products of inertia will be zero regardless of roll angle, ψ . (This will be shown in section II-2g.) Therefore, the roll and transverse moment of inertia can be obtained independent of ψ . This will simplify the equations and allow the angular momentum, \vec{h}_0 , to be written in the second rotation.

Therefore, equation (58) can be simplified and written in the X_2 , Y_2 , and Z_2 axes as

$$\begin{aligned}\omega_{x2} &= -\frac{d\phi}{dt} \cos \theta \\ \omega_{y2} &= \frac{d\theta}{dt} \\ \omega_{z2} &= -\frac{d\phi}{dt} \sin \theta + \frac{d\psi}{dt}\end{aligned}\quad (60)$$

which are the total rotation rates of the vehicle in the second rotated axes.

Now $\omega_{E_{xH}}$, $\omega_{E_{yH}}$, and $\omega_{E_{zH}}$ must also be written in the same axes system as the vehicle angular rates. This can be done by using the transformation equation (55), which will result in

$$\begin{aligned}\omega_{E_{x2}} &= \omega_{E_{xH}} \cos \theta - \omega_{E_{yH}} \sin \theta \sin \phi - \omega_{E_{zH}} \sin \theta \cos \phi \\ \omega_{E_{y2}} &= 0 + \omega_{E_{yH}} \cos \phi - \omega_{E_{zH}} \sin \phi \\ \omega_{E_{z2}} &= \omega_{E_{xH}} \sin \theta + \omega_{E_{yH}} \sin \phi \cos \theta + \omega_{E_{zH}} \cos \phi \cos \theta\end{aligned}\quad (61)$$

Therefore, equation (59) can be written as

$$\Omega_x = \omega_{x_2} + \omega_{Ex_2}$$

$$\Omega_y = \omega_{y_2} + \omega_{Ey_2}$$

$$\Omega_z = \omega_{z_2} + \omega_{Ez_2} \quad (62)$$

which are the inertial angular velocities of the vehicle in the X_2 , Y_2 , and Z_2 axes.

Since equation (62) is written in the second rotated axes system, it is also necessary to have the angular velocity of that coordinate system. Therefore,

$$\begin{aligned} \Omega_{x_2} &= -\frac{d\phi}{dt} \cos \theta + \omega_{Ex_2} \\ \Omega_{y_2} &= \frac{d\theta}{dt} + \omega_{Ey_2} \\ \Omega_{z_2} &= -\frac{d\psi}{dt} \sin \theta + \omega_{Ez_2} \end{aligned} \quad (63)$$

which completes the transformation of angular velocities.

g. Moment of Momentum

A particle of mass, m , moving with velocity, \vec{R} , figure 11, has a linear momentum (Ref. 13)

$$\vec{p} = m \vec{R}$$

The moment of this linear momentum about an arbitrary point, O , is defined as

$$\vec{h}_o = \vec{r} \times m \vec{R} \quad (64)$$

where

\vec{R} = absolute velocity of m

\vec{r} = radius drawn from O as shown in figure 11

\vec{h}_o = the angular momentum of the particle about the point O

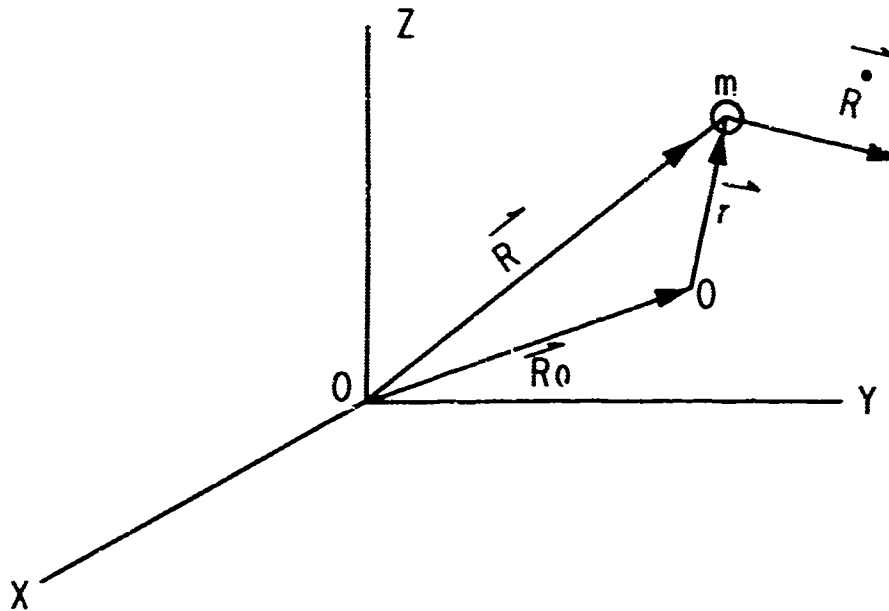


Figure 11. Moment of Momentum about 0

The angular momentum of a rigid body, figure 12, about any axis perpendicular to the plane of motion and passing through the point 0 fixed in a moving body is the sum of the moments of the linear momenta of all its particles about the axis. Therefore, equation (64) can be rewritten as

$$\vec{h}_o = \sum_i \vec{r}_i \times m_i \vec{v}_i$$

where \vec{v}_i = velocity of any point i on the body. The velocity of a representative particle of mass m_i may be expressed in terms of the velocity of 0 plus the velocity of m_i with respect to 0.

$$\vec{v}_i = \vec{v}_o + \vec{\omega} \times \vec{r}_i$$

Therefore,

$$\vec{h}_o = \sum_i \vec{r}_i \times m_i (\vec{v}_o + \vec{\omega} \times \vec{r}_i)$$

or is expanded from

$$\vec{h}_o = \sum_i \vec{r}_i \times (\vec{\omega} \times \vec{r}_i) m_i - \vec{v}_o \times \sum_i m_i \vec{r}_i$$

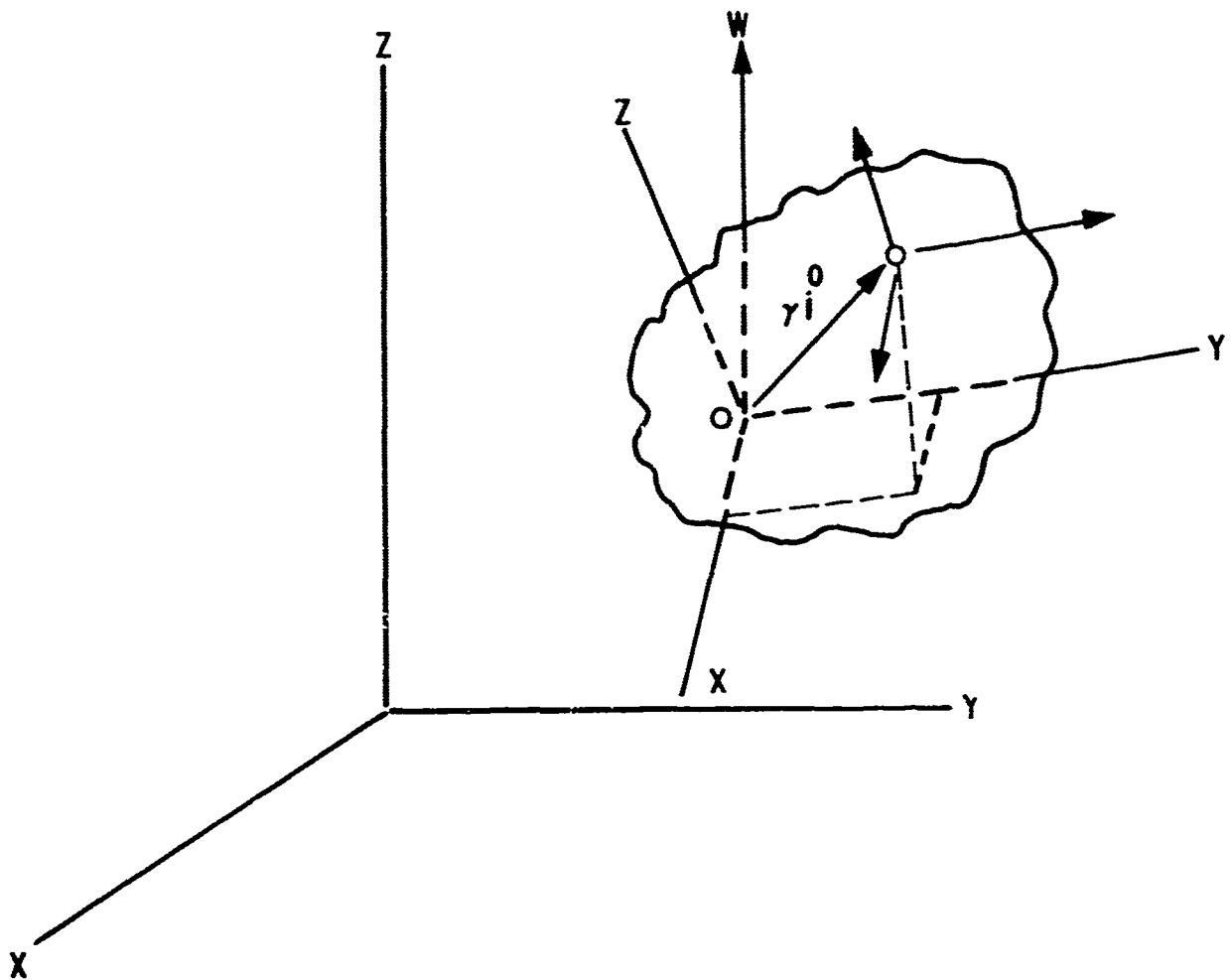


Figure 12. Components of Momentum

If, by definition, O coincides with the center of mass, the term $\sum_i m_i \dot{r}_i$ is equal to zero, the angular momentum can be expressed by the following integral

$$\vec{h}_c = \int \vec{r} \times (\vec{\omega} \times \vec{r}) dm \quad (65)$$

The relation between the angular momentum of a body and the applied moments, \vec{M}_o , of the forces $\sum \vec{F} = m\ddot{R}$ acting on m is obtained from rotational equation of motion.

$$\vec{M}_o = \sum \vec{r} \times m\ddot{R} \quad (66)$$

Taking the second derivative of the expression

$$\ddot{\vec{R}} = \ddot{\vec{R}}_o + \ddot{\vec{r}}$$

and substituting into equation (66)

$$\ddot{\vec{M}}_o = \sum \vec{r} \times m \left(\ddot{\vec{R}}_o + \ddot{\vec{r}} \right)$$

or

$$\ddot{\vec{M}}_o = \sum \frac{d}{dt} (\vec{r} \times m \vec{r}) - \ddot{\vec{R}}_o \times \sum m \vec{r} \quad (67)$$

Again $\sum m \vec{r} = 0$ when 0 coincides with center of mass. Equation (67) reduces to

$$\ddot{\vec{M}}_o = \sum \frac{d}{dt} (\vec{r} \times m \vec{r}) \quad (68)$$

but \vec{r} is equal to the following:

$$\vec{r} = \left(\frac{d\vec{r}}{dt} \right) = \left[\frac{d\vec{r}}{dt} \right] + \vec{\omega} \times \vec{r}$$

where

$$\left(\frac{d\vec{r}}{dt} \right) = \text{total derivative relative to inertial axis}$$

$$\left[\frac{d\vec{r}}{dt} \right] = \text{derivative relative to rotating axis and, since body is rigid, is equal to zero}$$

Therefore,

$$\vec{r} = \vec{\omega} \times \vec{r}$$

and substituting into equation (67) the relationship between $\ddot{\vec{M}}_o$ and $\ddot{\vec{h}}_o$ is established.

$$\ddot{\vec{M}}_o = \frac{d}{dt} \left(\vec{r} \times m (\vec{\omega} \times \vec{r}) \right) \quad (69)$$

or

$$\vec{M}_o = \frac{d \vec{h}_o}{dt} \quad (70)$$

With this relationship established, the derivation of \vec{h}_o can be continued. The integral in equation (65) must be evaluated and this is done by first expanding the cross product $\vec{\omega} \times \vec{r}$

$$\vec{\omega} \times \vec{r} = \begin{vmatrix} \vec{i} & \vec{j} & \vec{k} \\ \Omega_x & \Omega_y & \Omega_z \\ x & y & z \end{vmatrix} = (\Omega_y z - \Omega_z y) \vec{i} + (\Omega_z x - \Omega_x z) \vec{j} + (\Omega_x y - \Omega_y x) \vec{k} \quad (71)$$

where Ω_x , Ω_y , and Ω_z is defined by equation (62). Then expansion of the cross product $\vec{r} \times (\vec{\omega} \times \vec{r})$ is

$$\begin{aligned} \vec{r} \times (\vec{\omega} \times \vec{r}) &= \begin{vmatrix} \vec{i} & \vec{j} & \vec{k} \\ x & y & z \\ (\Omega_y z - \Omega_z y) & (\Omega_z x - \Omega_x z) & (\Omega_x y - \Omega_y x) \end{vmatrix} \\ &= \vec{i} \left[\Omega_x (y^2 + z^2) - \Omega_y (xy) - \Omega_z (xz) \right] \hat{m} \\ &+ \vec{j} \left[-\Omega_x (xy) + \Omega_y (x^2 + z^2) - \Omega_z (yz) \right] \hat{m} \\ &+ \vec{k} \left[-\Omega_x (xz) + \Omega_y (yz) + \Omega_z (x^2 + y^2) \right] \hat{m} \quad (72) \end{aligned}$$

By definition, the moments of inertia of a body about the x, y, z axes are

$$I_x = \int (y^2 + z^2) \hat{m}$$

$$I_y = \int (x^2 + z^2) \hat{m}$$

$$I_z = \int (x^2 + y^2) \hat{m}$$

and the products of inertia are

$$I_{xy} = \int xy dm$$

$$I_{xz} = \int xz dm$$

$$I_{yz} = \int yz dm$$

If the x , y , z axes are considered the principal axes, the products of inertia and the time derivatives of the moments of inertia are zero.

Therefore, by integrating equation (72) over the entire body and applying the above definition, the following is obtained:

$$h_o = I_x \Omega_x \vec{i} + I_y \Omega_y \vec{j} + I_z \Omega_z \vec{k} \quad (73)$$

in which case the moment of momentum components along the x , y , z axes are

$$h_x = I_x \Omega_x$$

$$h_y = I_y \Omega_y$$

$$h_z = I_z \Omega_z \quad (74)$$

It was shown previously that the moment about a body's center of gravity was equal to the time derivative of the moment of momentum.

$$\vec{M}_o = \frac{d \vec{h}_o}{dt}$$

which in general form can be expressed as

$$\left(\frac{d \vec{h}_o}{dt} \right) = \left[\frac{d \vec{h}_o}{dt} \right] + \vec{\omega} \times \vec{h}_o$$

Substitute this into equation (70), Euler's moment equation is obtained,

$$\vec{M}_o = \frac{d \vec{h}_o}{dt} + \vec{\Omega}_2 \times \vec{h}_o \quad (75)$$

where $\vec{\Omega}_2$ is the angular velocity of the second rotated axes system.

Taking the cross product $\vec{\Omega}_2 \times \vec{h}_o$ in a manner similar to equation (71), equation (75) becomes

$$\begin{aligned}\vec{M}_o = & \left[\frac{dhx}{dt} \vec{i} + \frac{dhy}{dt} \vec{j} + \frac{dhz}{dt} \vec{k} \right] + (\Omega_{y2} h_z - \Omega_{z2} h_y) \vec{i} \\ & + (\Omega_{z2} h_x - \Omega_{x2} h_z) \vec{j} + (\Omega_{x2} h_y - \Omega_{y2} h_x) \vec{k}\end{aligned}\quad (76)$$

and collecting terms yields

$$\begin{aligned}\vec{M}_o = & \left(\frac{dhx}{dt} + \Omega_{y2} h_z - \Omega_{y2} h_y \right) \vec{i} + \left(\frac{dhy}{dt} + \Omega_{z2} h_x - \Omega_{x2} h_z \right) \vec{j} \\ & + \left(\frac{dhz}{dt} + \Omega_{x2} h_y - \Omega_{y2} h_x \right) \vec{k}\end{aligned}\quad (77)$$

Now, taking the derivatives of equation (74) and remembering $d(I)/dt = 0$ for principal axes,

$$\begin{aligned}\frac{dhx}{dt} &= I_x \dot{\Omega}_x \\ \frac{dhy}{dt} &= I_y \dot{\Omega}_y \\ \frac{dhz}{dt} &= I_z \dot{\Omega}_z\end{aligned}\quad (78)$$

where $\dot{\Omega}_x$, $\dot{\Omega}_y$, $\dot{\Omega}_z$ are the derivatives of equation (62)

$$\begin{aligned}\dot{\Omega}_x &= \ddot{\phi} \cos \theta + \dot{\phi} \dot{\theta} \sin \theta + \dot{\omega}_{Ex_2} \\ \dot{\Omega}_y &= \ddot{\phi} + \dot{\omega}_{Ey_2} \\ \dot{\Omega}_z &= -\ddot{\phi} \sin \theta - \dot{\phi} \dot{\theta} \cos \theta + \dot{\omega}_{Ez_2}\end{aligned}\quad (79)$$

and $\dot{\omega}_{Ex_2}$, $\dot{\omega}_{Ey_2}$, $\dot{\omega}_{Ez_2}$ are the derivatives of equation (61). Before taking the derivatives of equation (61), let the following be elements of equation (55) where subscripts indicate row and columns:

$$\begin{aligned}
 B_{11} &= \cos \theta \\
 B_{12} &= -\sin \theta \sin \phi \\
 B_{13} &= -\sin \theta \cos \phi \\
 B_{21} &= 0 \\
 B_{22} &= \cos \phi \\
 B_{23} &= -\sin \phi \\
 B_{31} &= \sin \theta \\
 B_{32} &= \cos \theta \sin \phi \\
 B_{33} &= \cos \theta \cos \phi
 \end{aligned} \tag{80}$$

The derivatives of equation (80) are defined here

$$\begin{aligned}
 DB_{11} &= -\dot{\theta} \sin \theta \\
 DB_{12} &= -\dot{\theta} \cos \theta \sin \phi - \dot{\phi} \sin \theta \cos \phi \\
 DB_{13} &= -\dot{\theta} \cos \theta \cos \phi + \dot{\phi} \sin \theta \sin \phi \\
 DB_{21} &= 0 \\
 DB_{22} &= -\dot{\phi} \sin \phi \\
 DB_{23} &= -\dot{\phi} \cos \phi \\
 DB_{31} &= \dot{\theta} \cos \theta \\
 DB_{32} &= -\dot{\theta} \sin \theta \sin \phi + \dot{\phi} \cos \theta \cos \phi \\
 DB_{33} &= -\dot{\theta} \sin \theta \cos \phi - \dot{\phi} \cos \theta \sin \phi
 \end{aligned} \tag{81}$$

Therefore,

$$\begin{aligned}
 \dot{\omega}_{Ex_2} &= DB_{11}\omega_{Ex} + DB_{12}\omega_{Ey} + DB_{13}\omega_{Ez} \\
 \dot{\omega}_{Ey_2} &= DB_{21}\omega_{Ex} + DB_{22}\omega_{Ey} + DB_{23}\omega_{Ez} \\
 \dot{\omega}_{Ez_2} &= DB_{31}\omega_{Ex} + DB_{32}\omega_{Ey} + DB_{33}\omega_{Ez}
 \end{aligned} \tag{82}$$

Substituting equations (74) (76), and (79) into equation (77) and writing \vec{M}_o in component form with $I_x = I_y$,

$$M_x = I_x \left(\ddot{\phi} \cos \theta + \dot{\phi} \dot{\theta} \sin \theta + \dot{\omega}_{Ex_2} \right) + \Omega_{y2} \left(I_z \Omega_z \right) - \Omega_{z2} \left(I_x \Omega_y \right)$$

$$M_y = I_x \left(\ddot{\theta} + \dot{\omega}_{Ey_2} \right) + \Omega_{z2} \left(I_x \Omega_x \right) - \Omega_{x2} \left(I_z \Omega_z \right)$$

$$M_z = I_z \left(-\ddot{\phi} \sin \theta - \dot{\phi} \dot{\theta} \cos \theta + \ddot{\psi} + \dot{\omega}_{Ez_2} \right) + \Omega_{x2} \left(I_x \Omega_y \right)$$

$$- \Omega_{y2} \left(I_x \Omega_x \right) \quad (83)$$

h. Summary of Equations of Motion

For convenience, the equations of motion are restated here with all terms added and in a form similar to that used in the program.

$$\frac{d^2x}{dt^2} = \frac{Fx}{m} - 2\dot{A} - \omega_{EyH} C + \omega_{EzH} B - Gx$$

$$\frac{d^2y}{dt^2} = \frac{Fy}{m} - 2\dot{B} - \omega_{EzH} A + \omega_{ExH} C - Gy$$

$$\frac{d^2z}{dt^2} = \frac{Fz}{m} - 2\dot{C} - \omega_{ExH} B + \omega_{EyH} A - Gz$$

$$\frac{d^2\theta}{dt^2} = \frac{My}{Ix} - \Omega_{z2} \Omega_x + \frac{\Omega_{x2} I_z \Omega_z}{Ix} - \dot{\omega}_{Ey_2}$$

$$\frac{d^2\phi}{dt^2} = \left(\frac{\dot{A}x}{Ix} + \frac{\Omega_{y2} I_z \Omega_z}{Ix} - \Omega_{z2} \Omega_y + \frac{d\dot{\phi}}{dt} \frac{d\theta}{dt} \sin \phi + \dot{\omega}_{Ex_2} \right) / \cos \phi$$

$$\frac{d^2\psi}{dt^2} = \frac{Mz}{Iz} - \frac{\Omega_{x2} I_x \Omega_y}{Iz} + \frac{\Omega_{y2} I_x \Omega_x}{Iz} + \frac{d^2\dot{\psi}}{dt^2} \sin \psi$$

$$+ \frac{d\dot{\psi}}{dt} \frac{d\theta}{dt} \cos \phi - \dot{\omega}_{Ez_2}$$

where all term are known from the initialization or from the previous time step.

Although these equations have been written for a conical shaped body with weight change due only to ablation, it only a matter of modifying the equations to include thrust and additional forces and moments associated with a finned missile.

3. INTEGRATION TECHNIQUE

To integrate a set of n simultaneous second order differential equations of the form

$$\frac{d^2x_i}{dt^2} = f_i(t, x_1, x_2, \dots, x_n), \quad i = (1, 2, \dots, n)$$

The Runge-Kutta method of numerical integration is recommended for this type of application and especially where a high degree of accuracy is desired. Thus, the equations of motion in the preceding subsection are shown as six second-order differential equations, which are to be solved simultaneously. This method consists of four sets of equations which involve different substitutions into the differential equations. The equations are solved, and the increments of the functions are calculated as weighted averages of the solutions to the four equations. Therefore, the integration procedure for the expression of the form

$$\frac{d^2x}{dt^2} = f(t, x, x')$$

is described by the following generalized equations

$$x_{n+1} = x_n + x'_n$$

$$x'_{n+1} = x'_n + \frac{\Delta t}{6} (k_0 + 2k_1 + 2k_3 + k_4)$$

where

$$k_0 = \Delta t f(t_n, x_n, x'_n)$$

$$k_1 = \Delta t f\left(t_n + \frac{\Delta t}{2}, x_n + \frac{\Delta t}{2} x'_n, x'_n + \frac{k_0}{2}\right)$$

$$k_2 = \Delta t f \left(t_n + \frac{\Delta t}{2}, x_n + \left(x'_n + \frac{\Delta t}{2} k_1 \right) \frac{\Delta t}{2}, x'_n + \frac{k_1}{2} \right)$$

$$k_3 = \Delta t f \left(t_n + \Delta t, x_n + x'_n \Delta t + \frac{\Delta t}{2} k_1, x'_n + k_2 \right)$$

In integrating a differential equation numerically, the equation is replaced by a difference equation and solved accordingly. The Runge-Kutta method has excellent properties for stability in the integration and if the integration step is taken small enough, the difference equation is usually close to the differential equation solution. However, some variables in the equations of motion may have peculiar oscillations or increase very rapidly which could cause an unstable condition or an error in the solution. An unstable condition or solution can often be made stable by using a smaller integration step. The reason for this is that different step sizes change the parameters relating to the stability of the difference solution.

The integration step size, Δt , for this program is fixed, although the user could modify the integration method to use a variable step size under error control (Ref. 14). The user has the option to break into the program at exact specified values of the independent variable, t , for the printout step.

4. AERODYNAMIC HEATING AND ABLATION

The equations of heat transfer are general in that they apply to most axially symmetric vehicles of any composite skin structure. The vehicle skin is assumed to be made of discrete layers of material whose properties may vary from layer to layer and there is no limit on the number of layers. This program is specific in that the equations have been applied to a blunt-nosed, conical vehicle.

Hypersonic vehicles may be categorized into two general types. The first consists of those vehicles which must be propelled through the atmosphere to sustain flight. The second type comprises those that have a vast store of kinetic and potential energy which will be dissipated to the surrounding air during reentry. The latter type is of primary interest and for which this program was written, although it will handle either type.

In either case, some of this energy is expended against drag forces which assume the form of skin friction and pressure drag which produce heat. The heat equivalent of the kinetic energy contained within a body is approximately

$$v_{en}^2 \approx 50,000 \text{ (Btu/lb)}$$

where v_{en} is the reentry velocity in ft/sec. While only a fraction of this energy is actually transferred to the body as heat, this fraction is still a significant quantity and accurately illustrates the magnitude of the problem.

a. Heat Flux Equation

Experiments in high speed flow have verified that the magnitude and direction of heat flow at the surface does not depend on the difference between the wall temperature and the free-stream temperature as in low-speed flow, but rather on the difference between the wall temperature, T_w , and the adiabatic wall temperature, T_{aw} . It is apparent that the determination of the adiabatic wall temperature will be of prime importance in the calculation of heat transfer, since the transference of heat to or from the wall will depend upon whether the skin temperature is above or below T_{aw} . The adiabatic wall temperature can conveniently be expressed in terms of a dynamic-temperature rise

$$T_{aw} = T_{b/l} + RF \left(\frac{v_E^2}{2g_c C_{p2} J} \right) \quad (84)$$

where

$T_{b/l}$ = boundary layer (B/L) edge temperature, °R

v_E = B/L edge velocity, ft/sec

g_c = gravitational constant, ft/sec²

J = Joule's constant = 778

C_{p2} = specific heat of air, Btu/lb-°R

RF = recovery factor which is a measure of the fraction of the free-stream dynamic temperature rise recovered at the wall

Reference 15 shows that for practical purposes

$$RF \approx \sqrt{PR} \quad (85a)$$

for laminar flow and

$$RF \approx \sqrt[3]{PR} \quad (85b)$$

for turbulent flow where

PR* = Prandtl number

$$PR = \frac{C_p}{\rho a} \frac{\mu^*}{K^*}$$

μ^* = viscosity of air in lb/ft-sec evaluated at reference temperature (T_{REF})

K^* = thermal conductivity of air in Btu/ft-sec-°R evaluated at T_{REF}

Therefore, the unit surface convective heat rate for high-speed flow (Ref. 16) is

$$\dot{q}_c/A = \overline{h}_e (T_{AW} - T_w) \quad (86)$$

where

$$\dot{q}_c/A = \text{heating rate in Btu/sec-ft}^2$$

$$\overline{h}_e = \text{convective heat transfer coefficient in Btu/ft}^2\text{-sec-}^{\circ}\text{R}$$

$$A = \text{local wetted area in ft}^2$$

(1) Heat Transfer Coefficient

For determining the heat transfer coefficient in laminar flow over a flat plate, an empirical method using Blasius theory was developed by Rubesin and Johnson (Ref. 17) to account for the combined effects of the local Mach number and the temperature ratio of the wall, T_w , to the boundary layer edge, TEMPE. In this method, the conventional analysis of heat transfer by convection can be used, but the reference temperature, T_{REF} , for evaluating the fluid properties is expressed as a function of the local Mach number and of the ratio T_w/TEMPE . The method has been extended to cover turbulent flow, and has proved to be both convenient and useful.

Therefore, for laminar flow the reference temperature is

$$T_{REF} = \text{TEMPE} \left[1 + 0.58 \left(\frac{T_w}{\text{TEMPE}} - 1 \right) + 0.032 \text{ MACHE}^2 \right] \quad (87)$$

and for turbulent flow

$$T_{REF} = \text{TEMPE} \left[1 + 0.45 \left(\frac{T_w}{\text{TEMPE}} - 1 \right) + 0.035 \text{ MACHE}^2 \right] \quad (88)$$

Equations (87) and (88) can be expressed in the form for laminar flow as

$$T_{REF} = TEMPE + 0.58 (T_W - TEMPE) + 0.19 (T_{AW} - TEMPE) \quad (89)$$

and for turbulent flow as

$$T_{REF} = TEMPE + 0.45 (T_W - TEMPE) + 0.21 (T_{AW} - TEMPE) \quad (90)$$

The heat transfer coefficient (Refs. 16, 18) is related to the flow properties through the expression

$$Nu^* (PR^*)^{1/3} = C (R_e)^a \quad (91)$$

where

$$Nu_u^* = \text{Nusselt number} = h_e x / K^*$$

h_e = effective heat transfer coefficient

X = distance from nose, ft

K^* = thermal conductivity of air, Btu/ft-sec-°R, evaluated at T_{REF}

R_e = B/L edge Reynolds number = $\rho_e V_e X / \mu_e$

ρ_e = boundary layer edge density, lb-sec²/ft⁴

V_e = boundary layer edge velocity, ft/sec

C = 0.575 for laminar flow on cone

C = 0.0296 for turbulent flow on cone

C = 0.778 for laminar flow on blunt body

C = 0.0348 for turbulent flow on blunt body

a = 0.8 for turbulent flow

a = 0.5 for laminar flow

μ_e = B/L edge viscosity, lb-sec/ft²

The solutions to these equations for the heat transfer coefficient is obtained by the use of the Blasius incompressible flat plate skin friction coefficients modified for compressible flow by use of Eckert's reference enthalpy. For

laminar flow

$$\frac{C_{fc}}{C_f} = \sqrt{\frac{\rho^* u^*}{\rho_e u_e}} \quad (92a)$$

and for turbulent flow

$$\frac{C_{fc}}{C_f} = \left(\frac{u^*}{u_e} \right)^{0.2} \left(\frac{\rho^*}{\rho_e} \right)^{0.8} \quad (92b)$$

Good correlation with experimental data is obtained if the gas properties are evaluated at the reference temperature and the velocity is taken as the boundary layer edge velocity. For the case of mass addition, the properties of the injected gas are used to compute the Prandtl number and Nusselt number.

It is important in the selection of a suitable material for thermal protection by the ablative process that the products of decomposition have a high specific heat. This in turn produces a high effective mean specific heat of the gas-air mixture in the boundary layer and a high Prandtl number. It is also desirable that the ablator have a low thermal conductivity. This will decrease heat conducted to the interior of the vehicle. The surface of the vehicle also receives heat by radiation from the hot gas in the shock layer in addition to that by convection. As the air density is low, its emissivity is much less than 1 percent. Therefore, the rate of radiation heat transfer is negligible compared with that of aerodynamic convection and can be ignored.

b. Unsteady Heat Conduction

A means of applying the Schmidt graphical method for solving an unsteady heat conduction problem is presented here. A thorough discussion of this method can be found in any general text (Refs. 16, 19) and will not be attempted here. This method is quite flexible in that difficult boundary conditions can be handled easily.

This method is widely used for solving unsteady heat conduction problems because it gives an iterative profile of the temperature change. Because of its simplicity, mistakes, if they occur, are easily found, and relatively untrained personnel can accomplish the work. Numerical methods are especially convenient when a high-speed digital computer is available since the steps in a numerical solution can be programmed relatively easily.

The numerical method for solving unsteady-state heat conduction differs from that used to solve steady state. In the latter case, the temperature distribution in a body can be obtained for a network of points in a solid by solving a system of residual equations. In unsteady-state systems, the initial temperature profile is known, but its variation with time must be determined. Therefore, it is necessary to resolve the temperature profile at some future time from a given distribution at an earlier time.

To illustrate the numerical method, it is necessary to transform the Fourier conduction equation (a partial differential equation that is second order in space and first order in time) for the unsteady temperature distribution in a heat-conducting solid into a finite difference form.

$$\frac{\Delta_t T}{\Delta t} = \frac{\alpha \Delta_x^2 T}{(\Delta x)^2} \quad (93)$$

The subscripts denote the differentiation variable. Letting n denote position and t time, $\Delta_t T$ can be written as

$$\Delta_t T = T_{n,t+1} - T_{n,t}$$

and in a similar manner

$$\Delta_x T = T_{n,t+1} - T_{n,t}$$

The expression $\Delta_x^2 T$ thus becomes

$$\Delta_x^2 T = T_{n+1,t} - 2T_{n,t} + T_{n-1,t}$$

Substituting these expressions into the Fourier equation (93), gives

$$T_{n,t+1} - T_{n,t} = \frac{\alpha \Delta_t}{(\Delta x)^2} (T_{n+1,t} - 2T_{n,t} + T_{n-1,t}) \quad (94)$$

The temperature throughout a wall or slab can now be computed for any later time if the initial distribution is known. A Schmidt plot demonstrates the temperature profile versus time in a semi-infinite slab (figure 13).

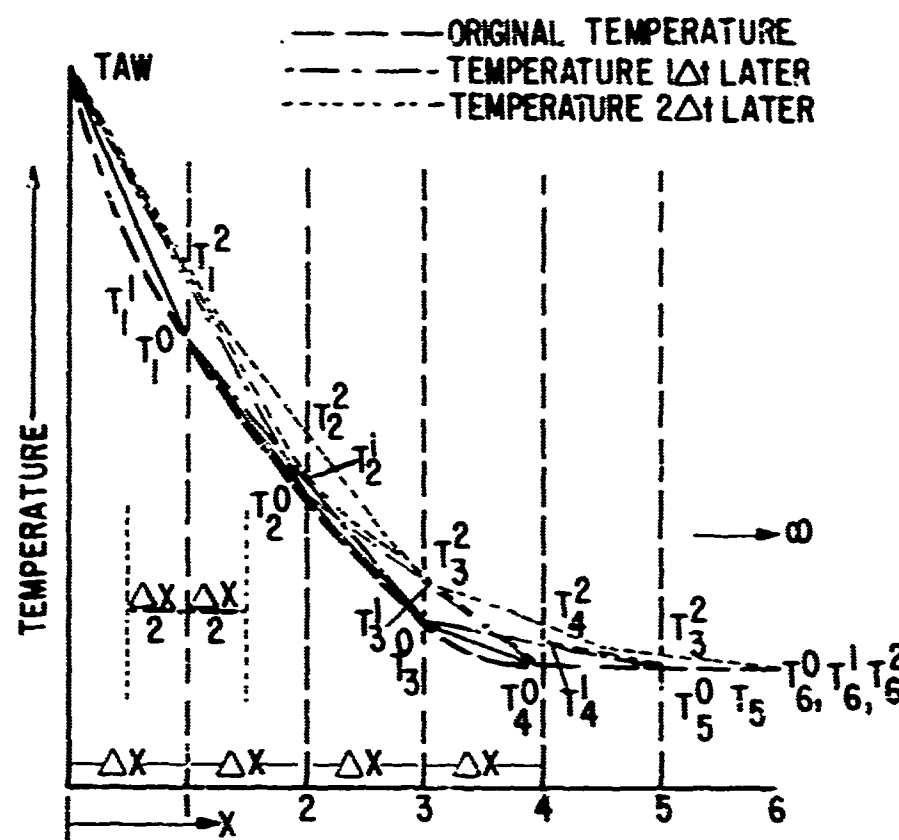


Figure 13. Schmidt Plot in an Infinitely Thick Wall

A constant wall temperature is assumed in the graphical example, but a varying wall temperature can be handled with equal ease. By letting the wall temperature vary with time, the distribution at each point within the body can be computed for each time increment.

c. Vehicle Thermal Model

To determine the time-temperature profile in the vehicle skin, the Fourier conduction equation was written as a finite difference equation and solved numerically. This method is a further adaptation of the Schmidt graphical method (Ref. 19). The wall is divided into a number of lamina with known thickness, specific heat, and thermal conductivity and with a known initial temperature distribution. Figure 14 illustrates the model with its associated nomenclature.

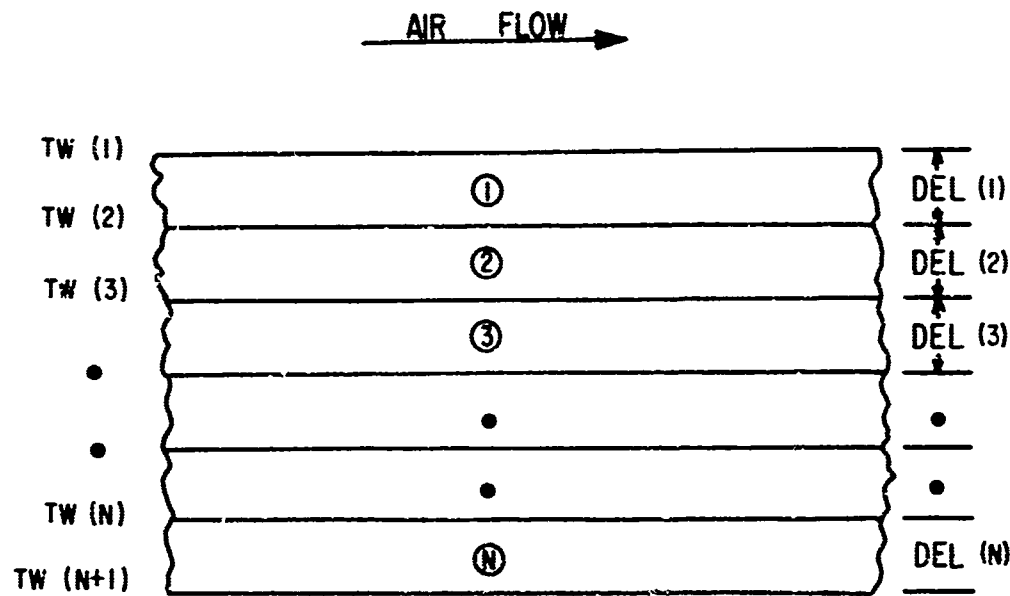


Figure 14. Model for Wall Temperature Profile and Ablation Recession Calculations

The difference equation for computing the temperature at position n at time $t + 1$ is

$$T_{n,t+1} = T_{n,t} + \frac{\alpha \Delta t}{(\Delta x)^2} (T_{n+1,t} - 2T_{n,t} + T_{n-1,t}) \quad (95)$$

In this form, the material properties cannot vary from layer to layer. If the properties vary from lamina to lamina, the above equation must be written in the form

$$T_{n,t+1} = T_{n,t} + \Delta t \left[\frac{\alpha_{n-1}}{(\Delta x_{n-1})^2} (T_{n-1,t} - T_{n,t}) - \frac{\alpha_n}{(\Delta x_n)^2} (T_{n,t} - T_{n+1,t}) \right] \quad (96)$$

Where α is the thermal diffusivity and may be replaced by its defined equivalent,

$$\alpha = \frac{K}{\rho c_p} \quad (97)$$

where

K = thermal conductivity of material in Btu/ft-sec-°R

ρ = density of material in lbs/ft³

c_p = specific heat of material in Btu/lb-°R

This step allows one to easily recognize certain groups of terms as the heat conducted through each lamina and permits the convective heat flux to be used in solving for the wall temperature. The equation for the wall temperature is

$$T_{n-1,t+1} = T_{n-1,t} + \frac{2\Delta t}{(\rho c_p \Delta X)_{n-1}} \left[h_e (T_{AW} - T_{n-1,t}) \right] - \frac{2\Delta t K_{n-1}}{(\rho c_p \Delta X^2)_{n-1}} (T_{n-1,t} - T_{n,t}) \quad (98)$$

The backface boundary condition can be specified in several ways. If internal heating (or cooling) is present, the backface may be held constant or allowed to vary in a specified manner. A conservative assumption is that no heat flows through the last lamina. This assumption will cause somewhat more ablation and higher temperatures than would be encountered with a cooled backface or other heat sink material.

d. Ablation

Advances in hypersonic atmospheric flight have resulted in environments of extremely high temperatures. Boundary layer temperatures in excess of 10,000°F are characteristic of vehicles entering the atmosphere at hypersonic speeds.

In hypersonic flight, it becomes obvious that capacitance or mass heat-sink protection, though simple, is an inefficient means of contending with the extremely high heat fluxes associated with certain reentries or with sustained

periods of thermal flight. Consequently, other means of cooling or protecting for operating beyond heat-sink limitations must be used. One convenient means of environmental protection and for which this program was primarily written is the ablation cooling method.

The ablative process is illustrated in figure 15. The ablation process works in the following manner: (1) the material or ablator acts as a heat sink; (2) when the critical or melting temperature of the ablator is reached, a thin layer of the material at the surface will begin successively to melt, vaporize, depolymerize, or decompose chemically; and (3) as the material vaporizes, the gaseous products of decomposition enter into the boundary layer. Being relatively cool, as compared to the boundary layer air, the injected gas forms a thin, but effective film that reduces the heat transfer to the vehicle skin. It is important in the selection of a suitable material for thermal protection by the ablative process that the thermal conductivity of the material should be as low as possible so as to confine the high-temperature zone at the surface to the thinnest layer possible. Likewise, to reduce the rate of mass loss, and hence, the required weight of protective ablator, the surface temperature at which decomposition and melting begins should be as high as practicable. The products of decomposition should preferably have a high Prandtl number, since it is defined as ratio of heat storage to heat conduction of a gas. This means it is desirable to have the mean effective specific heat of the gas-air mixture in the boundary layer as large as possible.

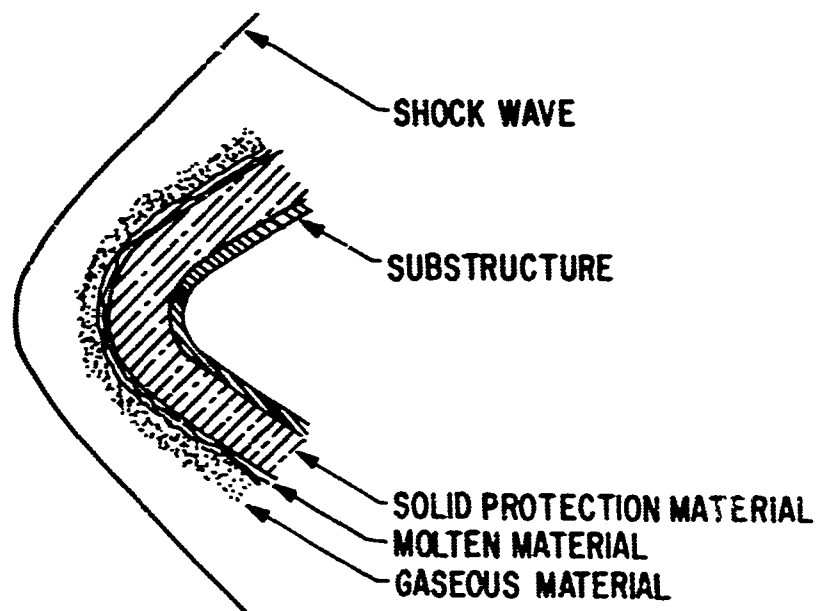


Figure 15. Ablative Process

Since the ablation process can be characterized by an exchange of material for thermal energy, the energy balance at the ablating surface, in its simplest form, is

$$\dot{q}_{\text{net}} = \dot{q}_c - \dot{q}_{\text{cond}} - \dot{q}_{\text{rad}} - \dot{q}_{\text{block}} \quad (99)$$

where \dot{q}_c is heat transferred to the surface by convection, \dot{q}_{cond} is the heat conducted from the surface to the substrate material, \dot{q}_{block} is the heat blockage by transpiration in the boundary layer, and \dot{q}_{rad} is negligible and has been ignored.

Ablation is assumed to occur when the temperature of the outermost lamina has reached the melting temperature of the material. The outer surface will recede and is assumed to take place normal to the local surface.

(1) Mass Loss and Surface Recession

Two mechanisms are involved in the loss of ablation material: (1) mass loss due to oxidation, and (2) mass loss due to sublimation. Oxidation is controlled by the diffusion of oxygen to the reacting carbon, and sublimation is controlled by local pressure and temperature. A detailed discussion on the theory of ablation and material decomposition and reaction is not the intent of this report, so only the results will be presented.

The efficiency of an ablation material is frequently defined for engineering use in terms of a quantity known as the effective heat of ablation, Q^* , in Btu/lb,

$$Q^* = \frac{\dot{q}_0}{\dot{m}} \quad (100)$$

where \dot{q}_0 is the surface heating rate of a nonablating calorimeter at the ablative temperature, and \dot{m} is the mass ablation rate. The term "effective heat of ablation" collectively expresses the ability of a material to absorb, block, and dissipate incident heat per unit mass expended. The effective heat of ablation value may also be expressed by using equations (99) and (100) as

$$Q^* = \frac{\dot{q}_{\text{cond}} + \dot{q}_{\text{block}}}{\left(1 - \frac{\dot{q}_{\text{rad}}}{\dot{q}_0}\right)} \quad (101)$$

or by substituting approximate equations for each gives

$$Q^* = \frac{C_p(T_w - T_b) + 0.7 \left(\frac{M_{air}}{M_v} \right)^{1/4} \dot{m}_v (\Delta h)_o}{\left(1 - \dot{q}_{rad}/\dot{q}_o \right)} \quad (102)$$

where

C_p = heat capacity of material

T_w = ablative surface temperature

T_b = temperature of unheated material

M_{air} = molecular weight of air

M_v = molecular weight of injected gas

\dot{m}_v = rate of mass injection

$(\Delta h)_o$ = enthalpy difference across boundary layer without transpiration

If the radiation, \dot{q}_{rad} , is insignificant, equation (102) can be reduced to the form

$$Q^* = A + B (\Delta h)_o \quad (103)$$

where A is an empirical value obtained from experimental investigations of different ablators and B is dependent on whether flow is laminar or turbulent.

The surface recession rate is obtained by

$$\dot{s} = \frac{\dot{q}_c}{Q^* \rho} \quad (104)$$

where

\dot{s} = recession rate, ft/sec

ρ = ablation material density, lb/ft³

The enthalpy difference across the boundary can be calculated from the following equations:

$$(\Delta h)_o = h_r - C_p T_w \quad (105)$$

where

$$h_r = C_p a \cdot \text{TEMPE} + R_F \cdot V_F^2 / (2g_c J)$$

The following are analytical expressions used in this program for determining mass loss and recession rates of three common ablators.

(a) Phenolic Refrasil (Silica)

The expression for obtaining the effective heat of ablation for Phenolic Refrasil is

$$Q^* = 4710 + B (\Delta h)_o \quad (106)$$

where

B = 0.58 for laminar flow

B = 0.32 for turbulent flow

(b) ATJ Graphite

The effective heat of ablation for ATJ graphite is

$$Q^* = 2000 + B (\Delta h)_o \quad (107)$$

where

B = 2 for either turbulent or laminar flow

(c) Carbon Phenolic

The expressions for carbon phenolic are more complicated than those used for the other materials due to reaction of carbon with atmospheric oxygen. This material has a very high melting temperature and a low thermal conductivity which gives it excellent insulation properties. Also, its products of decomposition have a high specific heat compared to that of air.

For laminar flow, the diffusion mass loss rate is given by
(Refs. 20, 21)

$$\dot{M}_d = \frac{q_c}{K1_L + K2_L (h_r - C_p_{BL} T_w)} \quad (108)$$

and for turbulent flow, the expression is

$$\dot{m}_d = \frac{\dot{q}_c}{K1_T + K2_T (h_r - Cp_{BL} T_w)} \quad (109)$$

where the constants $K1$ and $K2$ can be interpreted as the intercept and slope, respectively, on an effective heat of ablation versus enthalpy difference (between recovery and wall conditions) plot.

\dot{q}_c = convective heat flux, Btu/ft²-sec

h_r = recovered enthalpy, Btu/lb

Cp_{BL} = specific heat in boundary layer, Btu/lb-°R

T_w = wall temperature, °R

$K1_L$ = 5370

$K2_L$ = 5.37

$K1_T$ = 4240

$K2_T$ = 5.77

The total mass loss rate is given by

$$\dot{M}_T = \dot{M}_d \left[1 + 2.64 \times 10^4 (PBL)^{-0.67} \exp \left(\frac{-11.05 \times 10^4}{T_w} \right) \right] \quad (110)$$

where

\dot{M}_T = total mass loss rate, lb/ft²-sec

PBL = boundary layer edge pressure, lb/ft² (Ref. 20)

The surface recession rate is calculated by

$$\dot{s} = \dot{M}_T / \rho \quad (111)$$

where

\dot{s} = recession rate, ft/sec

ρ = ablation material density, lb/ft³

(2) Total Weight Loss Rate and Total Weight Loss

After the local instantaneous and total local recession rates have been computed, the local weight loss rate can be calculated, if needed, by determining the volume reduction of the local segment and multiplying by the material density. But the primary weight loss of interest is the total for the vehicle. To compute the total vehicle mass loss and mass loss rate, the following procedure is used. Using the local weight loss rate, the instantaneous and total recessions, and the initial radii and slant length of the particular segment of interest (see figure 16), the mass loss rate per unit area is multiplied by the appropriate surface area to give a local integrated mass loss rate. This is accomplished by the following equations:

$$\dot{W}_{(LEN)} = \pi \left(RL_{(LEN)} + RS_{(LEN)} - 2\dot{c}_{(LEN)} \right) \dot{s}_{c} \text{ SOL}_{(LEN)} \quad (112)$$

where

$\dot{W}_{(LEN)}$ = instantaneous mass loss rate of segment (LEN), lb/sec

(LEN) = number of particular segment of cone

RL = larger segment radius, ft

RS = smaller segment radius, ft

$\dot{c}_{(LEN)}$ = total recession of segment, ft

\dot{s} = instantaneous recession of segment, ft/sec

ρ_c = surface material density, lb/ft³

SOL_(LEN) = slant height of conical segment, ft

$$\dot{W} = \dot{W} + \dot{W}_{(LEN)} \quad (113)$$

will give total vehicle mass loss rate when the operations in equation (113) are accomplished in a program "Do Loop." Summing these local rates will result in the total vehicle weight loss.

e. Stagnation Heating

To evaluate stagnation point convective heat transfer rates, this program employs Lee's theory (Ref. 22), modified by use of Eckert's reference enthalpy techniques (Ref. 19), in Lee's equation

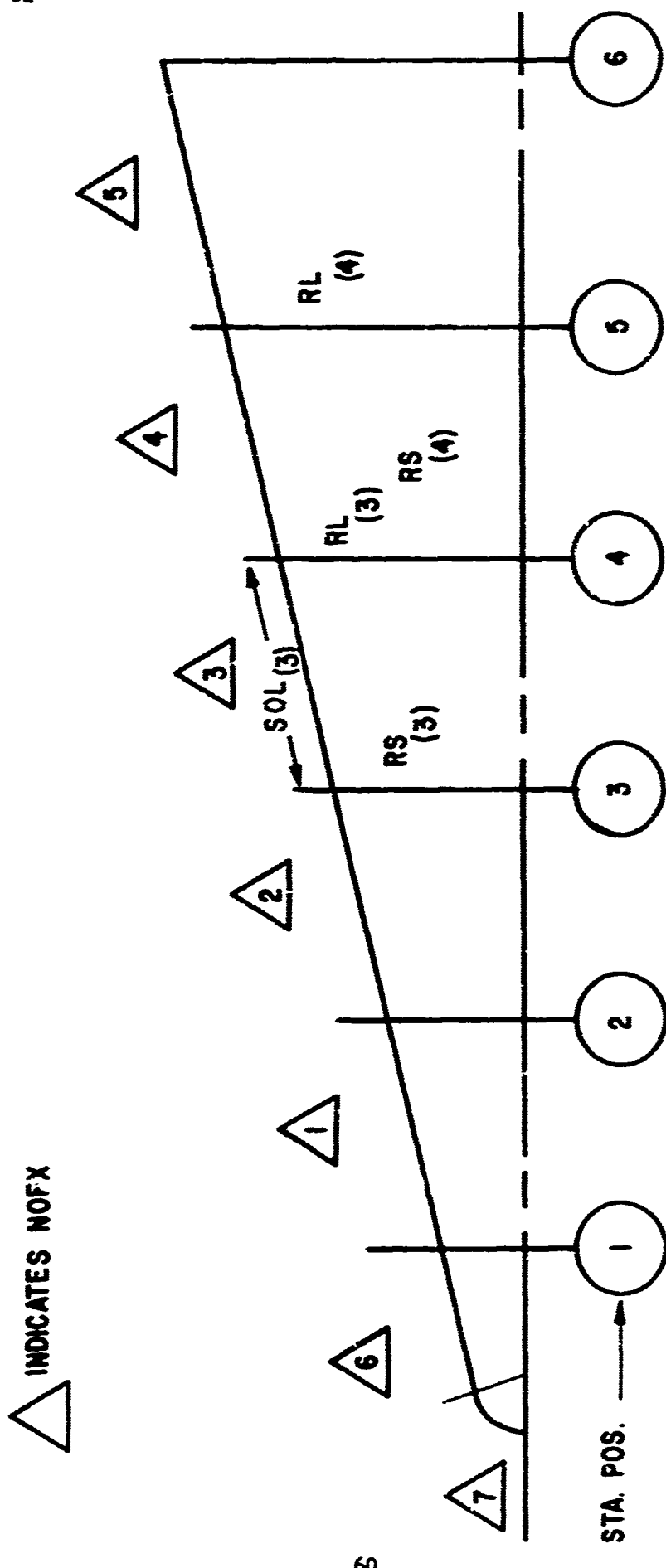


Figure 16. Vehicle Nomenclature

$$q_{c_{\text{STAG}}} = \frac{0.778}{(\text{PR})^{2/3}} \sqrt{\rho_{\text{IS}} \nu_{\text{IS}}} \sqrt{dV/dx} h_{\text{se}} \cdot G(M_{\infty}, \bar{\gamma}, \gamma_{\infty}) \quad (114)$$

where

$$G(M_{\infty}, \bar{\gamma}, \gamma_{\infty}) = \left(\frac{\bar{\gamma}-1}{\bar{\gamma}} \right)^{1/2} \left(1 + \frac{2}{\bar{\gamma}-1} \frac{1}{M_{\infty}^2} \right)^{1/2} \left(1 - \frac{1}{\bar{\gamma} M_{\infty}^2} \right)^{1/2}$$

$$\bar{\gamma} \approx 1.10 - 1.20 \text{ at high temperatures}$$

$$h_{\text{se}} = V_{\infty}^2 / 2GJ$$

$$\gamma_{\infty} = 1.4 \text{ ratio of specific heats for air}$$

$$\rho_{\text{IS}} = \text{density evaluated at stagnation reference conditions}$$

$$\nu_{\text{IS}} = \text{viscosity evaluated at stagnation reference conditions}$$

$$dV/dx = \text{velocity component gradient at the stagnation point (from Fay and Riddell)}$$

$$\frac{dV}{dx} = \frac{1}{SAR} \left[2(p_s - p_{\infty}) / \rho_{\text{IS}} \right]^{0.5}$$

$$p_s = \text{stagnation pressure (oblique shock)}$$

(1) Nose Blunting

In the determination of nose blunting, it is assumed that the initial nose shape of particular interest was a sphere-cone, and after ablation the final shape was a sphere-cone. Experimental evidence has shown that the final eroded shape could be approximated by a sphere-cone having a small deviation from a sphere. The reference sphere-cone configuration after erosion is obtained by placing a spherical surface tangent to a cone parallel to the original surface but displaced by the erosion on the cone and is located axially at a position on the vehicle center line in accordance with the erosion at the stagnation point (figure 17).

The experimental evidence of nose-shape change of reentry vehicles, as previously noted, can be represented by a sphere-cone which deviates from a spherical shape by an amount less than 10 percent of the final nose radius. The final eroded nose radius can be obtained in terms of the stagnation point erosion and cone erosion as shown in the following equation:

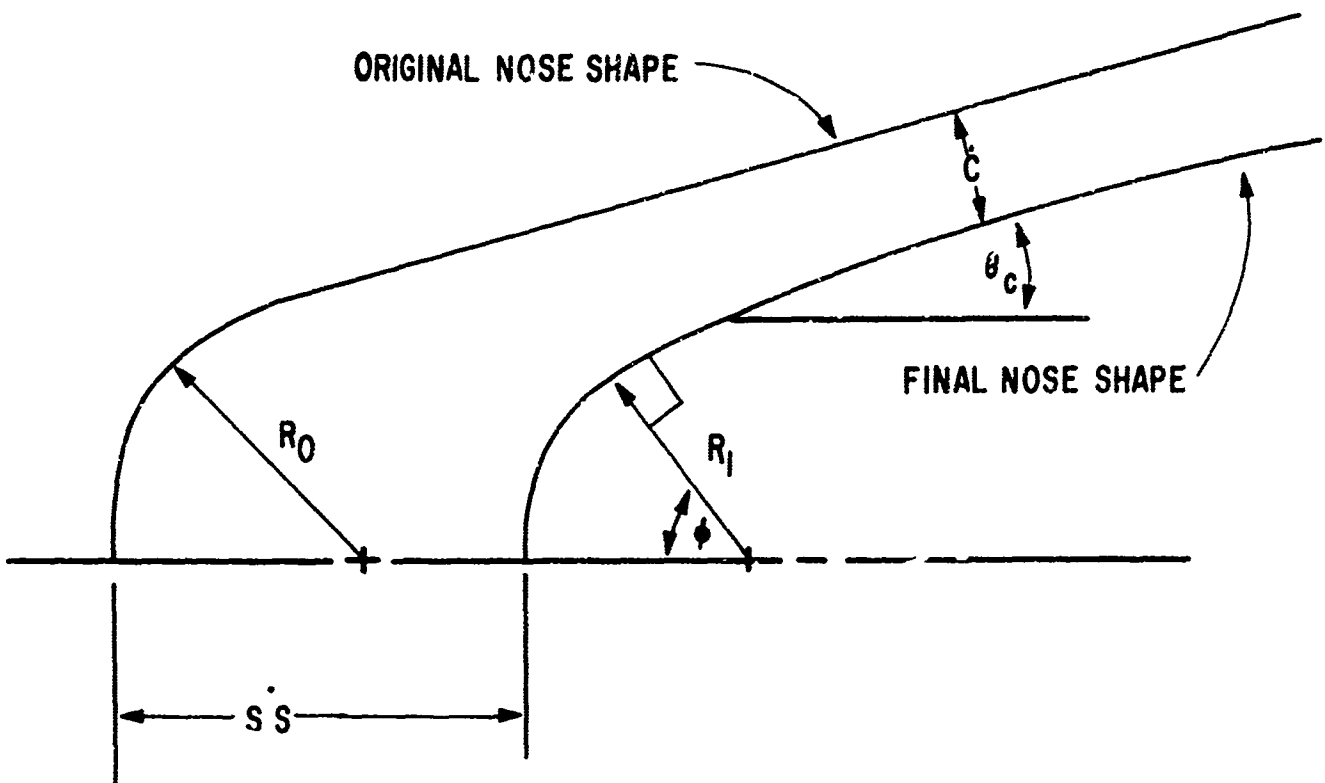


Figure 17. Vehicle Nose-Shape Change

$$R = R_0 + \frac{1}{(1 - \sin \theta_c)} \left[\sin \theta_c \int_0^t \left(\frac{\dot{q}_c}{\rho Q^*} \right)_S dt - \int_0^t \left(\frac{\dot{q}_c}{\rho Q^*} \right)_C dt \right]$$

The integral represents the erosion at a given time during the flight for the locations at the stagnation point S and a point on the cone C at a location of wetted length of about five times the nose radius.

It is now possible to evaluate the final nose radius for a given application. Let

$$\dot{S}_S = \int_0^t \left(\frac{\dot{q}_c}{\rho Q^*} \right)_S dt \quad (115)$$

and

$$\dot{c} = \int_0^t \left(\frac{\dot{q}_c}{\rho Q^*} \right) c \, dt \quad (116)$$

therefore

$$R = R_o + \frac{1}{(1 - \sin \theta_c)} \left[\sin \theta_c \dot{s}_s - \dot{c} \right] \quad (117)$$

where

R_o = original nose radius, ft

R = instantaneous nose radius, ft

θ_c = cone half-angle

\dot{s}_s = stagnation point recession rate, ft/sec

\dot{c} = recession rate at location, C, ft/sec (see figure 17)

f. Boundary Layer Transition

The problem of transition from laminar to turbulent boundary layer flow has always been a troublesome one for the aeronautical engineer. The standard approach usually has been to design conservatively, that is, for turbulent flow. In general, the transition Reynolds number has been found to primarily depend upon the local Mach number, which has been observed in the analysis of boundary layer transition on a series of flight vehicles. Transition on blunt spherical nose vehicles with low boundary layer edge Mach numbers appears to occur at Reynolds number of 1.5×10^6 , while on sharp bodies where the edge of the boundary layer edge Mach numbers approach 10 Reynolds numbers as high as 2.0×10^7 have been observed prior to transition. Thus, for untested vehicle configurations, it is necessary to investigate the relationship of the Mach number and the Reynolds number in both the high and low Mach number regions. This relationship between Mach number and Reynolds number stands to reason if their definitions are understood. The parameter Mach number describes the influence of compressibility on heat transfer and flow phenomena and is defined

as the ratio of the gas or flight velocity to the local or ambient speed of sound. The Reynolds number, which describes the nature of flow, is a dimensionless measure of the ratio of inertial to viscous forces.

It should be noted that flight data on sharp bodies indicate that, generally, transition does not occur instantaneously over the entire vehicle so that it may travel several thousand feet between the onset of transition and the establishment of a fully turbulent boundary layer. See references 23 and 24.

The approach used in this program is to apply the sharp and blunt body transition Reynolds numbers simultaneously. Therefore, the sharp body criterion is described by the expression

$$Re_{TRAN} = 6.6 \times 10^7$$

and the blunt body criterion is applied when either of the following two Reynolds numbers are reached with conditions stated

$$Re_{TRAN} = 1.5 \times 10^6 \text{ on the spherical nose}$$

$$Re_{TRAN} = 5.0 \times 10^6 \text{ on the conical portion aft of the spherical nose for a wetted length of five times the nose radius.}$$

The above criteria has been found to correlate with experimental data.

5. AERODYNAMICS

The one item that plays the most significant role in determining the performance of a high velocity or hypersonic reentry vehicle is aerodynamic drag. Experimental results have been correlated with theoretical studies of the nonsteady effects on a reentry vehicle or missile during its trajectory. These results indicate that the aerodynamic forces can be determined accurately by assuming quasi-steady flow conditions; that is, the flow field at any instant of time is the same as that associated with steady motion at the same velocity. Furthermore, it has been demonstrated that the boundary layer behaves in a quasi-steady manner. Therefore, assuming that the validity of these results carry over for an ablating blunt cone, the instantaneous drag coefficients can be obtained from equivalent steady-state conditions.

This program assumes that the drag consists of three components: cone pressure or forebody drag, base pressure drag, and skin friction or viscous drag. It is convenient to consider these quantities as distinct quantities which can be added together to obtain the total vehicle drag. Though all these quantities are distinct, some are dependent upon the boundary layer condition. For example, the condition of the boundary layer, laminar or turbulent, which influences the viscous drag can also influence the base drag.

a. Cone Pressure Drag

The forebody pressure drag for a slender body at zero angle-of-attack or at incidence can be calculated on the basis of the modified slender-body theory.

The forebody pressure drag is defined by the relation

$$D_p = - \iint_{S_m} P \cos(n, V_\infty) dS_m$$

where $\cos(n, V_\infty)$ is the cosine of the angle between V_∞ and the outward normal to the vehicle surface. The area S_m comprises the total area of the vehicle except base area.

For a sharp cone at $\alpha = 0$, the pressure P_c is constant over the entire body, and the forebody drag is then only a function of the pressure ratio P_c/P_∞ across the conical shock. Solutions for this pressure ratio as a function of Mach number and cone angle, θ_c , have been tabulated by Kopal (Ref. 25) for the ratio of specific heats of $\gamma = 1.405$. These results have been employed directly in the drag equation in order to obtain the forebody drag on a sharp cone. The analysis produced the equation

$$C_{Dp} = 4 \sin^2 \theta_c \left[\frac{2.5 + 8 M_\infty \sin \theta_c}{1 + 16 M_\infty \sin \theta_c} \right] \quad (118)$$

which is similar to the form of the Newtonian drag equation for a sharp cone. The last term represents the variation from the Newtonian theory due to Mach number effects.

Nose blunting of a cone will increase the pressure drag. Local overpressures are induced near a blunt nose by the strong nose-shock curvature. The results of sharp and blunt body solutions have been correlated as a function of M_∞ , θ_c , and R_N/R_B . However, for bluntness ratios, R_N/R_B less than 0.05, the values for the drag due to the overpressures are low compared to C_{Dp} .

This program does account for the drag due to the nose being blunt within the limits expressed above. The sharp cone drag is modified by assuming the nose drag to be that of a sphere minus that of the cone replaced by the sphere. Because both of these terms are referenced to the projected area of the sphere, the area or bluntness ratio, R_N/R_B , term is needed as a correctness factor. Therefore, the pressure coefficient for a blunt cone is (Ref. 26)

$$C_{Dp_{cone}} = C_{Dp} + \left[0.58 - C_{Dp} \right] \left(\frac{R_N}{R_B} \right)^2 \quad (119)$$

where 0.58 is drag coefficient for a sphere obtained from reference 27

C_{Dp} is from equation (118)

R_N/R_B is the bluntness ratio of nose radius to cone base radius

b. Skin-Friction Drag

The skin-friction or viscous drag is defined as

$$D_V = \iint_{S_m} \tau \cos(\theta, v_\infty) dS_m$$

where τ is the local skin friction per unit area due to viscosity, and $\cos(\theta, v_\infty)$ is the cosine of the angle between v_∞ and the tangent to the vehicle surface in the τ direction as shown in figure 18.

The skin-friction drag coefficient can be defined as

$$C_{Df} = \frac{2\pi}{A_B} \int_0^L C_{f_\infty} \cos \theta r dx \quad (120)$$

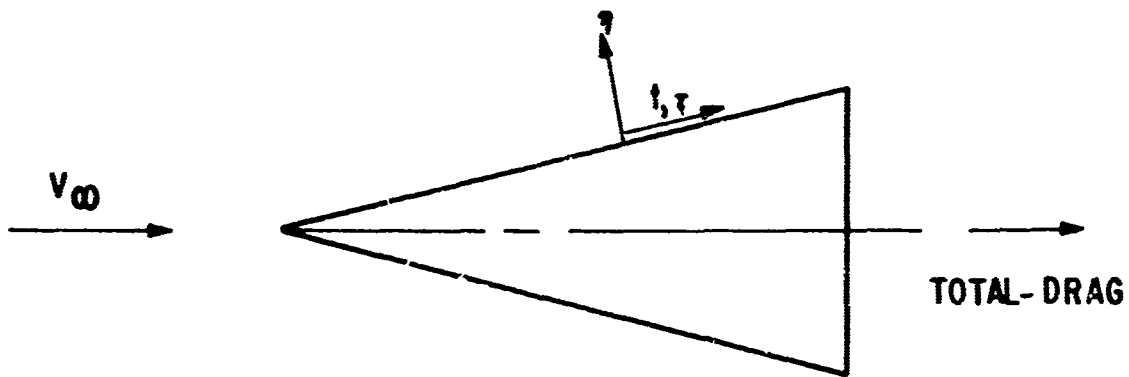


Figure 18. Aerodynamic Body Subject to Normal and Tangential Forces

where C_{f_∞} is the local skin-friction coefficient defined as

$$C_{f_\infty} = \frac{\tau}{1/2 \rho V_\infty^2} \quad (121)$$

(1) Local Skin-Friction Coefficient

(a) Laminar Flow, $\alpha = 0$

The local skin-friction coefficient is calculated using the Blasius flat plate in compressible solution. The flat plate solution was modified for conical flow by the Mangler transformation (Ref. 28) and for compressibility by Eckert's reference enthalpy method (Ref. 29).

The modified Blasius equation is

$$C_f = \frac{0.664}{\sqrt{Re_x}} \sqrt{3} \sqrt{\frac{c^* u^*}{\rho_e u_e} \left(\frac{\rho_e V_e^2}{\rho_\infty V_\infty^2} \right)} \quad (122)$$

where

$$Re_x = \frac{\rho_e V_e x}{\mu_e} \quad \text{boundary layer edge Reynolds number}$$

x = distance along sharp cone surface

ρ_e = density of air μ_e = viscosity of air v_e = velocity

The superscript * and subscripts e and ∞ signify the property is evaluated at the reference enthalpy or conditions at the edge of boundary layer or free stream, respectively.

Equation (121) can be simplified to

$$C_{f\infty} = \frac{1.15}{\sqrt{x}} \frac{v_e^{1.5} \left(\frac{\rho^* \mu^*}{\rho_\infty \mu_\infty}\right)^{0.5}}{\rho_\infty v_\infty^2} \quad (123)$$

Letting

$$\frac{R_\infty}{x} = \frac{\rho_\infty v_\infty x}{\mu_\infty}$$

and rearranging equation (123),

$$C_{f\infty} = \frac{1.15}{\sqrt{\frac{R_\infty}{x}}} \left(\frac{v_e}{v}\right)^{1.5} \sqrt{\frac{\rho^* \mu^*}{\rho_\infty \mu_\infty}} \quad (124)$$

From references 30 and 31, the quantity

$$\sqrt{\frac{\rho^* \mu^*}{\rho_\infty \mu_\infty}}$$

can be replaced by

$$\sqrt{\frac{\rho^* \mu^*}{\rho_\infty \mu_\infty}} = \left(\frac{p_c}{p_\infty}\right)^{0.5} \left(\frac{h^*}{h_\infty}\right)^{-0.185}$$

where

$$\frac{h^*}{h_\infty} = \frac{h^*}{h_e} \frac{T_e}{T_\infty}$$

It is assumed that cone pressure p_c is equal to boundary layer edge pressure, p_e , the free-stream specific heat is equal to the boundary layer edge specific heat, the specific heat ratio is $\gamma = 1.405$, and the recovery factor, R_F , is equal to 0.8426. Therefore, equation (123) for the local skin-friction coefficient can be written as

$$c_{f_\infty} = \frac{1.15}{\sqrt{R_\infty x}} \left(\frac{v_e}{v_\infty} \right)^{1.5} \left(\frac{p_e}{p_\infty} \right)^{0.5} \left(\frac{T_e}{T_\infty} \right)^{-0.185} \left(\frac{h^*}{h_e} \right)^{-0.185} \quad (125)$$

where

$$\frac{h^*}{h_e} = 0.5 + 0.5 \left(\frac{T_e}{T_\infty} \right)^{-1} + 0.0374 M_e^2 \quad (126)$$

The ratios,

$$\left(\frac{v_e}{v_\infty} \right)$$

$$\left(\frac{p_e}{p_\infty} \right)$$

$$\left(\frac{T_e}{T_\infty} \right)$$

are obtained from conical flow results given by Bertram (Refs. 31 and 32) which have been correlated as a function of the hypersonic similarity parameter, $M_\infty \sin \theta_c = K_c$. A curve-fit of these results produced the following relations:

$$\frac{v_e}{v_\infty} = \left[1 - \frac{1.4}{M_\infty^2} \left(K_c \right)^{1.9} \right]^{0.5} \quad (127)$$

$$\frac{p_e}{p_\infty} = 1 + 2.8 K_c^2 \left[\frac{2.5 + 8 K_c}{1 + 16 K_c} \right] \quad (128)$$

$$\frac{T_e}{T_\infty} = 1 + 0.0966 K_c + 0.2267 (K_c)^2 \quad (129)$$

The local Mach number can be computed from

$$\frac{M_e}{M_\infty} = \frac{V_e}{V_\infty} \cdot \frac{\sqrt{\gamma_e R_e T_\infty}}{V_\infty}$$

From previous assumptions and reducing

$$\frac{M_e}{M_\infty} = \frac{V_e}{V_\infty} \left(\frac{T_e}{T_\infty} \right)^{-0.5} \quad (130)$$

The local laminar skin-friction is now defined in terms of free-stream conditions, wall temperature, and cone angle.

(b) Turbulent Flow, $\alpha = 0$

Using the Blasius flat plate incompressible solution modified in a similar manner for conical flow and compressibility, the Blasius equation for the local skin friction coefficient in turbulent flow is

$$C_{f_\infty} = \frac{0.0698}{R_{ex}^{0.2}} \left(\frac{p_e}{p_\infty} \right)^{0.5} \left(\frac{u^*}{u_e} \right)^{0.2} \frac{\rho_e V_e^2}{\rho_\infty V_\infty^2} \quad (131)$$

By substituting in a manner similar to laminar flow, and using the same ratios and rearranging, the following expression for the turbulent skin-friction coefficient in terms of free-stream conditions, wall temperature, and cone angle is given by

$$C_{f_\infty} = \frac{0.0698}{(R_{ex})^{0.2}} \left(\frac{V_e}{V_\infty} \right)^{1.8} \left(\frac{p_e}{p_\infty} \right)^{0.6} \left(\frac{h^*}{h_e} \right)^{-0.55} \left(\frac{T_e}{T_\infty} \right)^{-0.58} \quad (132)$$

where

$$\left(\frac{h^*}{h_e} \right) = 0.5 + 0.5 \left(\frac{T_w}{T_\infty} \right) \left(\frac{T_e}{T_\infty} \right)^{-1} + 0.0388 M_e$$

for $R_F = 0.877$.

(2) Average Skin-Friction Coefficient

To obtain the average skin-friction coefficient for both laminar and turbulent flow, the local value must be integrated over the cone surface. Therefore, substituting πR_B^2 for A_B in equation (120) and rearranging

$$C_{Df} = \frac{2\pi}{\pi R_B^2} \int_0^L C_{f_\infty} \cos \theta(r) dx \quad (133)$$

but

$$C_{f_\infty} = \left(C_{f_\infty} \right)_{x=L} \left(\frac{L}{x} \right)^{0.5}$$

and

$$\frac{R_B^2}{B} = L^2 \sin^2 \theta_c$$

$$r = x \sin \theta_c$$

Substituting these relations into equation (133), then

$$C_{Df} = \frac{2}{L^2 \sin^2 \theta_c} \left(C_{f_\infty} \right)_{x=L} (L)^{0.5} \cos \theta_c \sin \theta_c \int_0^L (x)^{0.5} dx \quad (134)$$

Now, combining equation (134) with equations (125) and (133), the average skin-friction coefficients for laminar and turbulent flow are, respectively,

$$C_{Df_L} = \frac{1.533}{\sqrt{\frac{R_B}{L}}} \left(\frac{V_e}{V_\infty} \right)^{1.5} \left(\frac{P_e}{P_\infty} \right)^{0.5} \left(\frac{T_\infty}{T_e} \right)^{0.185} \left(\frac{h_e}{h^*} \right)^{0.185} \left(\cot \theta_c \right)$$

and

$$C_{Df_T} = \frac{0.0776}{\left(\frac{R_B}{L} \right)^{0.2}} \left(\frac{V_e}{V_\infty} \right)^{1.5} \left(\frac{P_e}{P_\infty} \right)^{0.5} \left(\frac{T_\infty}{T_e} \right)^{0.185} \left(\frac{h_e}{h^*} \right)^{0.185} \left(\cot \theta_c \right) \quad (135)$$

The wall temperature used in the enthalpy ratio equation is taken as an average temperature over the entire vehicle surface.

c. Base Drag

The base pressure drag is determined by the mechanics of the wake, for which there is as yet no complete theory. Values of the base pressure coefficient C_{PB} must be obtained experimentally. Because of this, analytical methods of treating base drag are usually replaced by a correlation of experimental results. As the vehicle velocity increases, the base pressure, and therefore, the base-drag coefficient are affected similarly to other pressures. Once the speed is well into the supersonic region, most base pressures for a cone approach about 70 percent of a vacuum. Hoerner (Ref. 33) has correlated a wide variety of data for conical flow with the following result:

$$C_{PB} = 1.43/M_\infty^2 \quad (136)$$

for a vacuum. Reducing this by 70 percent

$$C_{PB} = 1.001/M_\infty^2 \quad (137)$$

for $M \geq 2$.

d. Stability Derivatives

The stability derivatives used in this program are for a sharp cone and are easily derived from references 34 and 35. These derivatives consisted of the damping coefficient per radian of pitch angle of attack, CM_Q , and the rate of change of the normal force coefficient per degree of pitch angle of attack, CN_α . These values are for the following cone conditions:

$$4.0^\circ < \epsilon_c < 10^\circ$$

and

$$0 < R_N/R_B < 0.3$$

The rate of change of pitching moment coefficient, CM_A , can be computed as

$$CM_A = - (SM) (CN_A) / DIA \quad (138)$$

where

SM = static margin in feet

DIA = reference diameter in feet

Because of the symmetry of the conical vehicle used in this program, the values produced by yaw angle of attack and yaw angular velocities are equal in magnitude to pitch (data). Therefore,

$$CNR = CXQ \quad (139)$$

$$CNS = -CZA \quad (140)$$

$$CNS = -CZA \quad (141)$$

The derivatives are used to compute the aerodynamic forces and moments needed to restore the vehicle to zero angle of attack in pitch and yaw.

SECTION III
SUBROUTINES

1. ATMOSPHERIC PROPERTIES

The following list of subroutines are incorporated in STRAB-6 to compute the necessary atmospheric properties. This atmosphere uses the equations derived for the 1962 U.S. Standard atmosphere.

a. Subroutine RHOF

This subroutine computes the atmospheric density as a function of geometric altitude from the main program. The geometric altitude is converted to geopotential altitude in the subroutine and the density is computed accordingly. The units of density, Rho, are $\text{lbs-sec}^2/\text{ft}^4$.

b. Subroutine VSD

This subroutine calculates the velocity of sound, VS, in feet/sec as a function of geometric altitude.

c. Subroutine TEMPA

The ambient temperature, TEMP, is calculated in this subroutine as a function of geometric altitude. The units are degrees R.

d. Subroutine VISCO

This subroutine computes the viscosity of air as a function of geometric altitude. The units are $\text{lb-sec}/\text{ft}^2$.

e. Subroutine PRESS

The ambient pressure, PE, is calculated in this subroutine as a function of geometric altitude. The units are lb/ft^2 .

2. HOT AIR PROPERTIES

a. Subroutine VISCOT

This subroutine calculates the viscosity of air as a function of temperature. It is used primarily for the hot air in the nonablating boundary layer. The units are lb/sec-ft .

b. Subroutine TCAT

The thermal conductivity, TCA, of hot air is calculated in this subroutine as a function of temperature. The units of TCA are Btu/ft-sec-°R.

3. ABLATOR THERMAL PROPERTIES

The following subroutines are used to compute the thermal properties of carbon phenolic, phenolic silica (Refrasil), and ATJ graphite. The properties computed are the thermal conductivity and the specific heat. The carbon phenolic and phenolic silica ablator have both virgin and char properties as well as densities. From all available data for ATJ graphite, it appears that no distinction is made between virgin or char conditions. The subroutines that compute the thermal properties for carbon phenolic and phenolic silica have the same names to minimize card changes in the main program.

a. Subroutine VTCPC

This subroutine computes the virgin thermal conductivity for carbon phenolic or for phenolic refrasil as a function of wall temperature. The units are Btu/ft-sec-°R.

b. Subroutine VCPPC

The virgin specific heat for carbon phenolic or phenolic silica is calculated by this subroutine as a function of wall temperature. The units are Btu/lb-°R.

c. Subroutine CTCPC

The char thermal conductivity for carbon phenolic or phenolic silica is computed by this subroutine as a function of wall temperature. The units are in Btu/ft-sec-°R.

d. Subroutine CCPP

This subroutine computes the char specific heat of carbon phenolic or phenolic silica as a function of wall temperature. The units are Btu/lb-°R.

4. ABLATION GAS PROPERTIES

Subroutines GCPB and GASTC compute the thermal properties of the ablative gas-air mixture in the boundary layer. These subroutines are used with the carbon phenolic ablator only. They compute the gas specific heat and gas thermal conductivity. The values associated with phenolic refrasil and ATJ graphite are inputted as single values.

5. STABILITY DERIVATIVES SUBROUTINES

These subroutines are incorporated into STRAB-6 for computation of the necessary aerodynamics discussed in section II-5. The equations are general for the following cone parameters:

$$4.0^\circ < \theta_c < 10.0^\circ$$

$$0 < R_N/R_B < 0.3$$

$$3.0 < M_\infty < 30$$

a. Subroutine CDSF

This subroutine calculates the aerodynamic drag coefficients CP, CAN, CPB, and CDF as a function of M_∞ or Reynolds number. CDSF is called for in the main program.

(1) Subroutine CDFM

This subroutine computes the skin-friction drag, CDF, and is called into the program through subroutine CDSF. The boundary layer edge properties are calculated in this subroutine.

b. Subroutine ACMQ

The damping coefficient, CMQ, is calculated in this subroutine as a function of free-stream Mach number. CMQ is per radian.

c. Subroutine ACNA

This subroutine computes the normal force coefficient, CNA, as a function of free-stream Mach number. CNA is per radian.

6. SUBROUTINE INITIAL (Ref. 36)

This subroutine is incorporated into STRAB-6 to provide the necessary vehicle geometry calculations and changes in units. By reading in vehicle axial stations of interest, the subroutine will compute the transition Reynolds number, slant height (SQL), smaller radius (RS), and larger radius (RL) for each conical segment. It will also compute the appropriate cone base radius and total slant height. See figure 16 for further clarification.

7. SUBROUTINE ATTK AND SSLP

These subroutines are used to compute the complete range of angles of attack, ALP, and sideslip, BFT. These angles are computed as a function of the components of the relative velocity.

8. SUBROUTINE DLON

This subroutine computes the longitude of the vehicle with respect to the earth reference system. See section II-2c for derivation.

SECTION IV
PROGRAM OPERATION

1. INPUT DATA REQUIREMENT

All input data that is subject to change either due to vehicle or trajectory requirements are read into STRAB-6 from the data statement. The word data is punched first, then the FORTRAN symbol, and then the numerical values. The symbols and numerical values are punched in Columns 7 through 72, inclusive, with up to nine continuation cards if needed. Columns 73 to 80, inclusive, can be used for comments or identification. The numerical values can be punched in any format except "I." Care should be taken to keep the symbol and its corresponding value in the same sequence. For example:

DATA V. AZN, NOFX, NAL, GAMMA/22414., 123.003, 8, 4, -39.92/

Also,

DATA WE, REQ, ET/0.729E-04, 20,927491E+06, 8.18133302E-02/

Another method of data card is

DATA (POS (I), I = 1, 6)/3.338, 15.189, 27.040, 38.851, 50.742, 65.556/

Another flexibility of the input routine, aside from the fact that the data can be introduced in any order of the symbols (with their associated values), is the feature that permits inputting the same symbol (and an associated value) again, thus superseding the previous value. This feature is convenient when basically constant vehicle configurations and initial conditions are maintained in many runs with only a few quantities changing. The "Standard" input data cards may be kept intact, and only the varying quantities may be punched on a card after the data cards which may be removed later.

For the heating portion of the program, there are several "Do Loops" that initialize temperatures, ablator lamina thickness, control indicators, and thermal properties of the adhesive bond and backface aluminum shell. Also, there are various equations to obtain initial trajectory conditions as well as initial dummy program starters.

a. Multi-Case Run

This program readily lends itself for a multi-case run with a minimal change. If the need arises for a parametric study of various vehicle geometry and trajectory missions, the following changes can be made to some of the data inputs and check for completion of the multi-case run.

Read 1500, NCASE, (POS(J), J=1, 8) 1500 FORMAT (I2, 7A10, A8)

Print 1501, NCASE, (POS(J), J=1, 8) 1501 FORMAT (1H1, 30X, 7A10, A8)

These read and print statements allow the identifier to be read into the program and case heading to be printed out before that particular case data output. The 1500 format allows the case number to be punched in the first two columns. When a zero is in these columns, the program will go to end with this check statement.

```
If (NCASE.NE.0) go to 1700
END
```

where statement 1700 would be the return at the beginning of the program to start another case.

To update the vehicle configuration and trajectory parameters, the following data input is used

Read 1300, (POS(I), I=1,NOFX)

Read 1300, THETC, GAMMA, BI

Read 1300, V, AXN, GLAT, DLON

Read 1300, ALGTH, SNR 1300 Format (8F10.2)

All other data input cards would remain the same. See appendix II for multi-case listing and setup.

2. OUTPUT DATA REQUIREMENTS

The output quantities of the program and sample case are shown in appendixes I and III.

Before the printout of any results, a listing of the program and input data cards are printed. This record of the actual program listing and data input will assist in the identification of a run as well as an aid in troubleshooting in the event of arithmetic errors.

The first block of data printout of the matrix of temperatures, lamina thickness, etc., are obtained from the initialization "Do Loops" for heating portion of the program. This printout is done only once.

The second block of data is the trajectory output, aerodynamic coefficients, and boundary layer edge values. The next block of output is the wall and skin-profile temperatures, total recession, integrated weight loss rate, and total weight loss.

Printout is regulated by a time indicator. Data can be printed out at any time step desired. If a printout of data is wanted every 0.1 second, set $BT = .1$. The following method will then allow printout at that time step.

$BTL = BT - H/6$.

$BTH = BT + H/6$.

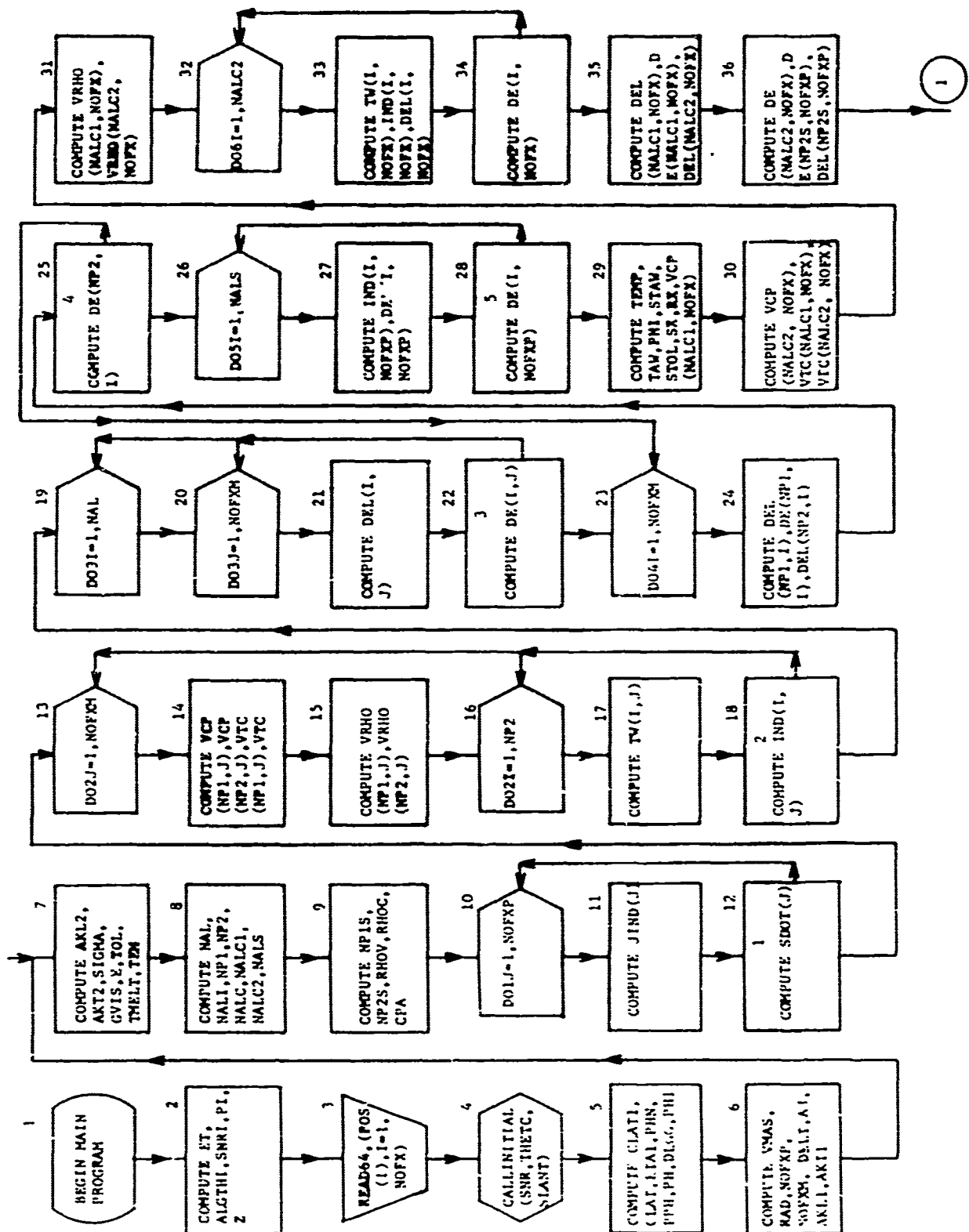
If ($T > BTL$. AND. $T < BTH$) go to (statement number)

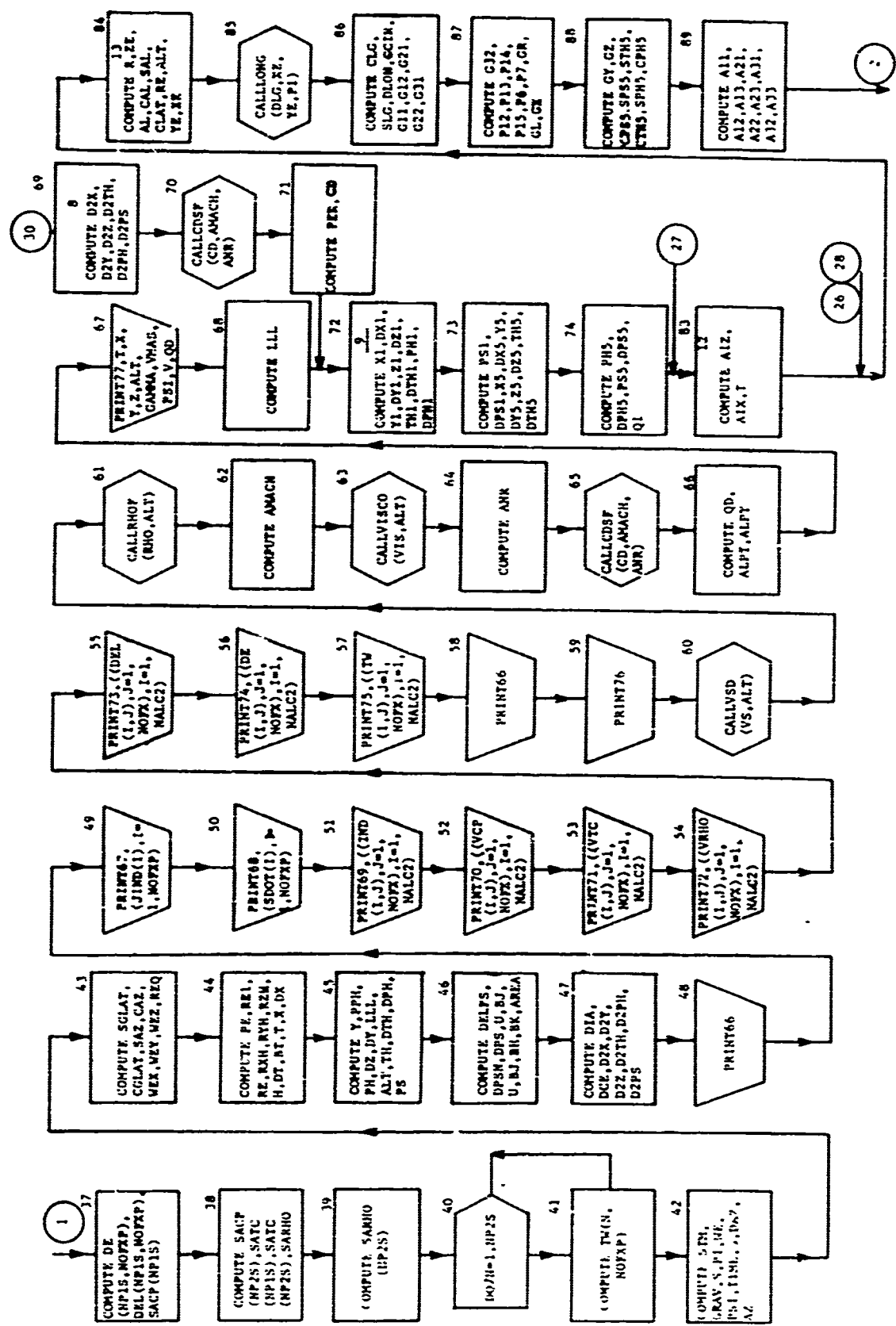
$BT = BT + .1$

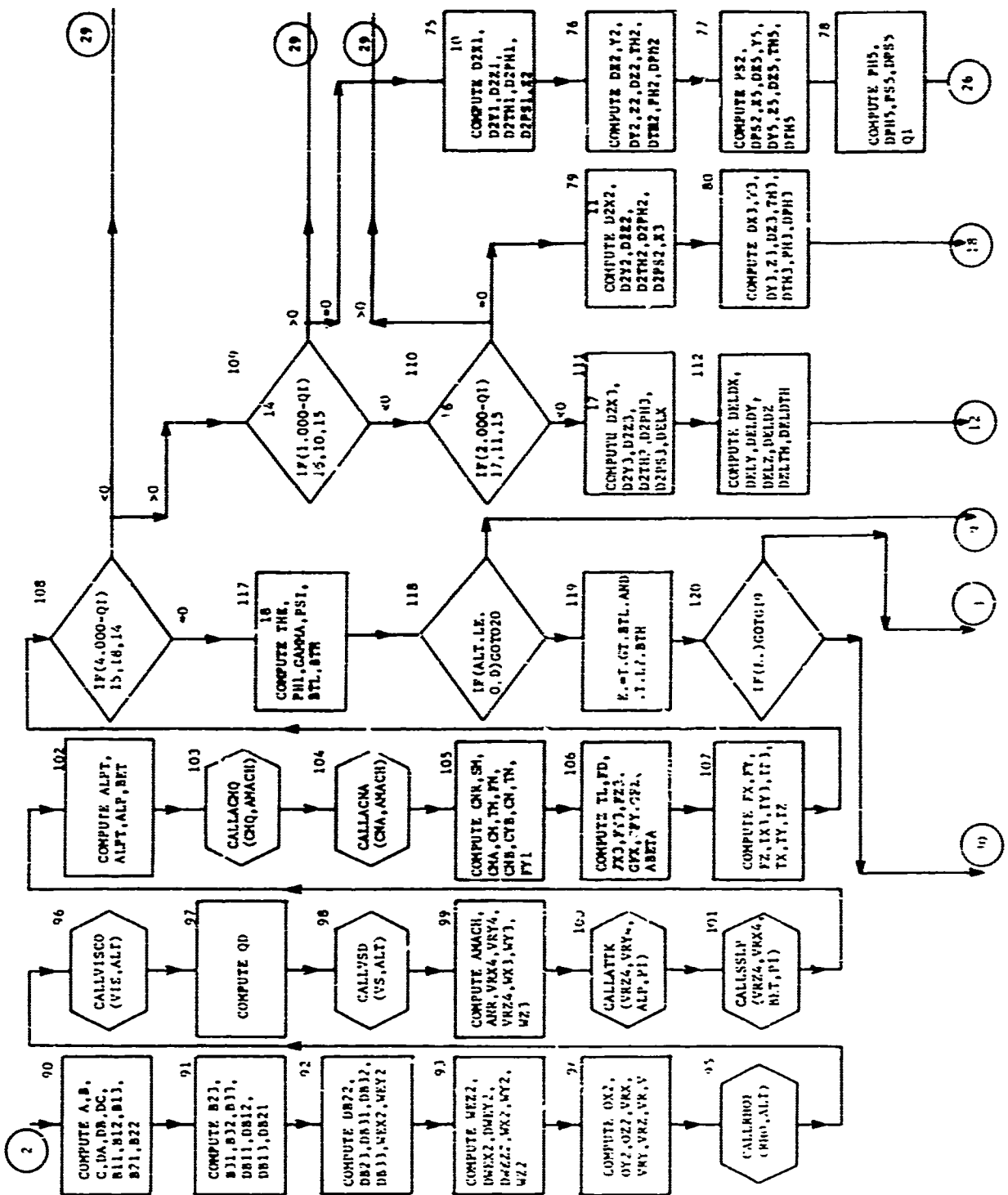
where H is the Runge-Kutta integration time step. This method will allow data printout and also go into the heating portion of the program.

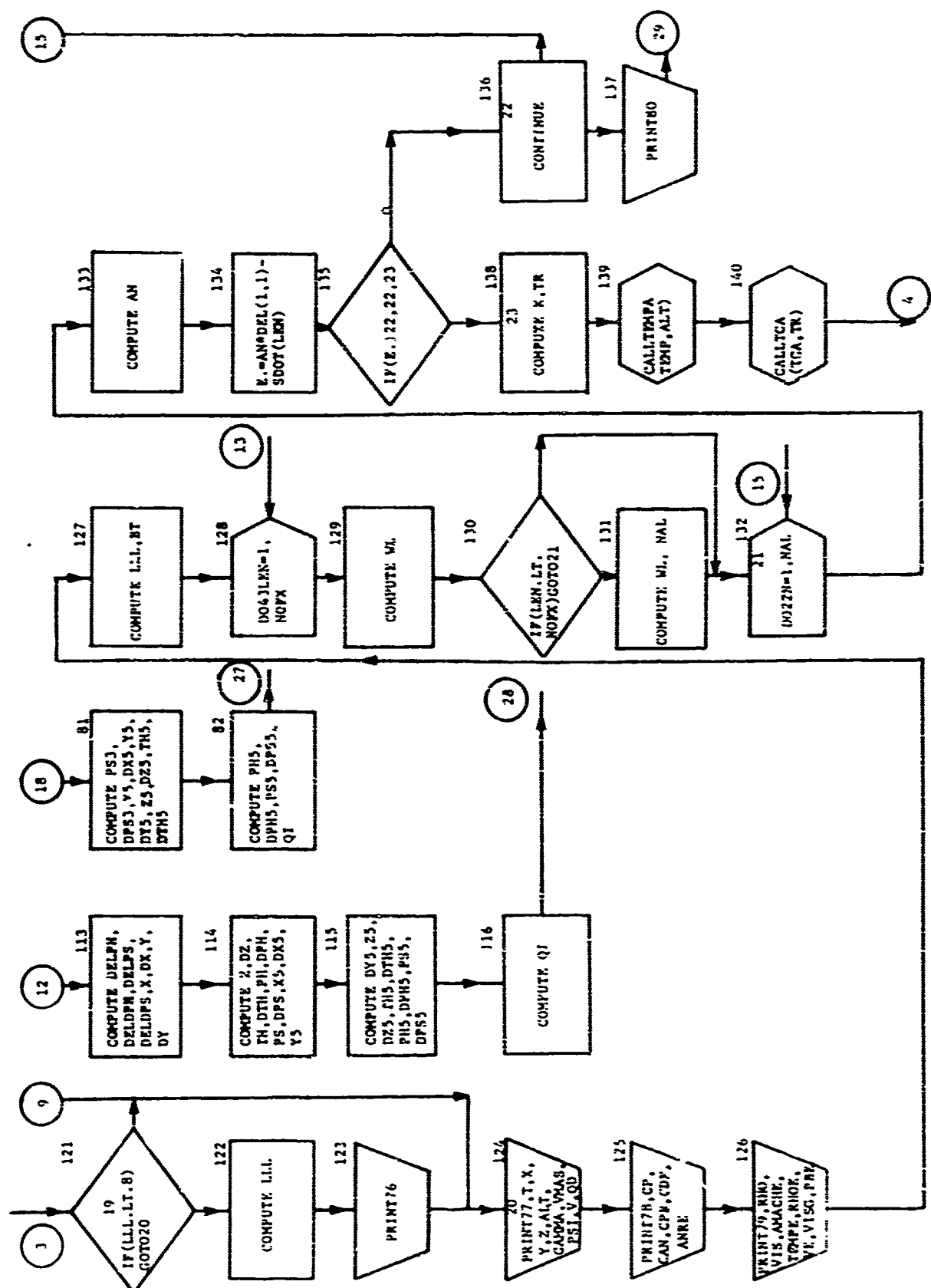
In addition to the printed output, selected quantities may also be obtained as punched output. The punched cards may be useful for machine plotting or as input to some other program.

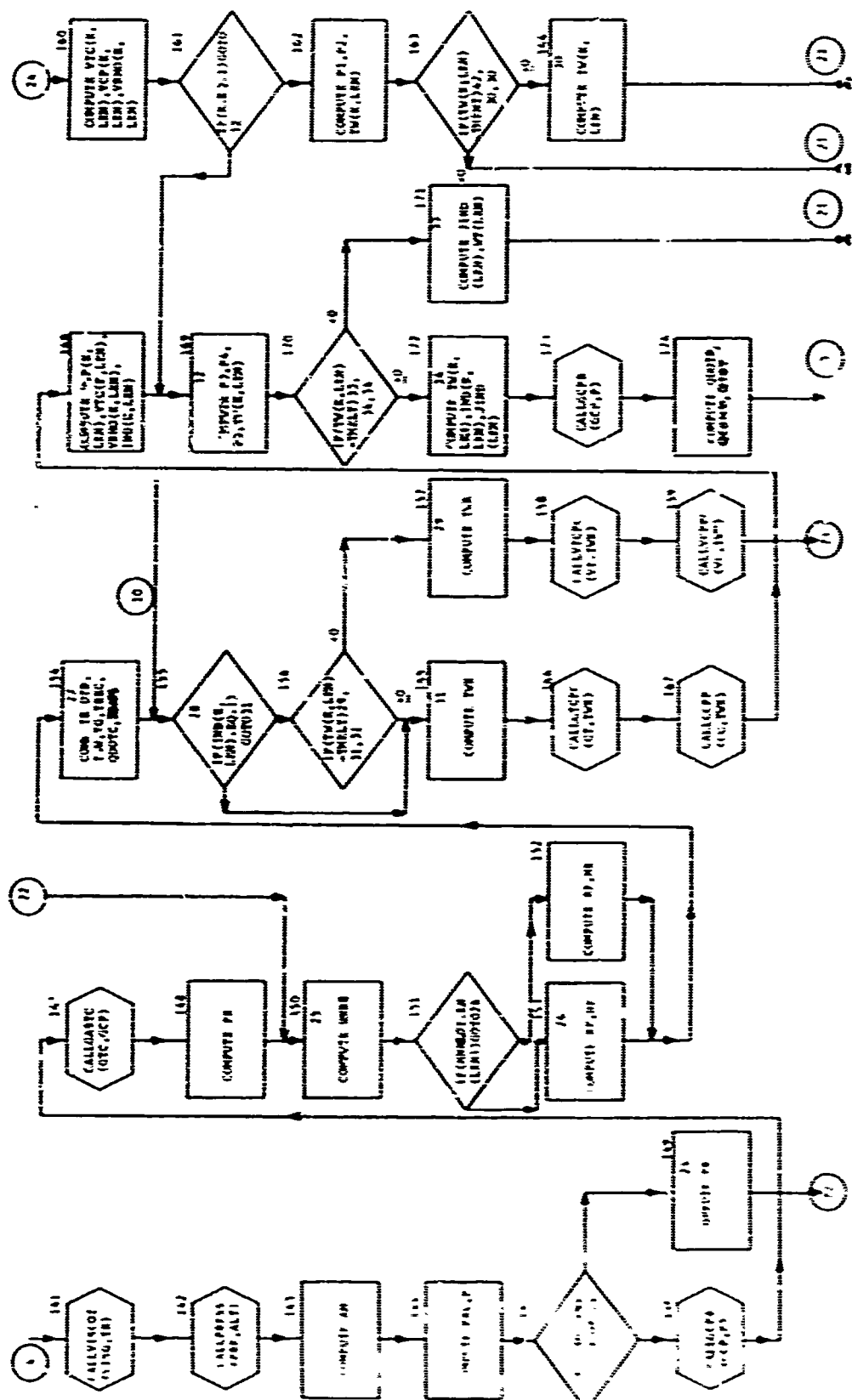
3. FLOW DIAGRAMS

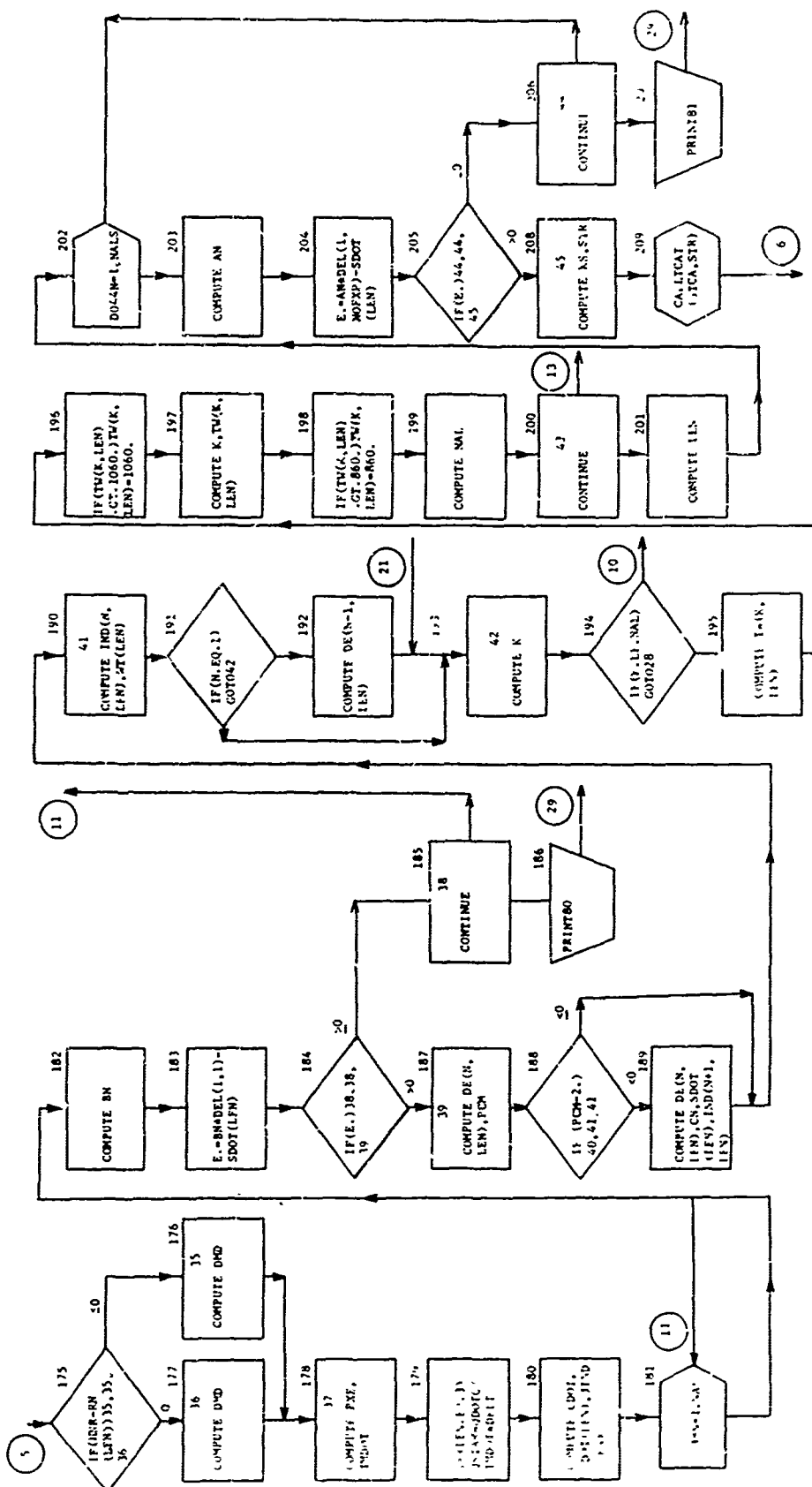


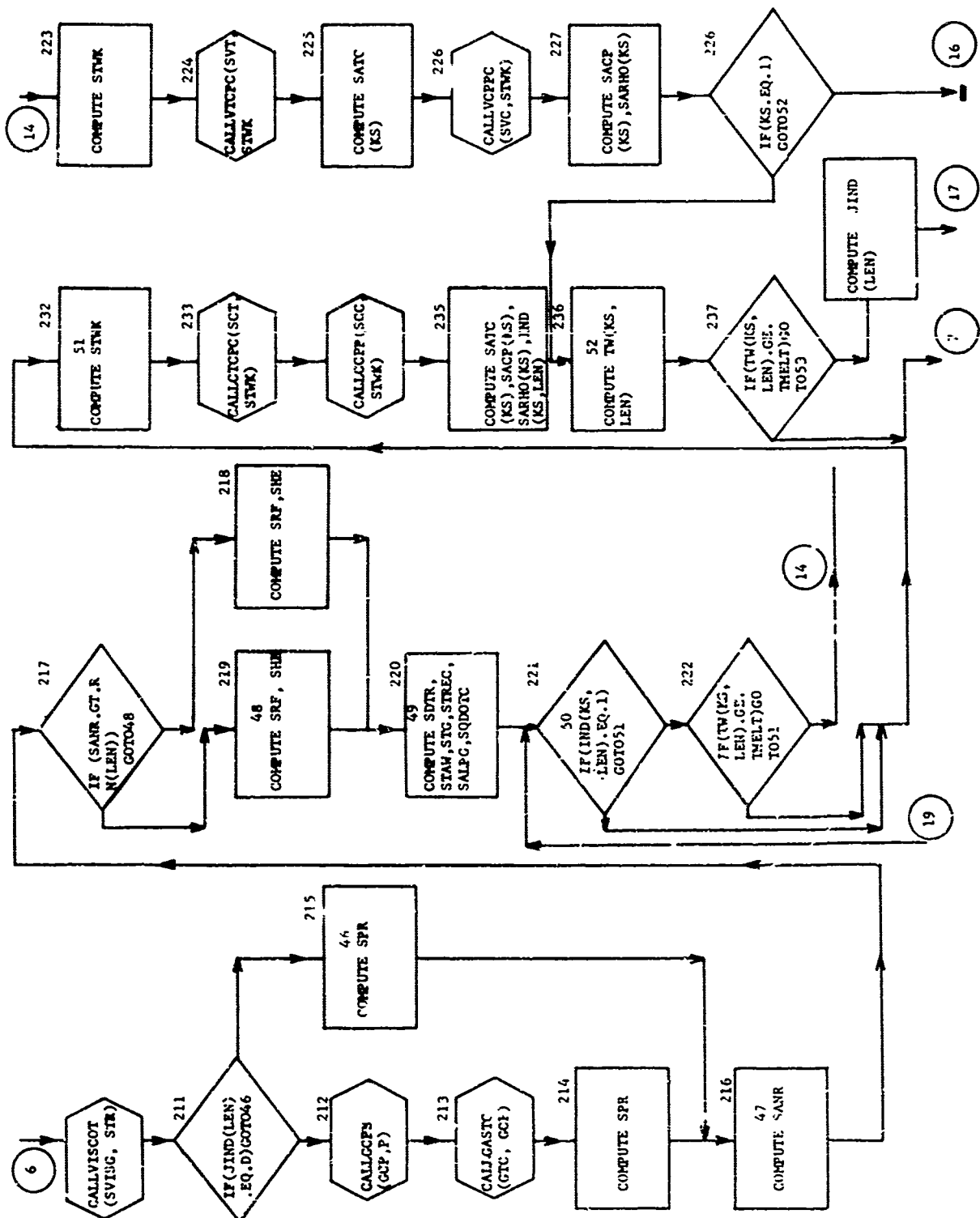


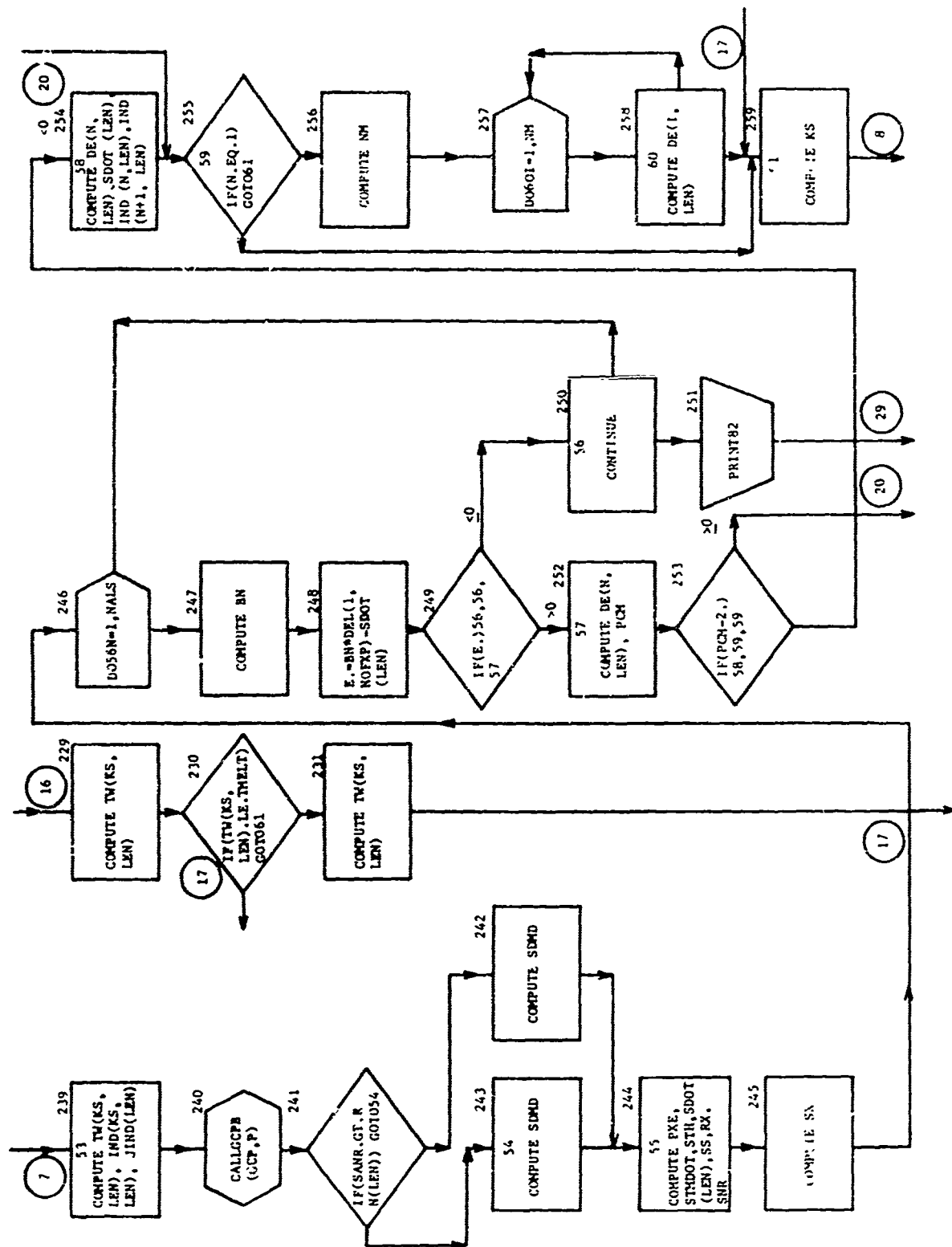


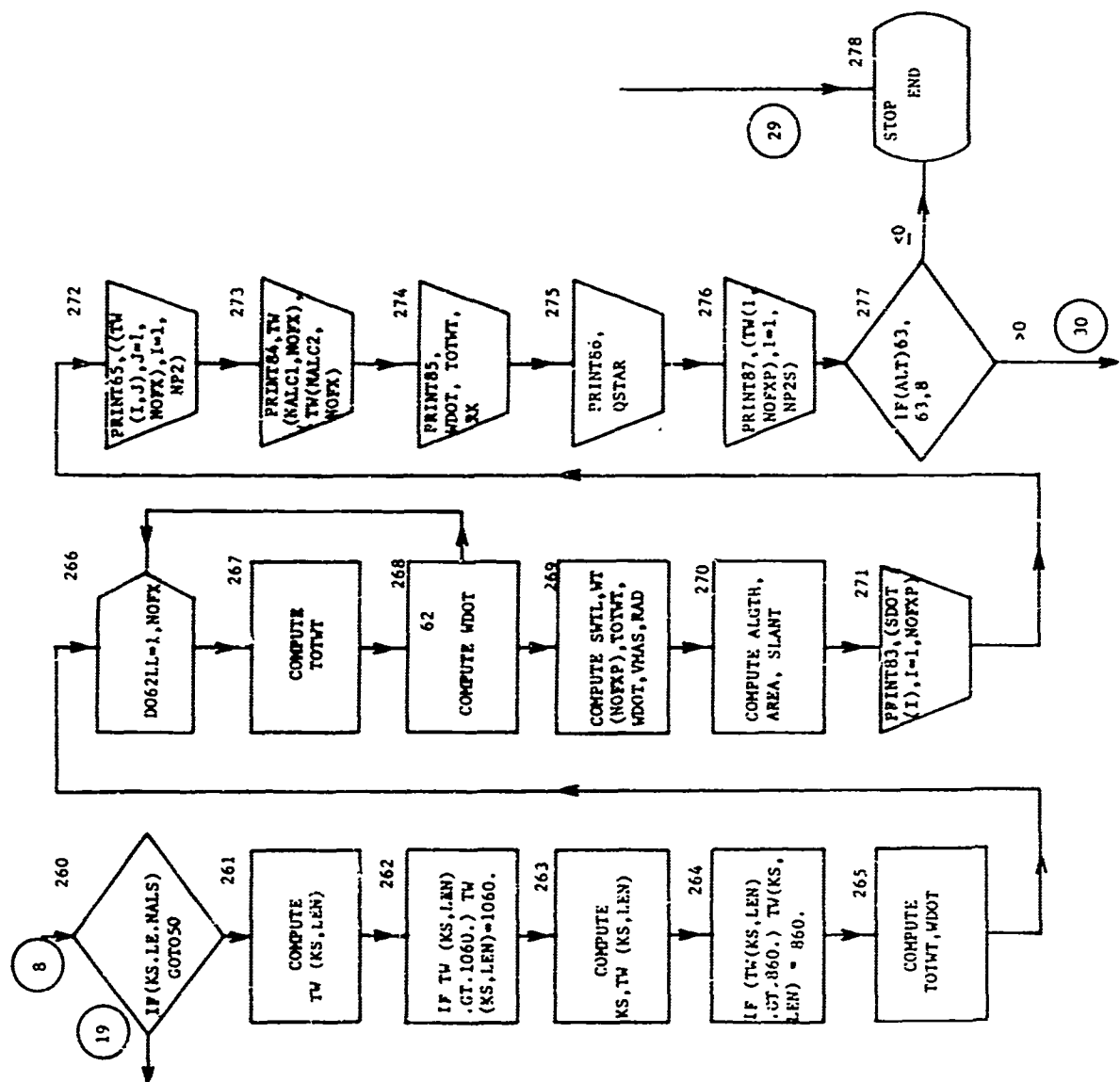












AFWL-TR-68-61

This page intentionally left blank.

AFWL-TR-68-61

APPENDIX I
STRAB-6 PROGRAM LISTING

PROGRAM STRAB62 (INPUT,OUTPUT)

C 6 DEGREE TRAJECTORY WITH ABLATION HEATING AND STAG

COMMON /A/ RE

COMMON /B/ AREA,RAD,SLANT,SNR,THETC,V

COMMON /C/ CPM,CP,CAN,CPR,CDF

COMMON /D/ TW(50,12),IND(50,12),JIND(12),VCP(50,12),VTC(50,12),VRH

10(50,12),DEL(50,12),DE(50,12),SDOT(12),XI(12),RS(12),RL(12),SOL(12)

2),WT(12),TM(12),TWT(12),SACP(50),SATC(50),SARHO(50),RN(12),QSTR(12)

3),QDOTC(12),QTOT(12),QCOND(12)

COMMON /E/ NOFXM,NAL,ALT,AMACH,QD,AMACHE,TEMPE,RHOE,VE,VISG,PBE,AN

IRE

COMMON /F/ NOFX,ALGTH,RADI,POS(11),AZN,GLAT

VEHICLE DATA

IF NOFX IS CHANGED CHANGE FORMAT 103

IF CONC ANGLE IS CHANGED SUB CDSF MUST BE CHANGED

DATA SNR,THETC,BI,SM/.0208,.07853,6.27836,.59718/

DATA PI,E,AJ,GRAV,G/3.14159,2.7183,778.,32.174,32.174/

DATA REQ,PE,ET,WE/20.927491E+06.,673852E-02,.08181333,0.7292E-04/

DATA NOFX,NAL,NALC,NALS/8,4,10,35/

DATA DELT,DT,H,RT,AT/.05,.0005,.001,.05,1./

DATA AZN,GLAT,DLON,GAMMA/154.,33.996,-107.5,-22.39/

DATA V+Z,ALPHA/15167.,2.50E+05,7./

DATA (POS(I),I=1,8)/6.607,18.570,30.533,42.496,54.459,66.422,78.38

15.86,469/

A12=0.51

ATX=23.08

CALL INITIAL (SNR,THETC,SLANT)

ALGTHI=ALGTH

SNRI=SNR

CLAT1=ATAN((1,-ET**2)*TAN(GLAT))

CLAT=CLAT1*180./PI

ETA1=GLAT-CLAT1

PHN=(90,-GAMMA-ALPHA)*PI/180.

PPH=0.0

PH=(1.+PPH)*PHN

DLGG=DLON

PH1=PH

VNAC=BI

RAD=RADI

NOFXP=NOFX+1

NOFXM=NOFX-1

AKL1=5370.

AKT1=4240.

AKL2=5.37

AKT2=5.77

GVIS=4.429E-5

TOL=.00854

TMELT=6760.

TEM=544.

NALT=NAL

NP1=NAL+1

NP2=NAL+2

NALC1=NALC+1

NALC2=NALC+2

NP1S=NALS+1

NP2S=NALS+2

RHCV=90.4

RHCC=74.

ATJRH0=120.96

CPA=.2395

DO 1 J=1,NOFXP

A 2

A 3

A 4

A 5

A 6

A 7

A 8

A 9

A 10

A 11

A 12

A 13

A 14

A 15

A 16

A 17

A 18

A 19

A 20

A 21

A 22

A 23

A 24

A 25

A 26

A 27

A 28

A 29

A 30

A 31

A 32

A 33

A 34

A 35

A 36

A 37

A 38

A 39

A 40

A 41

A 42

A 43

A 44

A 45

A 46

A 47

A 48

A 49

A 50

A 51

A 52

A 53

A 54

A 55

A 56

A 57

A 58

A 59

A 60

A 61

```

1 JIND(J)=0 A 62
  SDOIT(J)=0. A 63
  DO 2 J=1,NOFXM A 64
  VCP(NP1,J)=.315 A 65
  VCP(NP2,J)=.208 A 66
  VTC(NP1,J)=.74E-04 A 67
  VTC(NP2,J)=.03694 A 68
  VRHO(NP1,J)=91.7 A 69
  VRHO(NP2,J)=169. A 70
  DO 2 I=1,NP2 A 71
  TW(I,J)=TEM A 72
2 IND(I,J)=0 A 73
  DO 3 I=1,NAL A 74
  DO 3 J=1,NOFXM A 75
  DEL(I,J)=TOL A 76
3 DE(I,J)=TOL A 77
  DO 4 I=1,NOFXM A 78
  DEL(NP1,I)=.00333 A 79
  DE(NP1,I)=.00333 A 80
  DEL(NP2,I)=.005 A 81
4 DE(NP2,I)=.005 A 82
  DO 5 I=1,NALS A 83
  IND(I,NOFXP)=0 A 84
  DEL(I,NOFXP)=TOL A 85
5 DE(I,NOFXP)=TOL A 86
  TEMP=298.2 A 87
  TAW=TEMP A 88
  PHI=80.967 A 89
  STAW=TEMP A 90
  STOL=TOL A 91
  SX=.01745*RS(NOFXP)*PHI A 92
  RX=SNR A 93
  VCP(NALC1,NOFX)=.315 A 94
  VCP(NALC2,NOFX)=.208 A 95
  VTC(NALC1,NOFX)=.74E-04 A 96
  VTC(NALC2,NOFX)=.03694 A 97
  VRHO(NALC1,NOFX)=91.7 A 98
  VRHO(NALC2,NOFX)=169. A 99
  DO 6 I=1,NALC2 A 100
  TW(I,NOFX)=TEM A 101
  IND(I,NOFX)=0 A 102
  DEL(I,NOFX)=TOL A 103
6 DE(I,NOFX)=TOL A 104
  DEL(NALC1,NOFX)=.00333 A 105
  DE(NALC1,NOFX)=.00333 A 106
  DEL(NALC2,NOFX)=.005 A 107
  DE(NALC2,NOFX)=.005 A 108
  DE(NP2S,NOFXP)=.005 A 109
  DEL(NP2S,NOFXP)=.005 A 110
  DE(NP1S,NOFXP)=.00333 A 111
  DEL(NP1S,NOFXP)=.00333 A 112
  SACP(NP1S)=.315 A 113
  SACP(NP2S)=.208 A 114
  SATC(NP1S)=.74E-04 A 115
  SATC(NP2S)=.03694 A 116
  SARHO(NP1S)=91.7 A 117
  SARHO(NP2S)=169. A 118
  DO 7 N=1,NP2S A 119
  TW(N,NOFXP)=TEM A 120
7 PSI=0. A 121
  DAZ=0.0 A 122
  AZ=(1.000+DAZ)*4ZN A 123

```

```

SGLAT=SIN(GLAT) A 124
CGLAT=COS(GLAT)
SAZ=SIN(AZ)
CAZ=COS(AZ)
WEZ=-WE*CGLAT*SAZ
WEY=WE*CGLAT*CAZ
WEZ=WE*SGLAT
RE1=REQ/(1.000+PE*(SIN(CLAT1))**2)**.500
RE=RE1
RYH=RE1*SIN(ETA1)*SAZ
RYH=-RE1*SIN(ETA1)*CAZ
RZH=RE1*COS(ETA1)
T=0.0
X=0.0
DX=0.0
Y=0.0
PPH=0.0
PH=(1.0+PPH)*PHN
DZ=V*SIN(GAMMA*PI/180.)
DY=V*COS(GAMMA*PI/180.)
LLL=0
ALT=Z
TH=0.0
DTH=0.0
DPH=0.0
PS=0.0
DELPS=0.0
DPSN=2.*PI
DPS=(1.+DELPS)*DPSN
U=0.1407639E+17
BJ=1623.41E-06
BH=6.04E-06
BK=6.37E-06
AREA=PI*RAD**2
DIA=1.781
DCD=0.00
D2X=0.0
D2Y=0.0
D2Z=0.0
D2TH=0.0
D2PH=0.0
D2PS=0.0
PRINT 71
PRINT 72, (JIND(I),I=1,NOFXP)
PRINT 92, (SDOT(I),I=1,NOFXP)
PRINT 73, ((IND(I,J),J=1,NOFX),I=1,NALC2)
PRINT 74, ((VCP(I,J),J=1,NOFX),I=1,NALC2)
PRINT 75, ((VTC(I,J),J=1,NOFX),I=1,NALC2)
PRINT 76, ((VRHO(I,J),J=1,NOFX),I=1,NALC2)
PRINT 77, ((DEL(I,J),J=1,NOFX),I=1,NALC2)
PRINT 78, ((DE(I,J),J=1,NOFX),I=1,NALC2)
PRINT 79, ((TW(T,J),J=1,NOFX),I=1,NALC2)
PRINT 71
PRINT 80
CALL VSD (VS,ALT)
CALL RHO (RHO,ALT)
AMACH=V/VS
CALL VISCO (VIS,ALT)
ANR=RHO*V*SLANT/VIS
CALL CDSF (CD,AMACH,ANR)
QD=.5*RHO*V**2
ALPT=ABS(ALPHA)

```

```

PRINT B1, T,X,Y,Z,ALT,GAMMA,VMAS,PSI,V,QA,AMACH,CD,ANR,PH1,THE,ALP A 186
1,BET,PS,ALPT,XE,YE,ZE,FD,FN,GFZ,CLAT,DLON,ABETA,GCIR,AIZ,AIX A 187
LLL=LLL+1 A 188
GO TO 9 A 189
B D2X=FX/VMAS-2.*DA-C*WEY+B*WEZ+GX A 190
D2Y=FY/VMAS-2.*DB-A*WEZ+C*WEY+GY A 191
D2Z=FZ/VMAS-2.*DC-B*WEX+A*WEY+GZ A 192
D2TH=TY/AIX-WX2*0Z2+AIZ*WZ2*0X2/AIX-DWEY2 A 193
D2PH=(-TX/AIX+AIZ*WZ2*0Y2/AIX-WY2*0Z2+DPH*DTH*SIN(TH)+DWEY2)/COS(T A 194
1H) A 195
D2PS=TZ/AIZ-AIX-WY2*0X2/AIZ+AIX-WX2*0Y2/AIZ+D2PH*SIN(TH)+DPH*DTH+C A 196
10S(TH)=DWEY2 A 197
CALL CDSF (CD,AMACH,ANR) A 198
PER=1.+.0375*ALPT+.00156*ALPT**2. A 199
CD=CD*PER A 200
9 X1=X+DX*H/2. A 201
DX1=DX+D2X*H/2. A 202
Y1=Y+DY*H/2. A 203
DY1=DY+D2Y*H/2. A 204
Z1=Z+DZ*H/2. A 205
DZ1=DZ+D2Z*H/2. A 206
TH1=DTH+DTH*H/2. A 207
DTH1=DTH+D2TH*H/2. A 208
PH1=PH+DPH*H/2. A 209
DPH1=DPH+D2PH*H/2. A 210
PS1=PS+DPS*H/2. A 211
DPS1=DPS+D2PS*H/2. A 212
X5=X1 A 213
DX5=DX1 A 214
YS=Y1 A 215
DY5=DY1 A 216
Z5=Z1 A 217
DZ5=DZ1 A 218
TH5=TH1 A 219
DTH5=DTH1 A 220
PH5=PH1 A 221
DPH5=DPH1 A 222
PS5=PS1 A 223
DPS5=DPS1 A 224
QI=1.000 A 225
GO TO 12 A 226
10 D2X1=FX/VMAS-2.*DA-C*WEY+B*WEZ+GX A 227
D2Y1=FY/VMAS-2.*DB-A*WEZ+C*WEY+GY A 228
D2Z1=FZ/VMAS-2.*DC-B*WEX+A*WEY+GZ A 229
D2TH1=TY/AIX-WX2*0Z2+AIZ*WZ2*0X2/AIX-DWEY2 A 230
D2PH1=(-TX/AIX+AIZ*WZ2*0Y2/AIX-WY2*0Z2+DPH5*DTH5*STH5+DWEY2)/CTH5 A 231
D2PS1=TZ/AIZ-AIX-WY2*0X2/AIZ+AIX-WX2*0Y2/AIZ+D2PH1*STH5+DPH5*DTH5* A 232
1CTH5-DWEY2 A 233
X2=X+DX1*H/2. A 234
DX2=DX+D2X1*H/2. A 235
Y2=Y+DY1*H/2. A 236
DY2=DY+D2Y1*H/2. A 237
Z2=Z+DZ1*H/2. A 238
DZ2=DZ+D2Z1*H/2. A 239
TH2=TH+DTH1*H/2. A 240
DTH2=DTH+D2TH1*H/2. A 241
PH2=PH+DPH1*H/2. A 242
DPH2=DPH+D2PH1*H/2. A 243
PS2=PS+DPS1*H/2. A 244
DPS2=DPS+D2PS1*H/2. A 245
X5=X2 A 246
DX5=DX2 A 247

```

Y5=Y2	A 248
DY5=DY2	A 249
Z5=Z2	A 250
DZ5=DZ2	A 251
TH5=TH2	A 252
DTH5=DTH2	A 253
PH5=PH2	A 254
DPH5=DPH2	A 255
PS5=PS2	A 256
DPSS=DPS2	A 257
OJ=2,000	A 258
GO TO 13	A 259
11 D2X2=FX/VMAS-2.♦DA-C♦WEY♦B♦WEZ♦GX	A 260
D2Y2=FY/VMAS-2.♦DB-A♦WEZ♦C♦WEX♦GY	A 261
D2Z2=FZ/VMAS-2.♦DC-B♦WEX♦A♦WEY♦GZ	A 262
D2TH2=TY/AIX-WX2♦0Z2♦AIZ♦WZ2♦0X2/AIX-DWEY2	A 263
D2PH2=(-TX/AIX+AIZ♦WZ2♦0Y2/AIX-WY2♦0Z2♦DPH5♦DTH5♦STH5♦DWEX2)/CTH5	A 264
D2PS2=TZ/AIZ-AIX-WY2♦0X2/AIZ+AIX-WX2♦0Y2/AIZ-D2PH2♦STH5♦DPH5♦DTH5♦	A 265
1CTH5=DWEZ2	A 266
X3=X♦DX2♦H/2.	A 267
DX3=DX♦D2X2♦H/2.	A 268
Y3=Y♦DY2♦H/2.	A 269
DY3=DY♦D2Y2♦H/2.	A 270
Z3=Z♦DZ2♦H/2.	A 271
DZ3=DZ♦D2Z2♦H/2.	A 272
TH3=TH♦DTH2♦H/2.	A 273
DTH3=DTH♦D2TH2♦H/2.	A 274
PH3=PH♦DPH2♦H/2.	A 275
DPH3=DPH♦D2PH2♦H/2.	A 276
PS3=PS♦DPS2♦H/2.	A 277
DPS3=DPS♦D2PS2♦H/2.	A 278
X5=X3	A 279
DX5=DX3	A 280
Y5=Y3	A 281
DY5=DY3	A 282
Z5=Z3	A 283
DZ5=DZ3	A 284
TH5=YH3	A 285
DTH5=TH3	A 286
PH5=PH3	A 287
DPH5=DPH3	A 288
PS5=PS3	A 289
DPSS=DPS3	A 290
OJ=3,000	A 291
12 T=T+DT	A 292
13 R=SQRT((RXH+X5)♦♦2+(RYH+Y5)♦♦2+(RZH+Z5)♦♦2)	A 293
ZE=(RZH+Z5)♦SGLAT-CGLAT*((RXH+X5)♦SAZ-(RYH+Y5)♦CAZ)	A 294
AL=ASIN(ZE/R)	A 295
CAL=COS(AL)	A 296
SAL=SIN(AL)	A 297
CLAT=AL*180./PI	A 298
PE=REQ/(1.000+PE♦SAL♦♦2)♦♦.500	A 299
ALT=R-RE	A 300
YE=(RXH+X5)♦CAZ+(RYH+Y5)♦SAZ	A 301
XE=(RZH+Z5)♦CGLAT+SGLAT*((RXH+X5)♦SAZ-(RYH+Y5)♦CAZ)	A 302
CALL LONG (DLG,XE,YE,PI)	A 303
CLG=COS(DLG)	A 304
SLG=SIN(DLG)	A 305
DLON=DLGG+DLG*180./PI	A 306
GCIR=((RE+RE1)/2.)♦ACOS(SAL♦SIN(CLAT))♦CAL♦COS(CLAT))♦COS(AL-CLAT)	A 307
111 G11=-SGLAT♦CAL♦CLG♦CGLAT♦SAL	A 308
	A 309

G12=SGLAT*SAL*CLG*CGLAT=CAL
 G21=-CAL*SLG
 G22=SAL*SLG
 G31=-CGLAT=CAL*CLG=SGLAT*SAL
 G32=CGLAT=SAL*CLG=SGLAT=CAL
 P12=1.-3.*SAL**2
 P13=j.*SAL-5.*SAL**3
 P14=3.-30.*SAL**2+35.*SAL**4
 P15=SIN(2.*AL)
 P6=CAL*(1.-5.*SAL**2)
 P7=SAL*CAL*(-3.+7.*SAL**2)
 GR=U/R**2*(1.+BJ*(REQ/R)**2*P12+4./5.*RH*(REQ/R)**3*P13+3K/6.*
 (R/R)**4*P14)
 SL=U/R**2*(1.-BJ*(REQ/R)**2*P15+3./5.*RH*(REQ/R)**3*P6+2./3.*BK*(REQ
 /R)**4*P7)
 Gx=GR*(G11*SAZ+G21*CAZ)+GL*(G12*SAZ+G22*CAZ)
 Gy=GR*(G21*SAZ-G11*CAZ)+GL*(G22*SAZ-G12*CAZ)
 Gz=GR*G31+GL*G32
 CP55=COS(P55)
 SP55=SIN(P55)
 STH5=SIN(TH5)
 CTH5=COS(TH5)
 SPH5=SIN(PH5)
 CPH5=COS(PH5)
 A11=CP55*CTH5
 A12=SP55*CPH5-CTH5*SPH5*CP55
 A13=-CP55*STH5*CPH5-SP55*SPH5
 A21=-SP55*CTH5
 A22=SP55*STH5*SPH5+CP55*CPH5
 A23=SP55*STH5*CPH5-SPH5*CP55
 A31=STH5
 A32=CTH5*SPH5
 A33=CTH5*CPH5
 A=WEY*(R2H+Z5)-(RYH+Y5)*WEZ
 B=WFZ*(RXH+X5)-(RZH+Z5)*WFX
 C=WEX*(RYH+Y5)-(RZH+Z5)*WEY
 DA=DZ5*WEY-DYS*WEZ
 DR=DX5*WEZ-DZ5*WFX
 DC=DY5*WFX-DX5*WEY
 B11=CTH5
 ^12=-STH5*SPH5
 v13=-STH5*CPH5
 B21=0.
 B22=CPH5
 B23=-SPH5
 B31=STH5
 B32=CTH5*SPH5
 B33=CTH5*CPH5
 DB11=-DTH5*STH5
 DB12=-DTH5*CTH5*SPH5-CPH5*CPH5*STH5
 DR13=-DTH5*CTH5*CPH5-CPH5*SPH5*STH5
 DR21=0.
 DB22=-DPH5*SPH5
 DR23=-DPH5*CPH5
 D931=0.
 D932=DPH5*CPH5*CTH5-DTH5*STH5*SPH5
 DA33=-DTH5*STH5*CPH5-CPH5*SPH5*CTH5
 WEX2=B11*WEX+B12*WEY+B13*WEZ
 WEY2=B21*WEX+B22*WEY+B23*WEZ
 WEZ2=B31*WEX+B32*WEY+B33*WEZ
 DWEX2=DR11*WEX+DB12*WEY+DR13*WEZ
 DWEX2=DR21*WEX+DB22*WEY+DR23*WEZ

DWE72=DA31*WEX+DS32*WEY+DA33*WEZ A 372
 WX2=WFX2-DPH5*CTH5 A 373
 WY2=WEY2+DTH5 A 374
 WZ2=WFZ2+DPSS=DPH5*STH5 A 375
 DX2=WX2 A 376
 OY2=WY2 A 377
 OZ2=WEZ2=DPH5*STH5 A 378
 VRX=DX5 A 379
 VRY=DY5 A 380
 VRZ=DZ5 A 381
 VR=SQRT(VRX**2+VRY**2+VRZ**2) A 382
 V=SQRT(DX5**2+DY5**2+DZ5**2) A 383
 CALL RHOF (RHO,ALT) A 384
 CALL VISCO (VIS,ALT) A 385
 QDZ=5*RHO*V**2 A 386
 CALL VSD (VS,ALT) A 387
 AMACH=V/VS A 388
 ANR=RHO*V*SLANT/VIS A 389
 VRX4=A11*VRX+A12*VRY+A13*VRZ A 390
 VRY4=A21*VRX+A22*VRY+A23*VRZ A 391
 VRZ4=A31*VRX+A32*VRY+A33*VRZ A 392
 WX3=-DPH5*CTH5*CPSS+DTH5*SPSS A 393
 WY3=DPH5*CTH5*SPSS+DTH5*CPSS A 394
 WZ3=DPSS=DPH5*STH5 A 395
 CALL ATTK (VRZ4,VRY4,ALP,PI) A 396
 CALL SSLP (VRZ4,VRX4,BET,PI) A 397
 ALP7=A7*S(ALP) A 398
 ALPT=ALPT*180./PI A 399
 ALP=ALP*180./PI A 400
 BET=BET*180./PI A 401
 ALP1=ABSF(ALP) A 402
 BET1=ABSF(BET) A 403
 CALL ACMQ (CMQ,AMACH) A 404
 CALL ACNA (CNA,AMACH) A 405
 CNA PER DEGREE A 406
 CMQ PER RADIAN A 407
 CNR=CMQ A 408
 CMA=-SM*CNA/DIA A 409
 CM=CMA*ALP+CMQ*WX3*DIA/(2.*V) A 410
 TM=CM*QD*AREA*DIA A 411
 FN=CNA*QD*AREA*ALP A 412
 CNB=-CMA A 413
 CYB=-CNA A 414
 CN=CNB*BET+CNR*WY3*DIA/(2.*V) A 415
 TN=CN*QD*AREA*DIA A 416
 FY1=CYB*QD*AREA*BET A 417
 TL=0. A 418
 FD=CD*QD*AREA A 419
 FX3=FY1 A 420
 FY3=-FN A 421
 FZ3=-FD A 422
 GFX=FX3/(VMAS*GRAV) A 423
 GFY=(FY3-VMAS*GRAV*SIN(PH))/(VMAS*GRAV) A 424
 GFZ=(FZ3+VMAS*GRAV*COS(PH))/(VMAS*GRAV) A 425
 ABETA=VMAS*GRAV/(CD*AREA) A 426
 FX=A11*FX3+A21*FY3+A31*FZ3 A 427
 FY=A12*FX3+A22*FY3+A32*FZ3 A 428
 FZ=A13*FX3+A31*FY3+A33*FZ3 A 429
 TX3=TM A 430
 TY3=TN A 431
 TZ3=TL A 432
 TX=TX3*CPSS=TY3*SPSS A 433

```

TY=TX3*SP55+TY3*CP55          A 434
TZ=TZ3                         A 435
IF '4.000-QI) 15,18,14          A 436
14 IF (1.000-QI) 16,10,15          A 437
15 GO TO 69                      A 438
16 IF (2.000-QI) 17,11,15          A 439
17 D2X3=FX/VMAS-2.*DA-C*WEY+B*WEZ+GX  A 440
D2Y3=FY/VMAS-2.*DB-A*WEZ+C*WEX+GY  A 441
D2Z3=FZ/VMAS-2.*DC-B*WEX+A*WEY+GZ  A 442
D2TH3=TY/AIX-WX2*0Z2+AIZ*WZ2*0X2/AIX-DWEY2  A 443
D2PH3=(-TX/AIX+AIZ*WZ2*0Y2/AIX-WY2*0Z2+DPH5*DTH5*STH5*DWEY2)/CTHS  A 444
D2PS3=TZ+AIZ-AIX*WY2*0X2/AIZ+AIX*WX2*0Y2/AIZ+D2PH3*STH5+DPH5*DTH5*  A 445
1CTH5-DWEZ2                      A 446
DELX=H/6.* (DX+2.*DX1+2.*DX2+DX3)  A 447
DELDX=H/6.* (D2X+2.*D2X1+2.*D2X2+D2X3)  A 448
DELY=H/6.* (DY+2.*DY1+2.*DY2+DY3)  A 449
DELDY=H/6.* (D2Y+2.*D2Y1+2.*D2Y2+D2Y3)  A 450
DELZ=H/6.* (DZ+2.*DZ1+2.*DZ2+DZ3)  A 451
DELDZ=H/6.* (D2Z+2.*D2Z1+2.*D2Z2+D2Z3)  A 452
DELTH=H/6.* (DTH+2.*DTH1+2.*DTH2+DTH3)  A 453
DELDTH=H/6.* (D2TH+2.*D2TH1+2.*D2TH2+D2TH3)  A 454
DELPH=H/6.* (DPH+2.*DPH1+2.*DPH2+DPH3)  A 455
DELDPH=H/6.* (D2PH+2.*D2PH1+2.*D2PH2+D2PH3)  A 456
DELPS=H/6.* (DPS+2.*DPS1+2.*DPS2+DPS3)  A 457
DELPSS=H/6.* (D2PS+2.*D2PS1+2.*D2PS2+D2PS3)  A 458
X=X+DELX                         A 459
D=DX+DELDX                        A 460
Y=Y+DELY                         A 461
DY=DY+DELDY                        A 462
Z=Z+DELZ                         A 463
DZ=DZ+DELDZ                        A 464
TH=TH+DELTH                        A 465
DTH=DTH+DELDTH                      A 466
PH=PH+DELPH                        A 467
DPH=DPH+DELDPH                      A 468
PS=PS+DELPS                        A 469
DPS=DPS+DELPSS                      A 470
X5=X                               A 471
DX5=DX                            A 472
Y5=Y                               A 473
DY5=DY                            A 474
Z5=Z                               A 475
DZ5=DZ                            A 476
TH5=TH                            A 477
DTH5=DTH                          A 478
PH5=PH                            A 479
DPH5=DPH                          A 480
PS5=PS                            A 481
DPS5=DPS                          A 482
QI=4.000                           A 483
GO TO 13                            A 484
18 THE=TH*180./PI                  A 485
PH1=PH*180./PI                  A 486
GAMMA=ATAN(DZ5/DY5)*180./PI      A 487
PSI=ATAN(DX5/DY5)*180./PI       A 488
BTL=BT-H/4.                         A 489
BTH=BT+H/4.                         A 490
IF (ALT.LE.0.0) GO TO 20          A 491
IF (T.GT.BTL.AND.T.LT.BTH) GO TO 19  A 492
GO TO 8                            A 493
19 BT=BT+.05                         A 494
C *****                                A 495

```

```

C ***** ****
20  WL=0.0          A 496
    DO 49 LEN=1,NOFX
    WL=WL+SCL(LEN)
    IF (LEN.LT.NOFX) GO TO 21
    WL=.25
    NAL=NALC
21  DO 22 N=1,NAL
    AN=N
    IF (AN*DEL(1,1)-SDOT(LEN)) 22+22,23
22  CONTINUE
    PRINT 84
    GO TO 69
23  K=N
    IF (LEN.GE.NOFX) TMELT=6400.
    TR=TEMPE+.58*(TW(K,LEN)-TEMPE)+.19*(TAW-TEMPE)
    CALL TEMPA (TEMP,ALT)
    CALL TCAT (TCA,TR)
    CALL VISCOT (VISE,TEMPE)
    CALL VISCOT (VISG,TR)
    CALL PRESS (PRE,ALT)
    AM=AMACH
    PBL=PRE*(1.+2.8*AM**2*(SIN(THETC))**2*(2.5+8.*AM*SIN(THETC))/(1.+
16.*AM*SIN(THETC)))
    P=PBL/2116.2
    IF (JIND(LEN).EQ.0) GO TO 24
    ***** ****
    CALL GCPB (GCP,P)
    IF (LEN.GE.NOFX) GCP=.4
    ***** ****
    CALL GASTC (GTC,GCP)
    PR=GCP*GVIS/GTC
    GO TO 25
24  PR=CPA*VISG/TCA
25  HNRF=RHOE*VE*WL/VISE*G
    RHOS=PBE/(1716.*TR)
    ANRR=RHOS*VE*WL/VISG*G
    IF (HNRF.GT.RN(LEN)) GO TO 26
    RF=PR**.5
    HF=.575*TCA/WL*PR**.33*HNRF**.5*(VISG/VISE*RHOS/RHOE)**.5
    GO TO 27
26  RF=PR**.33
    HE=.0296*TCA/WL*PR**.33*HNRF**.8*(VISG/VISE)**.2*(RHOS/RHOE)**.8
27  DTR=VE**2/(2.*G*AJ*CPA)
    TAW=TEMPE+RF*DTR
    QDOTC(LEN)=HE*(TAW-TW(K,LEN))
28  IF (IND(K,LEN).EQ.1) GO TO 33
    IF (TH(K,LEN)-TMELT) 29,33,33
29  TWK=TW(K,LEN)
    IF (LEN.GE.NOFX) GO TO 30
    CALL VTCPC (VT,TWK)
    CALL VCPPC (VC,TWK)
    VRHO(K,LEN)=RHOV
    GO TO 31
30  CALL TCATJ (VT,TWK)
    CALL CPATJ (VC,TWK)
    VRHO(K,LEN)=ATJRHO
31  VTC(K,LEN)=VT
    VCP(K,LEN)=VC
    IF (K.EQ.1) GO TO 36
    P1=VTC(K-1,LEN)*(TW(K-1,LEN)-TW(K,LEN))/(VRHO(K-1,LEN)*VCP(K-1,LFN
1)*DE(K-1,LEN)**2)

```

```

P2=VTC(K,LEN)*(TW(K,LEN)-TW(K+1,LEN))/(VRHO(K,LEN)*VCP(K,LEN)*DE(K
1,LEN)**2) A 558
TW(K,LEN)=TW(K,LEN)+DELT*(P1-P2) A 559
IF (TW(K,LEN)-TMELT) 48,32,32 A 560
32 TW(K,LEN)=TMELT-1. A 561
GO TO 48 A 562
33 TWK=TW(K,LEN) A 563
IF (LEN.GE.NOFX) GO TO 34 A 564
CALL CTCPC (CT,TWK) A 565
CALL CCPP (CC,TWK) A 566
VRHO(K,LEN)=RHOC A 567
GO TO 35 A 568
34 CALL TCATJ (CT,TWK) A 569
CALL CPATJ (CC,TWK) A 570
VRHO(K,LEN)=ATJRHO A 571
35 VCP(K,LEN)=CC A 572
VTC(K,LEN)=CT A 573
IND(K,LEN)=1 A 574
36 P3=DELT/(VCP(K,LEN)*VRHO(K,LEN)*DE(K,LEN))*2. A 575
P4=HE*(TAW-TW(K,LEN)) A 576
P5=VTC(K,LEN)*(TW(K,LEN)-TW(K+1,LEN))/DE(K,LEN) A 577
HR=CPA*TEMPE*RF*VE**2/(2.*G*AJ) A 578
QCOND(LEN)=-VTC(K,LEN)*(TW(K,LEN)-TW(K+1,LEN))/DE(K,LEN) A 579
TW(K,LEN)=TW(K,LEN)+P3*(P4-P5) A 580
IF (TW(K,LEN)-TMELT) 37,38,38 A 581
37 JIND(LEN)=0 A 582
WT(LEN)=0. A 583
GO TO 48 A 584
38 TW(K,LEN)=TMELT A 585
IND(K,LEN)=1 A 586
JIND(LEN)=1 A 587
CALL GCPB (GCP,P) A 588
IF (LEN.GE.NOFX) GCP=.4 A 589
QDOTR=0. A 590
QTOT(LEN)=QDOTC(LEN)+QCOND(LEN) A 591
IF (QTOT(LEN).LE.0.0) GO TO 48 A 592
IF (LEN.LT.NOFX) GO TO 39 A 593
DELH=HR-CPA*TMELT A 594
QSTAR=2000.*2.*DELH A 595
CDOT=QTOT(LEN)/(QSTAR*AT.RHO) A 596
GO TO 43 A 597
39 IF (HNRE-RN(LEN)) 40,40,41 A 598
40 DMD=(QTOT(LEN))/(AKL)+AKL2*(HR-CPA*TMELT)) A 599
GO TO 42 A 600
41 DMD=(QTOT(LEN))/(AKT1+AKT2*(HR-CPA*TMELT)) A 601
42 PXE=11.05E-04/TMELT A 602
TMDOT=DMD*(1.+2.64E+09/(PBL**.67*E**PXE)) A 603
CDOT=TMDOT/RHOV A 604
43 SDOT(LEN)=SDOT(LEN)+CDOT*DELT A 605
JIND(LEN)=1 A 606
DO 44 N=1,NAL A 607
BN=N A 608
IF (BN*DEL(1,1)-SDOT(LEN)) 44,44,45 A 609
44 CONTINUE A 610
PRINT 84 A 611
GO TO 69 A 612
45 NE(N,LEN)=DEL(N,LEN)-(SDOT(LEN)-(BN-1.)*DEL(1,LEN)) A 613
PCM=VCP(N,LEN)*VRHO(N,LEN)*DE(N,LEN)**2/(DELT*VTC(N,LEN)) A 614
IF (PCM-2.) 46,47,47 A 615
46 DE(N,LEN)=0. A 616
CN=N A 617
SDOT(LEN)=CN*TOL A 618
A 619

```

```

1 IND(N+1,LEN)=1
2 IND(N,LEN)=1
3 WT(LEN)=PI*(RL(LEN)+RS(LEN)-2.*SDOT(LEN))*CDOT*RHOC*SOL(LEN)
4 IF (N.EQ.1) GO TO 48
5 DE(N-1,LEN)=0.
6 K=K+1
7 IF (K.LE.NAL) GO TO 28
8 TW(K,LEN)=TW(K,LEN)+DELT*(VTC(K-1,LEN)/(VRHO(K-1,LEN)*VCP(K-1,LEN)
9 1*DE(X-1,LEN)**2)*(TW(K-1,LEN)-TW(K,LEN))-VTC(K,LEN)/(VRHO(K,LEN)*V
10 2CP(K,LEN)*DEL(K,LEN)**2)*(TW(K,LEN)-TW(K+1,LEN)))
11 IF (TW(K,LEN).GT.1060.) TW(K,LEN)=1060.
12 K=K+1
13 TW(K,LEN)=TW(K,LEN)+DELT*(VTC(K-1,LEN)/(VRHO(K-1,LEN)*VCP(K-1,LEN)
14 1*DEL(K-1,LEN)**2)*(TW(K-1,LEN)-TW(K,LEN)))
15 IF (TW(K,LEN).GT.860.) TW(K,LEN)=860.
16 NAL=NALI
17 CONTINUE
18 *****
19 LEN=NOFXP
20 DO 50 N=1,NALS
21 AN=N
22 IF (AN*DEL(1,NOFXP)-SDOT(LEN)) 50,50,51
23 CONTINUE
24 PRINT 85
25 GO TO 69
26 KS=N
27 TMELT=6400.
28 STR=TEMP+.58*(TW(KS,LEN)-TEMP)+.19*(STAW-TEMP)
29 CALL TCAT (STCA,STR)
30 CALL VISCVT (SVISG,STR)
31 IF (JIND(LEN).EQ.0) GO TO 52
32 *****
33 CALL GCPB (GCP,P)
34 IF (LEN.GE.NOFX) GCP=.4
35 *****
36 CALL GASTC (GTC,GCP)
37 SPR=GCP*GVIS/GTC
38 GO TO 53
39 SPR=CPA*SVISG/STCA
40 SRF=SPR**.5
41 CALL PRESS(PRE,ALT)
42 PTS=PRE*((1.2*AMACH**2)**3.5)*((6.0/(17.0*AMACH**2-1.0))**2.5)
43 RHOVS=PTS
44 DV=1./SN**.5*(PTS-PRE)/RHOVS
45 GTAB=((1.0+5.0/(AMACH**2))**1.0-1.0/(1.4*AMACH**2))**0.25
46 SDOTC=0.6**3.3*GTAB*SQRT(RHOVS*SVISG*DVG)*(V**2)/(2.*G*AJ)
47 SDTR=V**2/(2.*G*AJ*CPA)
48 STAW=TEMP+SRF*SDTR
49 STG=TEMP+SDTR
50 STREC=TEMP+SRF*(STG-TEMP)
51 SHE=SDOTC/(STG-TW(KS,LEN))
52 IF (IND(KS,LEN).EQ.1) GO TO 57
53 IF (TW(KS,LEN).GE.TMELT) GO TO 57
54 STWK=TW(KS,LEN)
55 CALL TCATJ (SYT,STWK)
56 CALL CPATJ (SVC,STWK)
57 SARHO(KS)=ATJRHO
58 SATC(KS)=SVT
59 SACP(KS)=SVC
60 IF (KS.EQ.1) GO TO 58
61 TW(KS,LEN)=TW(KS,LEN)+DELT*(SATC(KS-1)/(SARHO(KS-1)*SACP(KS-1)*DE(
62 1*(KS-1,LEN)**2)*(TW(KS-1,LEN)-TW(KS,LEN))-SATC(KS)/(SARHO(KS)*SACP(K
63 1*(KS-1,LEN)**2)*(TW(KS-1,LEN)-TW(KS,LEN)))=SATC(KS)/(SARHO(KS)*SACP(K
64 1*(KS-1,LEN)**2)*(TW(KS-1,LEN)-TW(KS,LEN)))
65 A 620
66 A 621
67 A 622
68 A 623
69 A 624
70 A 625
71 A 626
72 A 627
73 A 628
74 A 629
75 A 630
76 A 631
77 A 632
78 A 633
79 A 634
80 A 635
81 A 636
82 A 637
83 A 638
84 A 639
85 A 640
86 A 641
87 A 642
88 A 643
89 A 644
90 A 645
91 A 646
92 A 647
93 A 648
94 A 649
95 A 650
96 A 651
97 A 652
98 A 653
99 A 654
100 A 655
101 A 656
102 A 657
103 A 658
104 A 659
105 A 660
106 A 661
107 A 662
108 A 663
109 A 664
110 A 665
111 A 666
112 A 667
113 A 668
114 A 669
115 A 670
116 A 671
117 A 672
118 A 673
119 A 674
120 A 675
121 A 676
122 A 677
123 A 678
124 A 679
125 A 680
126 A 681

```

```

2S)*DE(KS,LEN)**2)*(TW(KS,LEN)-TW(KS+1,LEN)))
IF (TW(KS,LEN).LE.TMELT) GO TO 65
TW(KS,LEN)=TMELT-1.
GO TO 65
57  STWK=TW(KS,LEN)
CALL TCATJ (SCT,STWK)
CALL CPATJ (SCC,STWK)
SARHO(KS)=ATJRHO
SATC(KS)=SCT
SACP(KS)=SCC
IND(KS,LEN)=1
58  TW(KS,LEN)=TW(KS,LEN)+DELT/(SACP(KS)*SARHO(KS)*DE(KS,LEN))*(SHE*(S
1TG-TW(KS,LEN))-SATC(KS)/DE(KS,LEN)*(TW(KS,LEN)-TW(KS+1,LEN)))*2.
IF (TW(KS,LEN).GE.TMELT) GO TO 59
JIND(LEN)=0
GO TO 65
59  TW(KS,LEN)=TMELT
HR=CPA*TEH*RF*V**2/(2.*G*AJ)
SQCOND=SATC(KS)*(TW(KS,LEN)-TW(KS+1,LEN))/DE(KS,LEN)
SQTOT=S00TC*SQCOND
IF (SQTOT.LE.0.0) GO TO 65
IND(KS,LEN)=1
JIND(LEN)=1
DELM=HR-CPA*TMELT
QSTARS=2000.*2.*DELM
CDOTS=SQTOT/(QSTARS*ATJRHO)
SDOT(LEN)=SDOT(LEN)+CDOTS*DELT
SS=CDOTS
RX=RX+1./{1.-SIN(THETC)}*(SIN(THETC)*SS-CDOT)
SX=.01745*RX*PHI
IF (SX.LE.0.0) SX=.01943
IF (RX.LE.0.0) RX=.01387
SNR=RX
DO 60 N=1,NALS
BN=N
IF (BN*DEL(1,NOFP)-SDOT(LEN)) 60,60,61
60  CONTINUE
PRINT 84
GO TO 69
61  DE(N,LEN)=DEL(N,LEN)-(SDOT(LEN)-(BN-1.)*DEL(1,NOFP))
PCM=SACP(N)*SARHO(N)*DE(N,LEN)**2/(DELT*SATC(N))
IF (PCM-2.) 62,63,63
62  DE(N,LEN)=0.
SDOT(LEN)=BN*STOL
IND(N,LEN)=1
IND(N+1,LEN)=1
63  IF (N.EQ.1) GO TO 65
NM=N-1
DO 64 I=1,NM
64  DE(I,LEN)=0.
65  KS=KS+1
IF (KS.LE.NALS) GO TO 56
TW(KS,LEN)=TW(KS,LEN)+DELT*(SATC(KS-1)/(SARHO(KS-1)*SACP(KS-1)*DF(
1KS-1,LEN)**2)*(TW(KS-1,LEN)-TW(KS,LEN))-SATC(KS)/(SARHO(KS)*SACP(K
2S)*DE(KS,LEN)**2)*(TW(KS,LEN)-TW(KS+1,LEN)))
IF (TW(KS,LEN).GT.1060.) TW(KS,LEN)=1060.
KS=KS+1
TW(KS,LEN)=TW(KS,LEN)+DELT*(SATC(KS-1)/(SARHO(KS-1)*SACP(KS-1)*DE(
1KS-1,LEN)**2)*(TW(KS-1,LEN)-TW(KS,LEN)))
IF (TW(KS,LEN).GT.860.) TW(KS,LEN)=860.
C ***** TMELT=6760. ***** A 742
A 743

```

```

C ***** A 744
TOTWT=0, A 745
WDOT=0.0 A 746
DO 66 LL=1,NOFX A 747
TOTWT=TOTWT+PI*(RS(LL)*RL(LL)-SDOT(LL))*SDOT(LL)*RHOV*SOL(LL) A 748
66 WDOT=WDOT+WT(LL) A 749
SWTL=.0698*PHI*SNRI**2*SDOT(NOFXP)*ATJRHO A 750
WT(NOFXP)=2.*PI*SNR**2*COOTS*ATJRHO A 751
TOTWT=TOTWT+SWTL A 752
WDOT=WDOT+WT(NOFXP) A 753
VMAS=BI-TOTWT/G A 754
RAD=RADI-SDOT(NOFXM) A 755
ALGTH=ALGTHI-SDOT(NOFXP) A 756
AREA=PI*RAD**2 A 757
SLANT=ALGTH/(COS(THETC)-SNR/RAD*(1.-SIN(THETC))) A 758
ATL=AT-DELT/6. A 759
ATH=AT+DELT/6. A 760
IF (ALT.LE.0.0) GO TO 68 A 761
IF (T.GT.ATL.AND.T.LT.ATH) GO TO 67 A 762
GO TO 8 A 763
67 IF (LLL.LT.8) GO TO 68 A 764
LLL=0 A 765
PRINT 80 A 766
68 PRINT 81, T,X,Y,Z,ALT,GAMMA,VMAS,PSI,V,QD,AMACH,CD,ANR,PHI,THE,ALP A 767
1,BET,PS,ALPT,XE,YE,ZE,FD,FN,GFZ,CLAT,DLON,ABETA,GCIR,AIZ,AIX A 768
PRINT 82, CP,CAN,CPB,CDF,ANRE A 769
PRINT 83, RHO,VIS,AMACHE,TEMPE,RHOE,VE,VISG,PBE A 770
LLL=LLL+1 A 771
AT=4T+1.0 A 772
PRINT 87, (SDOT(I),I=1,NOFXP) A 773
PRINT 70, ((TW(I,J),J=1,NOFX),I=1,NP2) A 774
PRINT 86, TW(NALC1,NOFX),TW(NALC2,NOFX) A 775
PRINT 89, WDOT,TOTWT,RX A 776
PRINT 90, QSTAR A 777
PRINT 91, (TW(I,NOFXP),I=1,NP25) A 778
IF (ALT) 69+69,R A 779
69 CONTINUE A 780
C A 781
C A 782
70 FORMAT (30X,8F8.0) A 783
71 FORMAT (1H1) A 784
72 FORMAT (*JIND*10I4) A 785
73 FORMAT (*IND*8I4/(10X,8I4)) A 786
74 FORMAT (*VCP*8E12.3/(11X,8E12.3)) A 787
75 FORMAT (*VTC*8E12.3/(11X,8E12.3)) A 788
76 FORMAT (*VRHO*8E12.3/(11X,8E12.3)) A 789
77 FORMAT (*DEL*8E12.3/(11X,8E12.3)) A 790
78 FORMAT (*DE*8E12.3/(11X,8E12.3)) A 791
79 FORMAT (*TW*8E12.3/(11X,8E12.3)) A 792
80 FORMAT (12X,4HTIME,14X,1HX,18X,1HY,15X,1HZ,16X,3HALT,13X,5HGAMMA,1 A 793
11X,4HVMAS/30X,4HPSI,15X,3HVEL,13X,2HOD,15X,5HAMACH,11X,2HCD,14X,3H A 794
2REN/30X,3HPHI,16X,5HTHETA,11X,5HALPHA,12X,3HBET,13X,2HPS,14X,4HALP A 795
3T/30X,2HXE,17X,2HYE,16X,2HZE,15X,2HFD,14X,2HFN,14X,3HGFZ/30X,3MLAT A 796
4,16X,4HLONG,12X,4HRETA,13X,4HGCTR,12X,2HIZ,14X,2HIX) A 797
81 FORMAT (1H0,4X,7E17.7/(22X,6E17.7)) A 798
82 FORMAT (10X,5E10.3) A 799
83 FORMAT (5X,AE,0.3) A 800
84 FORMAT (10H OVERHEAT/) A 801
85 FORMAT (*OVERHEATSTAG1*) A 802
86 FORMAT (*OVERHEATSTAG2*) A 803
87 FORMAT (10X*SDOT*9E12.3) A 804
88 FORMAT (86X,FR,0) A 805

```

```
89  FORMAT (10X*WTLOSSRATE:I$•E11.4•LBS/SECANDTOTALWTLOSS:I$•E13.4•LBS) A 806
10NOSERADIS•E11.4•FT•) A 807
90  FORMAT (10X*QSTARIS•E11.4•BTU/LB•) A 808
91  FORMAT (30X•13FA.0) A 809
92  FORMAT(*  SDOT*  10F8.5) A810
      END A811
```

C	SUBROUTINE ATTK (VRZ4, VRY4, ALP, PI)	1
	COMPUTES ANGLE OF ATTACK, ALP.	2
1	IF (VRZ4) 9,5,1	3
2	IF (VRY4) 4,3,2	4
	ALP=ATAN(VRY4/VRZ4)	5
	RETURN	6
3	ALP=0.	7
	RETURN	8
4	ALP=ATAN(VRY4/VRZ4)	9
	RETURN	10
5	IF (VRY4) 6,7,8	11
6	ALP=PI/2.	12
	RETURN	13
7	ALP=0.	14
	RETURN	15
8	ALP=PI/2.	16
	RETURN	17
9	IF (VRY4) 10,11,12	18
10	ALP=PI+ATAN(VRY4/VRZ4)	19
	RETURN	20
11	ALP=PI	21
	RETURN	22
12	ALP=PI+ATAN(VRY4/VRZ4)	23
	RETURN	24
	END	25-

C	SUBROUTINE CDSF (CD,AM,ANR)	1
C	COMPUTES INVISCID DRAG	2
C	COMMON /B/ AREA,RAD,SLANT,SNR,THETC,V	3
C	COMMON /C/ CPM,CP,CAN,CPB,CDF	4
C	PI=3.14159	5
C	G=32.174	6
C	ANOSE=PI*(SNR**2)	7
C	WAREA=PI*RAD*SLANT	8
C	AMACH=AM	9
C	PR=.89	10
C	CPM=1.42857/((AM**2)*((6.0*(AM**2)/5.0)**3.5*(6.0/(7.0*(AM**2)-1.0))**2.0))	11
C	CP=4.0*(SIN(THETC))**2*(2.5*8.0*AMACH*SIN(THETC))/(1.0+16.0*AMACH*SIN(THETC))	12
C	CAN=(.55-CP)*ANOSE/AREA	13
C	CPB=1.001/AM**2	14
C	CALL CDFM (CDF)	15
C	CD=CP+CAN+CPR+CDF	16
C	RETURN	17
C	END	18
C		19
C		20-

```

C      SUBROUTINE LONG (DLG,XE,YE,PI)
THIS SUB COMPUTES LONGITUDE
IF (YE) 1,6,4
1      IF (XE) 2,9,3
2      DLG=PI*ATAN(YE/XE)
      RETURN
3      DLG=ATAN(YE/XE)
      RETURN
4      IF (XE) 5,10,3
5      DLG=PI*ATAN(YE/XE)
      RETURN
6      IF (XE) 7,7,8
7      DLG=PI
      RETURN
8      DLG=0.0
      RETURN
9      DLG=PI/2.
      RETURN
10     DLG=PI/2.
      RETURN
      END

```

```

1
2
3
4
5
6
7
8
9
10
11
12
13
14
15
16
17
18
19
20
21-

```

```

SUBROUTINE INITIAL (SNR,THETC,SLANT)          E 1
C E 2
C E 3
C E 4
C E 5
C E 6
C E 7
C E 8
C E 9
C E 10
C E 11
C E 12
C E 13
C E 14
C E 15
C E 16
C E 17
C E 18
C E 19
C E 20
C E 21
C E 22
C E 23
C E 24
C E 25
C E 26
C E 27
C E 28
C E 29
C E 30
C E 31
C E 32
C E 33
C E 34
C E 35

THIS SUBROUTINE PROVIDES THE NECESSARY GEOMETRY CALCULATIONS AND
CHANGES IN UNITS FOR PROGRAM STRAR6

COMMON /D/ TW(50,12),IND(50,12),JIND(12),VCP(50,12),VTC(50,12),VRH
10(50,12),DEL(50,12),DE(50,12),SDOT(12),XI(12),RS(12),RL(12),SOL(12
2),WT(12),TM(12),TWT(12),SACP(50),SATC(50),SARHO(50),RN(12)
COMMON /F/ NOFX,ALGTH,RADI,POS(11),AZN,GLAT
AZN=AZN/57.296
GLAT=GLAT/57.296
ALGTH=POS(NCFX)/12.
IM=NOFX-1
STH=SIN(THETC)
CTH=COS(THETC)
DO 1 I=1,IM
RN(I)=6.6E-07
SOL(I)=(POS(I+1)-POS(I))/(12.0*CTH)
1 RS(I)=SNR*CTH*(POS(I)/12.0-SNR*(1.0-CTH))*STH/CTH
RN(NOFX)=5.0E-06
RN(NOFX+1)=1.5E-06
RS(NOFX)=SNR
RS(NOFX+1)=SNR
SOL(NOFX)=(POS(1)/12.0-SNR*(1.0-CTH))/CTH
RADI=SNR*CTH*(ALGTH-SNR*(1.0-CTH))*STH/CTH
IM=NOFX-2
DO 2 I=1,IM
2 RL(I)=RS(I+1)
RL(NOFX-1)=RADI
RL(NOFX)=RS(1)
SLANT=0.0
DO 3 I=1,NOFX
3 SLANT=SLANT+SOL(I)
RETURN
END

```

```

SUBROUTINE CDFM (CDF)
C THIS SUB COMPUTES SKIN FRICTION DRAG
COMMON /B/ AREA,RAD,SLANT,SNR,THETC,V
COMMON /D/ TW(50,12),IND(50,12),JIND(12),VCP(50,12),VTC(50,12),VRH
10(50,12),DEL(50,12),DE(50,12),SDOT(12),XI(12),RS(12),RL(12),SOL(12)
2,WT(12),TM(12),TWT(12),SACP(50),SATC(50),SARHO(50),RN(12)
COMMON /E/ NOFXM,NAL,ALT,AMACH,QA,AMACHE,TEMPE,RHOE,VE,VISG,PBE,AN
1RE
TWA=0.
CDF=0.0
SR=SNR/RAD
PI=3.14159
CALL RHOF (RHO,ALT)
CALL VISCO (VIS,ALT)
CALL VSD (VS,ALT)
CALL PRESS (PRE,ALT)
CALL TEMPA (TEMP,ALT)
AMACH=V/VS
TEMPE=TEMP*(1.+.0966*AMACH*SIN(THETC)+.2267*(AMACH*SIN(THETC))**2)
VE=V*(1.-1.4/AMACH**2*(AMACH*SIN(THETC))**1.9)**.5
AMACHE=AMACH*(VE/V)*(TEMP/TEMPE)**.5
R1=1716.
AM=AMACH
AM=AMACH
PBE=PRE*(1.+2.8*AM**2*(SIN(THETC))**2*(2.5+8.*AM*SIN(THETC))/(1.+
16.*AM*SIN(THETC)))
RHOE=PBE/(R1*TEMPE)
CALL VISCOT (VISG,TEMPE)
AREA=PI*RAD**2
ANRE=RHOE*VE*SLANT*32.174/VISG
COTT=1./TAN(THETC)
DO 2 K=1,NOFXM
DO 1 K=1,NAL
IF (DE(M,K).LE.0.) GO TO 1
TWA=TWA+TW(M,K)/8.
1 CONTINUE
2 CONTINUE
RE=RHO*V*SLANT/VIS
IF (ANRE-2.0E-07) 3,4,4
3 HSH=.5*(TWA/TEMPE)+.0374*(AMACHE)**2
CDF1=(1.53/RE**.5)*(VE/V)**1.5*(PBE/PRE)**.5*(TEMP/TEMPE)**.185*(1
1./HSH)**.185*COTT
CDF=CDF1*((1.+9.8842*SR-44.0235*SR**2+70.383*SR**3)-(SR**1.69+2.1*
1*SR)*ALOG1((RE)))
GO TO 5
4 HSH=.5*(TWA/TEMPE)+.0388*(AMACHE)**2
CDF1=(.0776/RE**.2)*(VE/V)**1.8*(PBE/PRE)**.8*(TEMP/TEMPE)**.58*(1
1./HSH)**.58*OTT
CDF=CDF1*(1.-(.8+.052*AMACH)*SR)
CDF=CDF
RETURN
END

```

SUBROUTINE VISCOT (VISG,TEMP)
THIS SUB COMPUTES VISCOSITY OF AIR VS TEMP
UNITS ARE LB/FT-SEC
IF (TEMP-2460.) 2,1,1
VISG=41.0E-10*TEMP+2.4414E-05
RETURN
IF (TEMP-1160.) 4,3,3
VISG=100.769E-10*TEMP+.97108E-05
RETURN
IF (TEMP-760.) 6,5,5
VISG=132.5E-10*TEMP+.603E-05
RETURN
VISG=166.666E-10*TEMP+.34334E-05
RETURN
END

1
2
3
4
5
6
7
8
9
10
11
12
13
14
15-

C SUBROUTINE PRESS (PE,ALT)
C COMPUTES PRESSURE PER ALTITUDE
LBS/FT2
PE=2116.2*EXP(-4.25509E-05*ALT)
RETURN
END

H 1
H 2
H 3
H 4
H 5
H 6-

```

C      SUBROUTINE VSD (VS,ALT)
C      THIS SUR COMPUTES SPEED OF SOUND
C      UNITS ARE FT/SEC.
C      IF (ALT>36000.) 1,1,2
1      VS=1116.9-.412E-02*ALT
      RETURN
2      IF (ALT>82000.) 3,3,4
3      VS=968.5
      RETURN
4      IF (ALT>154000.) 5,5,6
5      VS=814.+.191E-02*ALT
      RETURN
6      IF (ALT>172000.) 7,7,8
7      VS=1106.
      RETURN
8      IF (ALT>262000.) 9,9,10
9      VS=1527.+.245E-02*ALT
      RETURN
10     VS=846.
      RETURN
      END

```

I	1
I	2
I	3
I	4
I	5
I	6
I	7
I	8
I	9
I	10
I	11
I	12
I	13
I	14
I	15
I	16
I	17
I	18
I	19
I	20
I	21-

```

C SUBROUTINE GCPB (GCP,PBL)
C THIS SUB COMPUTES ABLATIVE GAS SPECIFIC HEAT
C UNITS ARE BTU/LB-DEG R
C IF (PBL<10.) 2,1,1
1 GCP=-.228* ALOG(PBL)+3.22
RETURN
2 IF (PBL<.009) 4,3,3
3 GCP=-.30882* ALOG(PBL)+3.4
RETURN
4 IF (PBL<.0001) 6,5,5
5 GCP=.7374* ALOG(PBL)+8.37
RETURN
6 IF (PBL<1.0E-05) 8,7,7
7 GCP=.12333* ALOG(PBL)+2.709
RETURN
8 GCP=1.284
RETURN
END

```

1 2 3 4 5 6 7 8 9
10 11 12 13 14 15 16 17 18-

```

SUBROUTINE TEMPA (TEMP,ALT)
C THIS SUB COMPUTES TEMP OF AIR VS ALT      TO 300,000
C TEMP IS IN DEGREES RANKINE
C IF (ALT>261000.) 2,1,1
1  TEMP=298.2
RETURN
2  IF (ALT>175500.) 4,3,3
3  TEMP=-2.463E-03*ALT+941.04
RETURN
4  IF (ALT>154000.) 6,5,5
5  TEMP=508.79
RETURN
6  IF (ALT>85000.) 8,7,7
7  TEMP=1.627E-03*ALT+256.05
RETURN
8  IF (ALT>35700.) 10,9,9
9  TEMP=389.99
RETURN
10 TEMP=-36.77E-04*ALT+518.7
RETURN
END

```

K	1
K	2
K	3
K	4
K	5
K	6
K	7
K	8
K	9
K	10
K	11
K	12
K	13
K	14
K	15
K	16
K	17
K	18
K	19
K	20
K	21-

SUBROUTINE TCAT (TCA,TEMP)
C THIS SUB COMPUTES THERMAL COND. OF AIR VS. TEMP
C UNITS ARE BTU/SEC-FT-DEGREE RANKINE
IF (TEMP-2960.) 2,1,1
1 TCA=6.0E-06*TEMP+.03324
GO TO 9
2 IF (TEMP-2460.) 4,3,3
3 TCA=7.8E-06*TEMP+.028
GO TO 9
4 IF (TEMP-1960.) 6,5,5
5 TCA=14.2E-06*TEMP+.01217
GO TO 9
6 IF (TEMP-1160.) 8,7,7
7 TCA=16.5E-06*TEMP+.00766
GO TO 9
8 TCA=19.28E-06*TEMP+.00444
9 TCA=TCA/3600.
RETURN
END

1
2
3
4
5
6
7
8
9
10
11
12
13
14
15
16
17
18
19-

```

SUBROUTINE VCPFC (VCP,TEMP)
C THIS SUB COMPUTES VIRGIN SPECIFIC HEAT VS. TEMP
C UNITS ARE BTU/LA-DEG R
C IF (TEMP=400.) 2,1,1
1 VCP=.55E-04*TEMP+.123
RETURN
2 IF (TEMP=2000.) 4,3,3
3 VCP=.19E-03*TEMP+.69
RETURN
4 IF (TEMP=1060.) 6,5,5
5 VCP=.554E-03*TEMP-.0423
RETURN
6 IF (TEMP=860.) 8,7,7
7 VCP=.975E-03*TEMP-.4865
RETURN
8 IF (TEMP=660.) 10,9,9
9 VCP=.21E-03*TEMP+.1714
RETURN
10 VCP=.375E-03*TEMP+.0625
RETURN
END

```

M	1
M	2
M	3
M	4
M	5
M	6
M	7
M	8
M	9
M	10
M	11
M	12
M	13
M	14
M	15
M	16
M	17
M	18
M	19
M	20
M	21-

```

C SUBROUTINE RHOF (RHO,ALT) 1
C THIS SUB COMPUTES DENSITY OF AIR VS. ALTITUDE 2
COMMON /A/ RE 3
GALT=RE*ALT/(RE+ALT) 4
RHO0=.0023769 5
R=53.352 6
E=2.7183 7
IF (GALT-36089.) 1,1,2 8
T=518.688-3.56616*GALT/1000. 9
RHO=RHO0*(T/518.668)**4.256 10
RETURN 11
1 IF (GALT-82021.) 3,3,4 12
3 EP2=(36089.-GALT)/(R*389.988) 13
RHO=RHO0*.297069*E**EP2 14
RETURN 15
4 IF (GALT-154199.) 5,5,6 16
5 T=254.988+1.64592*GALT/1000. 17
RHO=RHO0*.0326657*(T/389.988)**-12.388 18
RETURN 19
6 IF (GALT-173885.) 7,7,8 20
7 EP4=(154199.-GALT)/(R*508.788) 21
RHO=RHO0*.00121179*E**EP4 22
RETURN 23
8 IF (GALT-259186.) 9,9,10 24
9 T=938.088-2.46888*GALT/1000. 25
RHO=RHO0*5.86784E-04*(T/508.788)**6.592 26
RETURN 27
10 IF (GALT-295276.) 11,11,12 28
11 EP6=(259186.-GALT)/(R*298.186) 29
RHO=RHO0*1.73274E-05*E**EP6 30
RETURN 31
12 T=-349.912+2.19456*GALT/1000. 32
RHO=RHO0*1.792653E-06*(T/298.186)**-9.541 33
RETURN 34
END 35-

```

	0	1
C	0	2
C	0	3
	0	4
	0	5
1	0	6
VIS=2.35E-07	0	7
RETURN	0	8
2	0	9
IF (ALT-270000.) 2,1,1	0	10
3	0	11
VIS=-1.509E-12*ALT+6.333E-07	0	12
RETURN	0	13
4	0	14
IF (ALT-156000.) 6,5,5	0	15
5	0	16
VIS=3.68E-07	0	17
RETURN	0	18
6	0	19
IF (ALT-83250.) 8,7,7	0	20
7	0	21-
VIS=.973E-12*ALT+2.172E-07	0	
RETURN	0	
8	0	
IF (ALT-34500.) 10,9,9	0	
9	0	
VIS=2.969E-07	0	
RETURN	0	
10	0	
VIS=-2.124E-12*ALT+3.737E-07	0	
RETURN	0	
END	0	

```

C SUBROUTINE CCP (CCP,TEMP)
C THIS SUB COMPUTES CHAR SPECIFIC HEAT VS. TEMP
C UNITS ARE BTU/LA-DEG R
C IF (TEMP>6000.) 2+1+1
1 CCP=.4
RETURN
2 IF (TEMP>4000.) 4+3+3
3 CCP=.125E-04*TEMP+.3215
RETURN
4 IF (TEMP>3000.) 6+5+5
5 CCP=.305E-04*TEMP+.2495
RETURN
6 IF (TEMP>2000.) 8+7+7
7 CCP=.47E-04*TEMP+.14
RETURN
8 IF (TEMP>1060.) 10+9+9
9 CCP=.207E-03*TEMP-.14
RETURN
10 CCP=.96E-04*TEMP-.02236
RETURN
END

```

1 2 3 4 5 6 7 8 9
10 11 12 13 14 15 16 17 18 19 20 21-

```

C      SUBROUTINE SSLP (VRZ4,VRX4,BET,PI)
1      COMPUTES ANGLE OF SIDESLIP
2      IF (VRZ4) 9-5-1
3      IF (VRX4) 4-3-2
4      BET=ATAN(VRX4/VRZ4)
5      RETURN
6      BET=0.
7      RETURN
8      BET=ATAN(VRX4/VRZ4)
9      RETURN
10     IF (VRX4) 6-7-8
11     BET=PI/2.
12     RETURN
13     BET=0.
14     RETURN
15     BET=PI/2.
16     RETURN
17     IF (VRX4) 10-11-12
18     BET=PI+ATAN(VRX4/VRZ4)
19     RETURN
20     BET=PI
21     RETURN
22     BET=PI+ATAN(VRX4/VRZ4)
23     RETURN
24     END

```

0	1
2	2
0	3
0	4
0	5
0	6
0	7
0	8
0	9
0	10
0	11
0	12
0	13
0	14
0	15
0	16
0	17
0	18
0	19
0	20
0	21
0	22
0	23
0	24
0	25-

C SUBROUTINE VTCPC (VTC,TEMP)
1 UNITS ARE BTU/FT-SEC-DEG R
2 IF (TEMP=4000.) 2,1,i
3 VTC=.705E-07*TEMP+.58E-04
4 RETURN
5 IF (TEMP=2000.) 4,3,3
6 VTC=.695E-07*TEMP+.62E-04
7 RETURN
8 VTC=.7376E-07*TEMP+.5347E-04
9 RETURN
10 END

R 1
RR 2
RRR 3
RRRR 4
RRRRR 5
RRRRRR 6
RRRRRRR 7
RRRRRRRR 8
RRRRRRRRR 9
RRRRRRRRRR 10
RRRRRRRRRRR 11-

```

C      SUBROUTINE ACMQ (C,A)
      COMPUTES DAMPING COEFFICIENT
      IF (A.GT.17.) GO TO 1
      IF (A.GT.9.) GO TO 2
      IF (A.GT.7.) GO TO 3
      IF (A.GT.5.) GO TO 4
      IF (A.GT.4.) GO TO 5
      IF (A.GT.3.) GO TO 6
      C=2.5*A-10.
      RETURN
1     C=-2.4
      RETURN
2     C=.05*A-3.25
      RETURN
3     C=.1*A-3.7
      RETURN
4     C=.3*A-5.3
      RETURN
5     C=.7*A-7.3
      RETURN
6     C=A-8.5
      RETURN
      END

```

S	1
S	2
S	3
S	4
S	5
S	6
S	7
S	8
S	9
S	10
S	11
S	12
S	13
S	14
S	15
S	16
S	17
S	18
S	19
S	20
S	21
S	22
S	23-

C SUBROUTINE GASTC (GTC,GCP)
C COMPUTES ABLATIVE GAS THERMAL
C CONDUCTIVITY. BTU/SEC-FT-DEG.R.
C GTC=4.429E-05* (GCP+.297)
C RETURN
C END

1
2
3
4
5
6-

C

SUBROUTINE ACNA (C,A)
COMPUTES NORMAL FORCE COEFF.
CNA PER DEGREE
C=.034
RETURN
END

1
2
3
4
5
6-

SUBROUTINE CTCPC (CTC,TEMP)
THIS SUB COMPUTES CHAR THERMAL CONDUCTIVITY VS. TEMP
UNITS ARE BTU/FT-SEC-DEG R
IF (TEMP-6000.) 1,2,2
CTC=.56E-07*TEMP+.053E-03
RETURN
2 CTC=.389E-03
RETURN
END

1
2
3
4
5
6
7
8
9-

SUBROUTINE CPATJ (S,T)
C COMPUTES SPEC HEAT OF ATJ GRAPHITE VS. TEMP
C UNITS BTU/LB-DEG-R
IF (T-2000.) 1,2,2
1 IF (T-1000.) 4,3,3
2 S=3.482E-05*T+.35536
RETURN
3 S=1.25E-04*T+.175
RETURN
4 S=3.409E-04*T-.0409
RETURN
END

1
2
3
4
5
6
7
8
9
10
11
12-

SUBROUTINE TCATJ (C,T)
C COMPUTES THER. COND. OF ATJ GRAPHITE VS. TEMP
1 IF (T-3460.) 1,3,3
2 IF (T-2460.) 2,4,4
3 IF (T-1460.) 6,5,5
4 C=(2.E-05*T+.2808)/60.
5 RETURN
6 C=.35/60.
7 RETURN
8 C=(-1.84E-04*T+.80264)/60.
9 RETURN
10 C=(-3.82E-04*T+1.091)/60.
11 RETURN
12 END

1
2
3
4
5
6
7
8
9
10
11
12
13
14-

AFWL-TR-68-61

APPENDIX II

STRAB-6 PROGRAM LISTING FOR MULTIPLE CASE RUN

WJM62, 6,2500, 65000. MOULDS, 627A, WODE.
RUN J(S,40000, , , ,77000)
RFL(40000)
STRAB62.

PROGRAM STRAB62 (INPUT,OUTPUT)

C 6 DEGREE TRAJECTORY WITH ABLATION HEATING AND STAG

COMMON /A/ RE

COMMON /B/ AREA,RAD,SLANT,SNR,THETC,V

COMMON /C/ CPM,CP,CAN,CPR,CDF

COMMON /D/ TW(50,12),IND(50,12),JIND(12),VCP(50,12)VTC(50,12),VRH
10(50,12),DEL(50,12),DE(50,12)SDOT(12),XI(12),RS(12),RL(12),SOL(12
2),WT(12),TM(12),TWT(12),SACP(50),SATC(50),SARHO(50),RN(12),QSTR(12
3),QDOTC(12),QTOT(12),QCOND(12)

COMMON /E/ NOFXM,NAL,ALT,AMACH,QD,AMACHE,TEMPE, RHOE,VE,VISG,PRE,AN
IRE

COMMON /F/ NOFX,ALGTH,RADI,POS(11),AZN,GLAT

C VEHICLE DATA

C IF NOFX IS CHANGED CHANGE FORMAT 103

C IF CONE ANGLE IS CHANGED SUB CDSF MUST BE CHANGED

700 1500 READ 1500,NCASE,(POS(J),J=1,8)
FORMAT(11,7A10,A8)

PRINT 1501,NCASE,(POS(J),J=1,8)
1501 FORMAT(1H1,30X,7A10,A8)

ETC.

```

DATA SNR,THETC,BI,SM/.0208,.07853,6.27836,.59718/*      A 13
DATA PI,E,AJ,GRAV,C/3.14159,2.7183,778.,32.174,32.174/    A 17
DATA REQ,PE,ET,WE/20.927491E+06,.673852E-02,.08181333,0.7292E-04/ A 18
DATA NOFX,NAL,NALC,NALS/8,4,10,35/*                           A 19
DATA DELT,DT,H,BT,AT/.05,.0005,.001,.05,1./                 A 20
DATA AZN,GLAT,DLON,CMMA/154.,33.996,-107.5,-22.39/*      A 21
DATA V,Z,ALPHA/15167.,2.50E+05,7./*                          A 22
DATA (POS(1),I=1,8)/6.607,18.370,30.533,42.496,54.459,66.422,78.38/* A 23
AREA=PI*RAD**2                                              A 24
SLANT=ALGTH/(COS(THETC)-SNR/RAD*(1.-SIN(THETC)))        A 25
ATL=AT-DELT/6.                                              A 26
ATH=AT+DELT/6.                                              A 27
IF (ALT.LE.0.0) GO TO 68                                    A 28
IF (T.GT.ATL.AND.T.LT.ATH) GO TO 67                      A 29
GO TO 8                                                       A 30
67  IF (LL1,LT,0) GO TO 68
LL1=0
PRINT 80
80
68  PRINT BI, T,X,Y,Z,ALT,GAMMA,VMAS,PSI,V, QD,ANACH,CD,ANR,PHI,THE,ALP A 767
    1,BET,PS,ALPT,XE,YE,ZE,FD,PN,GFZ,CLAT,DLON,ABETA,GCIR,AIZ,AIX A 768
    PRINT B2, CP,CAN,CPL,CDF,ANRE A 769
    PRINT B3, RHO,VIS,ANACHE,TRPPE,RHOE,VE,VISG,PRE A 770
    LL1=LL1+1
    AT=AT+1.0

```

/*These data cards can be removed and read into program by multi-case read statement.

```
PRINT 87, (SDOT(I), I=1,NOFXP) A 773
PRINT 70, ((TW(I,J), J=1,NOFX), I=1, NP2) A 774
PRINT 88, TW(NALC1,NOFX), TW(NALC2,NOFX) A 775
PRINT 89, WDOT,TOTWT,RX A 776
PRINT 90, QSTAR A 777
PRINT 91, (TW(I,NOFXP), I=1, NP2S) A 778
IF (ALT) 69,69,8 A 779
IF (NCASE.NE.0) GO TO 700 A 780
69 C A 781
C A 782
FORMAT (30X,8F8.0) A 783
FORMAT (1H1) A 784
```

AFWL-TR-68-61

APPENDIX III
SAMPLE CASE OUTPUT

TIME	X PSI PHI XF LAT	Y VEL THETA LONG	Z QD ALPHA ZETA BETA	ALT			GAMMA			VMAS		
				AMACH	BET	FO	CO	PS	FN	REN	ALPT	GFZ
0.	0. 1.0394009E+00 0. 3.3617746E+01	0. 1.5167000E+04 0. -1.0750000E+02	2.5000000E+05 8.9088100E+00 0. 0.	2.5000000E+05 1.6585019E+01 0. 0.	2.5000000E+05 1.6585019E+01 0. 0.	-2.2390000E+01 1.394224E+01 0. 5.1000000E-01	-2.2390000E+01 1.394224E+01 0. 5.1000000E-01	0. 0. 0. 2.3080000E+01	0.2783600E+00 3.374106E+04 7.0E+00 0.	0. 0. 0. 0.		
1.0000000E+00	2.1707650E-01 1.932203E-03 1.071799E-02 1.757827E+07 1.460E-02 1.019E-07 SNOT 0.	1.4023633E+04 1.5176582E+04 1.5176582E+04 -7.9831134E-02 6.144736E+03 -1.077998E+02 3.747E-03 1.034E-01 0. 0.	2.4420767E+05 1.1740936E+01 5.1578359E+00 1.761207E+07 1.2290268E+03 1.5223763E+04 0. 0. 0.	2.4421349E+05 1.6344308E+01 8.1503590E+02 1.9297120E+07 1.5223763E+04 0. 0.	2.4421349E+05 1.6344308E+01 8.1503590E+02 1.9297120E+07 1.5223763E+04 0. 0.	-2.2495287E+01 1.522152E+01 6.2831227E+00 2.2912934E+00 5.1000000E-01 0. 0.	-2.2495287E+01 1.522152E+01 6.2831227E+00 2.2912934E+00 5.1000000E-01 0. 0.	0.2783600E+00 4.3663176E+04 5.315835E+00 -3.049921E+01 2.3080000E+01	0. 0. 0. 0. 0.			
2.0000000E+00	610 546 544 544 544 544 SNOT 0.	593 584 545 544 544 544 0.	579 575 545 544 544 544 0.	573 545 544 544 544 544 0.	571 545 544 544 544 544 0.	593 585 578 572 572 567 0.	567 545 544 544 544 544 0.	567 545 544 544 544 544 0.	0.2783600E+00 4.3663176E+04 5.315835E+00 -3.049921E+01 2.3080000E+01	0. 0. 0. 0. 0.		
3.0000000E+00	871 953 944 SNOT 0.	676 551 544 0.	629 550 544 0.	612 547 544 0.	599 547 544 0.	586 546 544 0.	579 546 544 544 544 544 0.	572 545 544 544 544 544 0.	559 545 544 544 544 544 0.	0.2783600E+00 4.3663176E+04 5.315835E+00 -3.049921E+01 2.3080000E+01	0. 0. 0. 0. 0.	
4.0000000E+00	9.3634264E-01 3.6812522E-03 1.1207642E-02 1.758n437E-07 1.467E-02 1.328E-07 SNOT 0.	2.8047303E+04 1.5190215E+04 -5.575552E+01 1.229456E+04 -1.074599E+02 3.85E-03 9.08E-02 1.317E-01 0.	2.3838059E+05 1.5321872E+01 5.49952E+01 1.174501E+07 1.6671809E+03 3.1459681E+04 0.	2.3838059E+05 1.6109963E+01 5.6678651E+01 1.8664377E+00 3.1459681E+04 0.	2.3838059E+05 1.6109963E+01 5.6678651E+01 1.8664377E+00 3.1459681E+04 0.	-2.2601020E+01 1.2221335E+01 1.2565903E+01 5.1000000E-01 2.3080000E+01	-2.2601020E+01 1.2221335E+01 1.2565903E+01 5.1000000E-01 2.3080000E+01	0.2783600E+00 4.3663176E+04 5.315835E+00 -3.049921E+01 2.3080000E+01	0. 0. 0. 0. 0.			
5.0000000E+00	673 550 544 544 544 544 SNOT 0.	639 549 544 544 544 544 0.	622 547 544 544 544 544 0.	605 547 544 544 544 544 0.	600 547 544 544 544 544 0.	597 547 544 544 544 544 0.	597 547 544 544 544 544 0.	597 547 544 544 544 544 0.	0.2783600E+00 4.3663176E+04 5.315835E+00 -3.049921E+01 2.3080000E+01	0. 0. 0. 0. 0.		
6.0000000E+00	779 569 546 SNOT 0.	739 562 546 0.	707 559 545 0.	680 557 545 0.	641 553 545 0.	626 551 545 0.	613 550 545 0.	603 549 545 0.	586 548 544 0.	0.2783600E+00 4.3663176E+04 5.315835E+00 -3.049921E+01 2.3080000E+01	0. 0. 0. 0. 0.	

5.3070469E-03	1.5201846E+04	1.9812465E+01	1.5881724E+01	1.1877684E-01	6.899143E+04
1.171130E+02	-1.257004E+00	-4.4033889E+00	1.270951E+00	1.8844709E+01	4.4033888E+00
1.7582632E+07	1.84120E+04	1.1733778E+07	2.540946E+00	-3.2028473E+00	-4.6832508E-01
3.371197E+01	-1.0733991E+02	1.5750261E+03	4.7708987E+04	5.100000E+01	2.300000E+01
1.466E+02	6.739E-04	3.969E-03	1.200E+05		
1.715E-07	2.823E-07	1.303E+01	5.421E+02	4.110E-07	1.514E+04
1.1	0.	0.	0.	0.	0.
WTLOSSRATEIS 0.	LBS/SECANDTOTALWTLOSSIS	0.	LBSANDNOSERADIS 2.0800E-02FT	554	
QSTARTS 0.	BTU/LB	839	792	754	698
		586	581	576	572
		550	549	548	548
4.0000000E+00	3.5091109E+00	5.6094057E+04	2.2664794E+05	2.2672359E+05	-2.2817118E+01
	6.5437958E+03	1.5213389E+04	2.5401848E+01	1.56592465E+01	6.2703600E+00
	1.1761076E+02	-1.0329000E+00	-4.7921722E+00	1.989069E+00	8.5707484E+04
	1.7584801E+07	2.4580738E+04	1.1722038E+07	3.013942E+00	2.5130669E+01
	3.3682934E+01	-1.0741999E+02	1.7022705E+03	6.3971352E+04	4.791722E+00
	2.195E-02	6.739E-04	4.082E-03	7.097E-02	1.434E+05
	2.195E-07	2.912E-07	1.589E-01	5.589E-02	5.019E-07
1.	0.	0.	0.	1.515E+04	3.865E+05
WTLOSSRATEIS 0.	LBS/SECANDTOTALWTLOSSIS	0.	LBSANDNOSERADIS 2.0800E-02FT	563	
QSTARTS 0.	BTU/LB	697	842	726	695
		603	596	561	576
		555	554	553	552
5.0000000E-11	5.2969119E+00	7.0116701E+04	2.2073285E+05	2.2085044E+05	-2.2924659E+01
	8.2545221E+03	1.5224966E+04	3.2311195E+01	1.5442517E+01	6.2703600E+00
	1.1245779E+02	6.958708E+01	4.6595769E+01	-6.890516E+01	1.057193E+05
	1.7586695E+07	3.0133030E+04	1.1706281E+07	2.935225E+00	4.6595769E+01
	3.3644650E+01	-1.0739988E+02	2.223255E+03	8.0246683E+04	-3.965344E+01
	2.768E-07	6.739E-04	4.197E-03	6.311E-02	1.19E+05
	2.768E-07	3.000E-07	1.277E+01	5.757E+02	6.143E+07
1.	0.	0.	0.	1.516E+04	3.875E+05
WTLOSSRATEIS 0.	LBS/SECANDTOTALWTLOSSIS	0.	LBSANDNOSERADIS 2.0800E-02FT	572	

QSTARTS 0.	BTU/LB	954 619 561	892 604 559	842 597 556	602 591 555	766 586 554	741 582 554	717 578 553	696 574 553	679 574 553	664 571 552	650 568 546	636 565 546
6.0000000E+00	7.675045E+00 1.140396E+02 1.0859402E+02 1.7589063E+07 3.36143E+01 3.515E-02	8.4139046E+04 1.5236403E+04 1.9306128E+00 3.6878014E+04 -1.0737987E+02 5.264E+01	2.1478733E+05 4.0795372E+01 4.4368445E+00 1.1092506E+07 2.0559880E+03 5.6335456E+04	2.1495622E+05 1.5231041E+01 -1.9350533E+00 -3.0081282E+00 9.6535456E+04 5.1000000E+01	-2.3028772E+01 9.099106E+01 3.7695339E+01 6.636061E+00 5.1000000E+01	6.2763600E+00 1.2933782E+05 4.108445E+00 -3.3870110E+01 2.3080000E+01							
5.0000000E+00	0.	0.	0.	0.	0.	0.	0.	0.	0.	0.	0.	0.	0.
6.0000000E+00	7.675045E+00 1.140396E+02 1.0859402E+02 1.7589063E+07 3.36143E+01 3.515E-02	8.4139046E+04 1.5236403E+04 1.9306128E+00 3.6878014E+04 -1.0737987E+02 5.264E+01	2.1478733E+05 4.0795372E+01 4.4368445E+00 1.1092506E+07 2.0559880E+03 5.6335456E+04	2.1495622E+05 1.5231041E+01 -1.9350533E+00 -3.0081282E+00 9.6535456E+04 5.1000000E+01	-2.3028772E+01 9.099106E+01 3.7695339E+01 6.636061E+00 5.1000000E+01	6.2763600E+00 1.2933782E+05 4.108445E+00 -3.3870110E+01 2.3080000E+01							
WTLOSSRATEIS 0.	BTU/LB	1014 635 568	942 625 565	885 617 564	840 610 562	802 603 561	771 597 559	744 592 558	722 587 558	702 583 557	685 579 557	670 576 548	657 573 546
QSTARTS 0.	BTU/LB	1014 635 568	942 625 565	885 617 564	840 610 562	802 603 561	771 597 559	744 592 558	722 587 558	702 583 557	685 579 557	670 576 548	657 573 546
7.0000000E+00	1.00867732E+01 1.4311788E+02 1.128524E+02 -3.549790E+01 1.759115E+07 4.302219E+04 -1.07358E+01	9.0161217E+04 1.5247948E+04 -3.549790E+01 2.8738864E+01 1.1678716E+07 -1.07358E+02 3.044E+02	2.0061210E+05 5.148558E+01 1.5048658E+01 3.6746377E+01 1.1678716E+07 2.608850E+03 1.1263880E+05	2.0061210E+05 5.148558E+01 1.5048658E+01 3.6746377E+01 3.927198E+00 5.271643E+01 5.1000000E+01	-2.3132163E+01 7.110766E+02 4.3979803E+01 5.271643E+01 5.1000000E+01	6.2763600E+00 1.577332E+05 2.807388E+01 -4.079878E+01 2.3080000E+01							
4.000E-07	3.179E-07	1.252E+01	6.089E-02	9.262E-07	1.518E+04	3.898E-05	9.678E-01	0.	0.	0.	0.	0.	0.
WTLOSSRATEIS 0.	BTU/LB	1002 650 574	960 590 572	888 582 570	776 577 568	754 574 548	738 572 547	720 570 547	712 567 544	704 567 544	696 563 544	688 562 544	675 562 542
QSTARTS 0.	BTU/LB	1002 650 574	960 590 572	888 582 570	776 577 568	754 574 548	738 572 547	720 570 547	712 567 544	704 567 544	696 563 544	688 562 544	675 562 542
TIME	X PSI PHI XF LAT	954 561 544 544 0.	999 640 549 544 0.	932 631 548 544 0.	879 622 568 544 0.	837 615 566 544 0.	802 608 565 544 0.	772 602 564 544 0.	747 597 563 544 0.	725 592 562 544 0.	706 588 562 544 0.	686 584 550 544 0.	675 580 550 544 0.
8.0000000E+00	1.4381999E+01 1.3913329E+02 1.169185E+02 1.7591225E+07 3.3545661E+01	1.1210205E+05 1.5259356E+04 -2.134005E+00 4.9168840E+04 -1.0733988E+02	2.02306641E+05 6.011759E+01 -3.609579E+00 1.1664908E+01 2.416173E+03	2.02306641E+05 1.4823682E+01 2.162250E+00 5.207241E+00 1.2915398E+03	-2.3241265E+01 7.366991E+02 5.026139E+01 -6.588763E+00 5.1000000E+01	6.2763600E+00 1.609483E+05 3.670959E+00 -4.784986E+01 2.3080000E+01							

1.492E-02	0.737E-04	4.555E-03	4.531E-02	3.008E+05	0.	0.	0.
3.472E-07	3.240E-07	1.239E+01	6.254E+02	1.141E+02	1.519E+04	3.006E-05	1.224E+00
5.001	0.	0.	0.	0.	0.	0.	0.
0.	0.	0.	0.	0.	0.	0.	0.
1011	906	849	812	787	768	757	758
615	601	592	586	562	549	548	740
553	551	550	549	549	544	544	724
545	545	545	545	544	544	544	711
544	544	544	544	544	544	544	700
544	544	544	544	544	544	544	690
544	544	544	544	544	544	544	665
WTLOSSRATEIS 0.	LBS/SECANDTOTALWTLOSSIS	0.	LBSANDNOSERADIUS 2.000E-02FT	608			
OSTARIS 0.	ATU/LB	1159	1061	984	923	874	801
666	654	654	635	627	619	613	772
562	579	577	574	573	571	570	568
562	562	562	562	570	569	568	567
9.0000000E+00	1.7769750E+01	1.2620338E+05	1.9674934E+05	1.9714632E+05	-2.1349328E+01	6.2783600E+00	
1.4980356E-02	1.5270724E+00	7.8877520E+01	1.4677316E+01	6.4934661E+02	2.2990097E+05		
1.1172722E+02	1.5733559E+00	1.6204045E+00	1.5533704E+00	5.6544901E+01	1.6204055E+01		
1.7595266E+07	5.50910E+04	1.1650883E+07	5.5312056E+07	4.6923173E+00	-1.975126E+01		
1.7595266E+07	5.50910E+04	2.9880398E+03	1.45568170E+05	5.1000000E+01	2.3080000E+01		
3.3511208E+01	-7.0713199E+01	4.062E-02	3.643E+05	1.921E+06	0.	0.	0.
1.685E-02	6.736E-04	4.070E-07	1.4086E-06	1.921E+04	3.917E-05	1.551E+00	0.
6.765E-07	3.350E-07	1.427E+01	6.419E+02	1.4086E-06	1.921E+04	3.917E-05	1.551E+00
5.907	0.	0.	0.	0.	0.	0.	0.
1061	949	900	890	822	800	788	785
628	613	603	596	591	567	565	764
556	554	552	551	550	550	550	747
545	545	545	545	545	545	545	732
544	544	544	544	544	544	544	720
544	544	544	544	544	544	544	710
544	544	544	544	544	544	544	681
WTLOSSRATEIS 0.	LBS/SECANDTOTALWTLOSSIS	0.	LBSANDNOSERADIUS 2.000E-02FT	622			
OSTARIS 0.	ATU/LB	1244	1130	1041	970	914	868
681	669	658	648	639	631	623	799
589	586	584	581	579	577	576	575
589	586	584	581	579	577	576	557
1.0000000E+01	2.2179234E+01	1.4022131E+05	1.9070245E+05	1.9117014E+05	-2.3450480E+01	6.2783600E+00	
2.0068170E+02	1.528092E+04	9.7046730E+01	1.4425528E+01	6.0280028E+02	2.7536953E+05		
1.121066E+02	6.505710E+01	1.3319386E+00	-6.1675739E+01	6.2827999E+01	1.3374986E+00		
1.7597280E+07	6.145221E+04	1.1637262E+07	6.31493270E+00	4.768773E+00	-4.0767238E+01		
3.3476892E+01	-1.0726992E+02	4.424E+05	3.1034183E+03	1.61892328E+03	5.1000000E+01	2.3080000E+01	
1.498E-02	6.736E-04	4.070E-07	1.688E-02	4.424E+05	3.928E+04	1.947E+00	0.
A.314E-07	3.44AE-07	1.215E+01	6.503E+02	1.772E-06	1.522E+04	3.928E+04	1.947E+00
SHOT 0.	0.	0.	0.	0.	0.	0.	0.
1111	993	931	889	858	834	821	813
660	624	614	607	601	597	594	790
559	556	554	553	552	551	551	771
546	546	545	545	545	545	545	755
544	544	544	544	544	544	544	741
544	544	544	544	544	544	544	730
544	544	544	544	544	544	544	694
WTLOSSRATEIS 0.	ATU/LB	1241	1204	1102	1022	947	905
681	663	671	661	651	642	634	627
589	591	588	586	586	586	586	581
589	591	588	586	586	586	586	581
*WTLOSSRATEIS 0.	LBS/SECANDTOTALWTLOSSIS	0.	LBSANDNOSERADIUS 2.000E-02FT	636			

1.100000E+01	2.7141567E+01	1.5424243E+05	1.840552E+05	1.0517134E+05	-2.3559782E+01	6.2763600E+00
1.1A47117E+02	1.5293059E+04	1.1664707E+02	1.4248242E+01	5.9491393E-02	5.9491393E-02	3.222690E+05
1.1607068E+02	-2.1130595E+00	-2.5018530E+00	2.1425745E+00	6.911021E+01	6.911021E+01	2.5018530E+00
1.1759927E+07	6.759267E+04	1.072795E+02	7.6343866E+00	-1.0515935E+01	-1.0515935E+01	-4.727204E+01
3.3442475E+01	-1.072795E+02	3.1446013E+03	1.7817803E+05	5.1000000E-01	5.1000000E-01	2.3060000E+01
1.492E-02 6.735E-04 4.931E-03 3.341E-02 5.383E-05	1.203E+01 6.747E+02 2.158E+06	1.523E+04 3.949E+05 2.498E+00	0.	0.	0.	0.
1.016E-06 3.539E-07 1.203E+01 6.747E+02 2.158E+06	0.	0.	0.	0.	0.	0.
5D0T 0.	0.	0.	0.	0.	0.	0.
WTLOSSRATEIS 0.	BTU/LB	WTLOSS/SECANDTOTALWTLOSSIS	0.	WTLOSSANDNOSERADIS 2.0800E-02FT	451	
1.1227757E+02	1.285	1167	1076	1003	944	856
1.1227757E+02	698	625	616	612	607	604
1.2612230E+07	563	559	557	556	555	553
3.344038E+01	547	546	546	545	545	545
1.493E-02 6.735E+04 5.060E+03 3.034E-02 6.566E+05	544	544	544	544	544	544
1.2336E-06 3.630E-07 1.191E+01 6.910E+02 2.679E+06	544	544	544	544	544	544
5D0T 0.	0.	0.	0.	0.	0.	0.
WTLOSSRATEIS 0.	BTU/LB	WTLOSS/SECANDTOTALWTLOSSIS	0.	WTLOSSANDNOSERADIS 2.0800E-02FT	451	
3.1786459E+01	1.6826004E+05	1.7847741E+05	1.7915075E+05	-2.3664901E+01	6.2783600E+00	
2.226869E+02	1.3040988E+04	1.4473631E+02	1.4652232E+01	5.597081E+02	3.894401E+05	
1.1227757E+02	2.5862576E+00	2.3753900E+00	-2.5191627E+00	7.5392619E+01	2.375390E+00	
1.2612230E+07	1.3334220E+04	1.609111E+07	8.786103E+00	1.2622072E+01	-4.061989E+01	
3.344038E+01	1.0725999E+02	3.3419180E+03	1.9544488E+05	9.1000000E-01	2.3060000E+01	
1.493E-02 6.735E+04 5.060E+03 3.034E-02 6.566E+05	0.	0.	0.	0.	0.	0.
1.2336E-06 3.630E-07 1.191E+01 6.910E+02 2.679E+06	1.924E+04 3.952E+05 3.177E+00	0.	0.	0.	0.	0.
5D0T 0.	0.	0.	0.	0.	0.	0.
WTLOSSRATEIS 0.	BTU/LB	WTLOSS/SECANDTOTALWTLOSSIS	0.	WTLOSSANDNOSERADIS 2.0800E-02FT	666	
1.1567	1375	1237	1134	1052	985	911
1.1567	714	701	687	676	665	656
613	609	596	603	600	598	596
1.300000E+01	3.7894799E+01	1.8227671E+05	1.7231992E+05	1.7311017E+05	-2.3769556E+01	6.2783600E+00
2.3877170E+02	1.5314961E+04	1.7734565E+02	1.788634E+01	5.188634E+01	5.188634E+01	4.703151E+05
1.1577706E+02	-2.5029488E+00	-1.5942149E+00	2.596809E+00	8.167520E+01	8.167520E+01	1.0942149E+00
1.7403180E+07	7.9812485E+04	1.1595622E+07	9.9548854E+00	-1.283843E+01	-1.283843E+01	-4.641493E+01
1.337178E+01	-1.0240035E+02	3.5986894E+03	2.1092497E+05	9.1000000E-01	9.1000000E-01	2.3060000E+01
1.493E-02 6.735E+04 5.060E+03 3.034E-02 6.566E+05	0.	0.	0.	0.	0.	0.
1.512E+06 3.630E-07 1.179E+01 6.992E+02 3.370E+06	1.523E+04 3.963E+05 4.043E+00	0.	0.	0.	0.	0.
5D0T 0.	0.	0.	0.	0.	0.	0.
WTLOSSRATEIS 0.	BTU/LB	WTLOSS/SECANDTOTALWTLOSSIS	0.	WTLOSSANDNOSERADIS 2.0800E-02FT	734	
1.1227757E+02	1220	1061	1012	967	933	906
1.1227757E+02	667	647	636	626	622	617
1.2612230E+07	567	563	560	559	557	556
3.344038E+01	547	547	546	546	546	546
1.493E-02 6.735E+04 5.060E+03 3.034E-02 6.566E+05	544	544	544	544	544	544
1.2336E-06 3.630E-07 1.191E+01 6.910E+02 2.679E+06	544	544	544	544	544	544
5D0T 0.	0.	0.	0.	0.	0.	0.
WTLOSSRATEIS 0.	BTU/LB	WTLOSS/SECANDTOTALWTLOSSIS	0.	WTLOSSANDNOSERADIS 2.0800E-02FT	666	
1.1567	1375	1237	1134	1052	985	911
1.1567	714	701	687	676	665	656
613	609	596	603	600	598	596
1.300000E+01	3.7894799E+01	1.8227671E+05	1.7231992E+05	1.7311017E+05	-2.3769556E+01	6.2783600E+00
2.3877170E+02	1.5314961E+04	1.7734565E+02	1.788634E+01	5.188634E+01	5.188634E+01	4.703151E+05
1.1577706E+02	-2.5029488E+00	-1.5942149E+00	2.596809E+00	8.167520E+01	8.167520E+01	1.0942149E+00
1.7403180E+07	7.9812485E+04	1.1595622E+07	9.9548854E+00	-1.283843E+01	-1.283843E+01	-4.641493E+01
1.337178E+01	-1.0240035E+02	3.5986894E+03	2.1092497E+05	9.1000000E-01	9.1000000E-01	2.3060000E+01
1.493E-02 6.735E+04 5.060E+03 3.034E-02 6.566E+05	0.	0.	0.	0.	0.	0.
1.512E+06 3.630E-07 1.179E+01 6.992E+02 3.370E+06	1.523E+04 3.963E+05 4.043E+00	0.	0.	0.	0.	0.
5D0T 0.	0.	0.	0.	0.	0.	0.
WTLOSSRATEIS 0.	BTU/LB	WTLOSS/SECANDTOTALWTLOSSIS	0.	WTLOSSANDNOSERADIS 2.0800E-02FT	748	
1.1567	1375	1237	1134	1052	985	911
1.1567	714	701	687	676	665	656
613	609	596	603	600	598	596
1.300000E+01	3.7894799E+01	1.8227671E+05	1.7231992E+05	1.7311017E+05	-2.3769556E+01	6.2783600E+00
2.3877170E+02	1.5314961E+04	1.7734565E+02	1.788634E+01	5.188634E+01	5.188634E+01	4.703151E+05
1.1577706E+02	-2.5029488E+00	-1.5942149E+00	2.596809E+00	8.167520E+01	8.167520E+01	1.0942149E+00
1.7403180E+07	7.9812485E+04	1.1595622E+07	9.9548854E+00	-1.283843E+01	-1.283843E+01	-4.641493E+01
1.337178E+01	-1.0240035E+02	3.5986894E+03	2.1092497E+05	9.1000000E-01	9.1000000E-01	2.3060000E+01
1.493E-02 6.735E+04 5.060E+03 3.034E-02 6.566E+05	0.	0.	0.	0.	0.	0.
1.512E+06 3.630E-07 1.179E+01 6.992E+02 3.370E+06	1.523E+04 3.963E+05 4.043E+00	0.	0.	0.	0.	0.
5D0T 0.	0.	0.	0.	0.	0.	0.

LOSSRATES 0.		RTU/LA		LBS/SEC AND TOTAL LOSSIS		0.		LBS AND NOSE RADIUS 2.0000E-02FT		753 683	
1.4000000E+01	4.3341126E+01	1.9629119E+05	1.6663146E+05	1.6704201E+05	1.6704201E+05	1.2956791E+01	1.2956791E+01	4.8235510E-02	4.8235510E-02	5.8630253E+05	5.8630253E+05
2.5599236E+02	2.5325611E+04	2.2125979E+02	1.7731313E+01	-2.502164E+01	-2.502164E+01	1.7731313E+00	1.7731313E+00	1.440147E+01	1.440147E+01	1.3308828E+01	1.3308828E+01
1.1204902E+02	2.6024638E+00	1.077162E+00	1.1561716E+00	1.1561716E+00	1.1561716E+00	2.2731682E+05	2.2731682E+05	5.100000E-01	5.100000E-01	2.308000E+01	2.308000E+01
1.7605094E+07	8.6011395E+04	1.0722009E+02	3.876004E+03	3.876004E+03	3.876004E+03	0.	0.	0.	0.	0.	0.
1.499E-02	6.735E-07	1.170E+03	4.354E-06	1.526E+04	3.974E-05	5.219E+00	5.219E+00	0.	0.	0.	0.
1.004E-06	3.680E-07	1.170E+03	4.354E-02	4.354E-06	1.526E+04	3.974E-05	5.219E+00	5.219E+00	0.	0.	0.
5.007	0.	0.	0.	0.	0.	0.	0.	0.	0.	0.	0.
1.342	1179	1099	1049	1011	982	965	949	949	949	949	949
696	671	656	649	643	638	634	634	634	634	634	634
578	570	567	565	563	562	561	561	561	561	561	561
549	548	548	547	547	547	547	547	547	547	547	547
545	545	545	544	544	544	544	544	544	544	544	544
544	544	544	544	544	544	544	544	544	544	544	544
0.	0.	0.	0.	0.	0.	0.	0.	0.	0.	0.	0.
LOSSRATES 0.		RTU/LA		LBS/SEC AND TOTAL LOSSIS		0.		LBS AND NOSE RADIUS 2.0000E-02FT		699	
0.	0.	0.	0.	0.	0.	0.	0.	0.	0.	0.	0.
1.5000000E+01	5.0261525E+01	2.103077E+05	1.5591357E+05	1.6096542E+05	1.6096542E+05	1.3866177E+01	1.3866177E+01	4.72258E-02	4.72258E-02	7.3150487E+05	7.3150487E+05
2.4918789E-02	1.5335992E-04	2.7621350E-02	1.1632230E-02	2.1032230E-02	2.1032230E-02	9.424271E+00	9.424271E+00	1.4502537E+00	1.4502537E+00	1.4502537E+00	1.4502537E+00
1.1544586E+02	-2.1510748E+00	-1.1567795E+00	-1.1567795E+00	1.333636E+00	1.333636E+00	-4.1706170E+01	-4.1706170E+01	-4.958730E+01	-4.958730E+01	-4.958730E+01	-4.958730E+01
1.760492E+07	9.218122E+04	1.1567795E+00	1.333636E+00	2.4372149E+05	2.4372149E+05	5.100000E+01	5.100000E+01	2.308000E+01	2.308000E+01	2.308000E+01	2.308000E+01
3.3304595E+01	-1.072014E+02	4.1330579E+03	4.1330579E+03	0.	0.	0.	0.	0.	0.	0.	0.
1.499E-02	6.735E-07	1.170E+03	2.144E+02	2.137E+02	2.137E+02	1.988E+04	1.988E+04	6.767E+00	6.767E+00	0.	0.
2.140E-06	3.680E-07	1.170E+03	2.137E+02	2.137E+02	2.137E+02	1.988E+04	1.988E+04	6.767E+00	6.767E+00	0.	0.
5.007	0.	0.	0.	0.	0.	0.	0.	0.	0.	0.	0.
1411	1235	1148	1093	1053	1023	1005	992	992	992	992	992
712	684	670	660	653	648	645	645	645	645	645	645
580	574	571	566	563	562	561	561	561	561	561	561
551	549	549	548	548	548	547	547	547	547	547	547
545	545	545	544	544	544	544	544	544	544	544	544
544	544	544	544	544	544	544	544	544	544	544	544
0.	0.	0.	0.	0.	0.	0.	0.	0.	0.	0.	0.
ATR15 0.		RTU/LA		LBS/SEC AND TOTAL LOSSIS		0.		LBS AND NOSE RADIUS 2.0000E-02FT		717	
0.	5.0.	2025	1700	1465	1328	1212	1122	1049	998	937	895
782	762	744	728	715	702	691	681	672	664	656	644
639	634	630	626	623	620	618	616	615	614	614	614
TIME	X	Y	Z	0	0	ALT	ALT	0	0	0	0
PAI	VEL	0	0	0	0	AHCH	AHCH	0	0	0	0
PHI	THETA	0	0	0	0	BET	BET	0	0	0	0
XF	YE	0	0	0	0	FD	FD	0	0	0	0
LAT	LONG	0	0	0	0	GCIR	GCIR	0	0	0	0
0.	0.	0.	0.	0.	0.	0.	0.	0.	0.	0.	0.
1.4000000E+01	9.4861058E+01	2.241970E+05	1.5366519E+05	1.5406234E+05	1.5406234E+05	2.4059095E+01	2.4059095E+01	6.2783600E+00	6.2783600E+00	9.1525671E+05	9.1525671E+05
1.3477400E+02	1.5346097E+06	1.3571440E+02	1.367531E+02	1.367531E+02	1.367531E+02	4.043911E+02	4.043911E+02	9.1525671E+05	9.1525671E+05	9.1525671E+05	9.1525671E+05

1.13669795E-02 2.06788500E-01 3.9423557E-01 -1.7378043E-01 1.0052448E-02
 1.7606649E-07 9.0284511E-04 1.1621856E-01 1.50956116E-01 5.0036538E-00
 3.32700860E-01 -1.0718020E-02 1.098E-02 1.7635E-06 2.0613750E-05 5.1000000E-01
 2.938E-06 3.879E-07 6.735E-04 5.19E-03 1.498E-02 7.32E-06 1.928E-06 3.999E-05 6.780E-00 2.308000E-01

5001 0. 1486 1207 1202 1142 1099 1066 1040 1041 0. 0. 0.
 7286 698 682 672 664 658 655 655 980 0.
 586 578 575 572 568 568 568 568 940 0.
 552 550 549 549 549 549 549 549 910 0.
 545 545 545 545 545 545 545 545 889 0.
 544 544 544 544 544 544 544 544 867 0.
 544 544 544 544 544 544 544 544 813 0.

WTLOSSRATEIS 0. RTU/LB 685/SECANDTOTALWTLOSSIS 0. LOSANDNOSERADIS 2.0800E-02PT

0.74046918E-01 2.3832232E-05 1.4738711E-05 1.8738864E-05 -2.419351E-01 6.273360E-00
 2.07404866E-02 1.95556302E-04 4.4209780E-02 1.398411E-01 3.854400E-01 1.154423E-00
 1.0324732E-02 2.3936164E-00 9.265087E-01 -2.3733225E-00 1.068008E-02 9.295087E-01
 1.7616681E-07 1.0441926E-05 1.1539907E-07 1.840907E-01 1.509195E-01 4.658327E-01
 3.322554E-01 -1.0716628E-02 4.8510681E-03 2.7656510E-05 5.100000E-01 2.308000E-01

1.7000000E-01 6.38846918E-01 2.3832232E-05 1.4738711E-05 1.8738864E-05 -2.419351E-01 6.273360E-00
 2.07404866E-02 1.95556302E-04 4.4209780E-02 1.398411E-01 3.854400E-01 1.154423E-00
 1.0324732E-02 2.3936164E-00 9.265087E-01 -2.3733225E-00 1.068008E-02 9.295087E-01
 1.7616681E-07 1.0441926E-05 1.1539907E-07 1.840907E-01 1.509195E-01 4.658327E-01
 3.322554E-01 -1.0716628E-02 4.8510681E-03 2.7656510E-05 5.100000E-01 2.308000E-01

1.759E-06 3.619E-07 6.735E-04 5.19E-03 1.498E-02 1.732E-06 1.928E-06 3.012E-05 1.150E-01 0. 0.
 9001 0. 1364 1262 1197 1150 1114 1095 1095 0. 0. 0.
 746 712 695 684 675 669 665 665 1030 0.
 991 963 959 959 956 954 952 952 989 0.
 553 552 551 550 549 549 549 549 950 0.
 549 548 548 548 548 548 548 548 920 0.
 545 545 544 544 544 544 544 544 895 0.
 545 545 545 545 545 545 545 545 859 0.

WTLOSSRATEIS 0. RTU/LB 685/SECANDTOTALWTLOSSIS 0. LOSANDNOSERADIS 2.0800E-02PT

1.4000000E-01 2.92322085E-05 1.4107951E-05 1.425952E-05 -2.4299920E-01 6.273360E-00
 2.0031116E-02 1.9365921E-04 5.665921E-02 1.414361E-01 3.4902213E-02 1.1550608E-00
 1.023316E-02 7.719941E-01 1.11727E-02 7.475812E-01 1.3086982E-02 1.11727E-02
 1.7612492E-07 1.0555600E-05 1.125941E-02 2.1430784E-01 2.3140784E-01 5.1134083E-01
 3.32009868E-01 -1.071636E-02 5.3000642E-03 2.9300400E-05 5.1000000E-01 2.308000E-01

1.4017E-02 6.735E-04 5.00E-03 1.429E-02 1.305E-05 1.530E-04 4.037E-05 1.615E-01 0. 0.
 9001 0. 1660 1440 1329 1258 1208 1169 1167 1167 0. 0. 0.
 768 726 709 696 687 676 676 676 1094 0.
 997 968 953 950 951 950 950 950 1036 0.
 555 553 552 551 551 550 550 550 991 0.
 549 548 548 547 547 546 546 546 955 0.
 545 545 545 544 544 544 544 544 920 0.
 545 545 545 545 545 545 545 545 896 0.

WTLOSSRATEIS 0. RTU/LB 685/SECANDTOTALWTLOSSIS 0. LOSANDNOSERADIS 2.0800E-02PT

1.4000000E-01 2.92322085E-05 1.4107951E-05 1.425952E-05 -2.4299920E-01 6.273360E-00
 2.0031116E-02 1.9365921E-04 5.665921E-02 1.414361E-01 3.4902213E-02 1.1550608E-00
 1.023316E-02 7.719941E-01 1.11727E-02 7.475812E-01 1.3086982E-02 1.11727E-02
 1.7612492E-07 1.0555600E-05 1.125941E-02 2.1430784E-01 2.3140784E-01 5.1134083E-01
 3.32009868E-01 -1.071636E-02 5.3000642E-03 2.9300400E-05 5.1000000E-01 2.308000E-01

1.4017E-02 6.735E-04 5.00E-03 1.429E-02 1.305E-05 1.530E-04 4.037E-05 1.615E-01 0. 0.
 9001 0. 1660 1440 1329 1258 1208 1169 1167 1167 0. 0. 0.
 768 726 709 696 687 676 676 676 1094 0.
 997 968 953 950 951 950 950 950 1036 0.
 555 553 552 551 551 550 550 550 991 0.
 549 548 548 547 547 546 546 546 955 0.
 545 545 545 544 544 544 544 544 920 0.
 545 545 545 545 545 545 545 545 896 0.

WLOSSRATEIS N. OSTARIS 0.		LHS/SECANDTOTALWTLOSSIS 0.		LBSANDNOSERADIS 2.0800E-02FT			
561	556	556	555	555	555	555	1160
547	545	545	546	546	546	546	1084
546	545	545	545	545	545	545	1040
							936
							637
2.2000000E+01	1.0674520E+02	3.0830039E+05	1.19556025E+05	1.1782398E+05	-2.4718546E+01	6.27836C0E+00	
	4.0507221E+02	1.5390041E+04	1.05038060E+03	1.4914639E+01	2.769914E+02	4.052456E+06	
	1.477229E+02	-1.680097E+00	-3.042728E+02	1.721235E+00	1.3020492E+02	3.842728E+02	
	1.761947E+07	1.0700043E+05	1.1469946E+07	6.982207E+01	-2.335696E+00	-6.658130E-01	
	3.2062627E+01	-1.0700041E+02	6.7197269E+03	3.5885364E+05	5.100000E+01	2.3080000E+01	
	1.4922E-02	6.737E-04	4.61E-03	7.757E+07	1.118E+05	4.699E+01	
	1.4000000E-05	3.18E-07	1.239E+01	6.35E+02	4.22E+05	1.533E+04	
	5907	0.	0.	0.	0.	0.	
WTLOSSRATEIS N. OSTARIS 0.	ATU/LA	LHS/SECANDTOTALWTLOSSIS 0.	LBSANDNOSERADIS 2.0800E-02FT				
2124	1825	1674	1576	1506	1451	1420	960
651	800	774	757	745	735	730	1400
626	612	605	600	597	594	592	1284
563	560	556	557	556	555	555	1200
547	547	546	546	546	546	546	1135
546	545	545	545	545	545	515	1095
							967
WTLOSSRATEIS N. OSTARIS 0.	ATU/LA	LHS/SECANDTOTALWTLOSSIS 0.	LBSANDNOSERADIS 2.0800E-02FT				
4390	3396	2663	2133	1797	1575	1414	960
321	888	860	836	814	795	770	1059
703	696	690	669	660	677	673	636
							959
							710
2.3000000E+01	1.1606612E+02	3.22286667E+05	1.0910768E+05	1.158354E+05	-2.4825204E+01	6.2783300E+00	
	4.4441915E+02	1.53900386E+04	2.045365E+03	1.499768E+01	2.6796779E+02	6.5691916E+06	
	1.1466330E+02	1.427387E+00	4.0749556E+02	1.375029E+00	1.4450371E+02	4.8745256E+02	
	1.762192E+07	1.01179803E+05	1.1455916E+07	6.396796E+01	3.9454066E+01	-7.317247E+01	
	3.3020146E+01	-1.0704096E+02	7.046521E+03	3.7333334E+05	5.1000000E+01	2.3080000E+01	
	1.4799E-02	6.7717E-04	4.4595E-03	1.5156E+07			
	1.8600E-05	3.2594E-07	1.249E+01	6.249E+02	5.694E+05	1.531E+04	
	5907	0.	0.	0.	0.	0.	
WTLOSSRATEIS N. OSTARIS 0.	ATU/LA	LHS/SECANDTOTALWTLOSSIS 0.	LBSANDNOSERADIS 2.0800E-02FT				
4994	3764	2940	2346	1934	1671	1468	998
944	909	879	853	830	810	792	750
712	705	699	694	684	685	692	670
							643
TIME	X	Y	Z	00	00	00	
	PC1	VEL		AMACH	CO	VMAS	
	PC2	THETA		BET	PS	REN	
	XP	YF		FD	PN	ALPT	
	LAT	LONG		BETA	QF2	QF1	
2.4500000E+01	1.2614421E+02	3.3625501E+05	1.0263060E+05	1.04932647E+05	-2.493328E+01	6.27833600E+00	

690	669	618	651	645	640	638	2047
584	578	575	572	571	569	568	1777
552	551	550	550	549	549	549	1592
549	548	548	548	547	547	547	1454
OSTARIS 0.	RTU/LB	6400	5978	4854	3921	3161	2135
		1108	1055	1009	969	935	881
		773	764	756	749	743	738
WTLOSSRATE15 9.7374E-04 LBS/SEC AND TOTALWTLOSSIS		1.0924E-03 LBSANDNOSEERRDIS 2.7088E-02 FT					860
3.0000000E+01		1.9415298E+02	4.1937260E+05	6.3431662E+04	6.7638309E+04	-2.5561643E+01	6.2782796E+00
		4.5493393E-02	1.51549119E+04	1.7967255E+04	1.5617826E+01	3.3701085E+02	6.0622161E+07
		1.1552821E+02	-6.3148071E+02	4.6528955E+03	1.044372E+01	1.684435E+02	4.652859E+03
		1.7632037E+07	1.367024E+05	1.1358009E+07	6.555272E+02	3.072579E+00	-3.6718282E+00
		3.27886897E+01	-1.06903168E+02	5.5509558E+03	4.9820732E+05	5.1000000E-01	2.3080000E+01
		1.4699E-02 1.435E-03 4.086E-03 1.341E-02 1.6220E+08					
		1.566E-04 2.969E-07 1.289E+01 5.695E+02 4.284E+04	1.509E+04 4.597E-05 4.107E+02				
		510T 0.	0.	0.	0.	0.	0.
		3864	3216	2863	2686	0.	0.
		1232	1080	1009	966	946	915
		702	678	667	659	653	649
		588	581	578	575	573	572
		553	552	551	550	550	550
		550	549	549	548	548	548
WTLOSSRATE15 9.63117E-04 LBS/SEC AND TOTALWTLOSSIS		2.58554E-03 LBSANDNOSEERRDIS 3.0470E-02 FT					860
OSTARIS 0.	RTU/LB	6400	6400	5156	4176	3394	2767
		1140	1082	1034	992	955	924
		784	774	766	759	752	747
		510T 0.	0.	0.	0.	0.	0.
3.1000000E+01		2.06507334E+02	4.3299196E+05	5.6907058E+04	6.13862985E+04	-2.5673637E+01	6.2782652E+00
		5.475747E-02	1.5048255E+04	2.3907315E+04	1.55376945E+01	3.2987327E+02	8.1444728E+07
		1.1583447E+02	2.2928605E+01	-1.63818699E+01	-2.816731E+01	1.946779E+02	1.6301669E+01
		1.76320353E+07	8.962950E+05	1.1344205E+07	8.5154908E+02	-1.437823E+02	-4.654248E+00
		3.272972E+01	-1.0688380E+02	5.6710814E+03	5.06838062E+05	5.1000000E-01	2.3080000E+01
		1.471E-02 1.696E-03 4.146E-03 1.222E-02 1.504E+08					
		2.111E-04 2.969E-07 1.289E+01 5.673E+02 5.560E+04	1.498E+04 4.722E-05 5.412E+02				
		510T 0.	0.	0.	0.	0.	0.
		4148	3452	3102	0.	0.	0.
		1311	1140	1059	1028	1030	1041
		715	689	676	668	663	659
		592	585	581	578	576	575
		554	553	552	551	550	550
		551	550	549	548	548	548
WTLOSSRATE15 1.1771E-03 LBS/SEC AND TOTALWTLOSSIS		3.04698E-03 LBSANDNOSEERRDIS 3.3143E-02 FT					860
OSTARIS 0.	RTU/LB	6400	6400	5557	4481	3631	2957
		1112	1111	1059	1015	976	943
		794	785	776	768	762	757
		510T 0.	0.	0.	0.	0.	0.
		X	Y	Z	Q	AL	AMACH
		PSI	VEL	THETA	ALPHA	BET	CD
		1.1	Y	Z	Z	FO	PS
		XF	LONG	LONG	BETA	GCIR	FN
		LAT				12	IX

3.200000E+01	2.1916943E+02	4.4648801E+05	5.040296E+04	5.5168526E+04	*2.5782704E+01	6.2762479E+00
5.791008E-02	1.490709E+04	3.1570669E+04	1.5391944E+01	3.2028597E+02	1.0990181E+08	
1.157786E+02	6.3920392E+02	3.670442E+03	3.58318E+02	2.0105108E+02	3.670442E+03	
1.0734924E+07	1.9553492E+05	1.133507E+07	1.0921373E+03	4.2550177E+00	-5.846131E+00	
1.2719328E+01	-1.0664473E+02	5.840212E+03	5.2442198E+05	5.1000000E+01	2.3080000E+01	
2.842E-04	2.038E-02	3.034225E+03	1.03E+01	2.047E+00		
2.969E-07	1.224E+01	5.664E+02	7.191E+01	1.484E+04	4.952E+05	6.965E+02
SNOT 0.	0.	0.	0.	0.	0.	1.220E-02
0.	446	3694	4232	4804	5029	5138
1401	1206	1132	1153	1172	1182	1182
729	700	686	678	673	670	668
596	588	584	581	579	578	577
556	554	553	552	551	551	551
552	550	550	549	549	549	549
WTLOSSRATEIS 2.1233E-03LBS/SECANDTOTALWTLOSSIS		3.6074E-03LBSANDNOSERADIS 3.6353E-02FT				
OSTARIS 0.	RTU/LA	6400	5947	4800	3869	3166
1205	1140	1085	1038	997	962	932
806	795	786	778	772	766	761
146	SNOT 0.	0.	0.	0.	0.	0.
3.300000E+01	2.3600755E+02	4.5982552E+05	4.3946687E+04	4.9001293E+04	*2.5891421E+01	6.2781990E+00
5.8101429E-02	1.4721659E+04	*1.366030E+04	1.5200439E+01	3.1563017E+02	1.4570261E+08	
2.055339E+02	2.6563303E+02	3.683340E+02	2.529353E+02	2.033341E+02	3.683305E+02	
1.7664270E+07	2.0136999E+05	1.1316953E+07	1.4097204E+03	5.8283006E+01	-7.4150638E+01	
3.6884555E+01	-1.0684545E+02	5.9269317E+03	5.3828916E+05	5.1000000E+01	2.3080000E+01	
1.476E-04	2.512E-03	4.332E-03	9.017E-03	2.631E+08		
2.969E-07	1.262E+01	5.606E+02	9.259E-04	1.466E+04	5.092E-05	8.908E+02
SNOT 0.	0.	0.	0.	0.	0.	1.752E-02
1501	1279	1262	1293	1320	1342	1352
745	713	698	691	687	685	684
601	592	598	585	583	581	580
597	553	554	553	553	552	552
553	551	551	550	550	549	549
WTLOSSRATEIS 2.2213E-03LBS/SECANDTOTALWTLOSSIS		5.1812E-03LBSANDNOSERADIS 4.0316E-02FT				
OSTARIS 0.	RTU/LA	6400	6400	5174	4167	3388
1239	1170	1112	1062	1019	982	932
817	806	797	788	781	776	771
146	SNOT 0.	0.	0.	0.	0.	0.
3.401000E+01	2.4497912E+02	4.7295956E+05	3.7556386E+04	4.2905430E+04	*2.6001686E+01	6.2781758E+00
5.0331901E-02	1.4430170E+04	5.3572294E+04	1.4951131E+01	3.117063E+02	1.02291094E+08	
1.594520E+02	2.203593E+02	3.6884319E+02	2.136776E+02	3.6884319E+02		
1.7637582E+07	2.0711004E+05	1.1303509E+07	1.803059E+05	7.2542527E+01	-9.3641090E+01	
3.6651266E+01	-1.0682212E+02	6.0016335E+03	5.5392817E+05	5.1000000E+01	2.3080000E+01	
1.480E-04	2.959E-03	4.47E-03	8.893E-03	3.351E+06		
2.969E-07	1.247E+01	5.558E+02	1.185E+02	1.462E+04	5.201E+05	1.130E+03
SNOT 0.	0.	0.	0.	0.	0.	1.148E-05
1613	1409	1452	1498	1528	1550	1487
763	727	714	708	705	703	710
606	597	592	599	587	585	584
558	556	555	554	553	553	553
554	552	551	551	549	549	549

WTLOSSRAT15 5.6249E-03BLT/LB	5.9280E-03LBSANDNOSERADIS 4.3532E-02FT	1060
OSTARIS 6.252RE+03BLT/LB		860
6400 6400 6400 5660 4521 3650 2975 2462 2072 1611 1622 1479 1365		
1275 1201 1139 1087 1042 1002 968 939 914 892 873 856 841		
828 817 807 799 791 785 780 776 773 771 773 773 773		
3.5000000E+01 2.500174E+02 4.05003481E+05 3.1260008E+04 3.6906678E+04 -2.6114147E+01 4.2421419E+00		
5.8779700E+02 1.4172297E+04 6.8392552E+04 1.4613244E+01 3.5227403E+01 2.5000007E+08		
1.109253E+02 3.3166191E+02 2.1895002E+02 1.9158201E+02 2.190112E+02 2.1895502E+02		
1.7398136E+07 1.2905805E+05 1.02600897E+02 6.175312E+03 5.6927256E+03 5.804465E+01		
3.2201099E+01 "1.06703489E+02 6.175312E+03 5.6927256E+03 5.1000000E+01 2.1080000E+01		
1.4955E-02 2.4888E-03 4.674E-03 8.190E-03 4.171E+06 1.411E+04 5.318E-05 1.419E+03 9.860E-04 4.149E-04 2.234E-02		
6.810E-04 2.969E-07 1.27E+01 5.498E+02 1.505E-03 1.121E+03 1.130E-03 1.080E-03 1.060E-03 1.050E-03 1.040E-03		
5324 5324 6760 6760 6760 6760 6760 6760 6760 6760 6760 6400 6400		
1735 1651 2100 2261 2321 2333 2333 2333 2333 2333 2333 5200 5200		
782 744 737 739 733 733 733 733 733 733 733 4077 4077		
612 601 596 593 591 591 590 589 589 589 589 3181 3181		
560 557 556 555 555 555 554 554 554 554 554 2507 2507		
555 553 552 552 551 551 551 551 551 551 551 2014 2014		
WTLOSSRAT15 1.4796E+00LBS/SECANDTOTALWTLOSSIS 1.1653E+00LBSANDNOSERADIS 3.9515E-02FT		1060
OSTARIS 5.8218E+03BLT/LB		860
6400 6400 6400 6182 4918 3950 3204 2634 2198 1899 1689 1532 1410		
1312 1233 1167 1112 1064 1023 987 956 930 906 886 869 843		
840 828 818 809 801 795 795 786 782 780 780 742 742		
3.6000000E+01 2.7104423E+02 4.9839173E+05 2.50897133E+04 3.1032908E+04 -2.6230124E+01 6.1844773E+00		
6.0004137E+02 1.3801112E+04 8.1666356E+04 1.3054017E+01 2.9191509E+02 2.8949270E+08		
1.1622653E+02 5.008753E+02 3.7060172E+03 3.001607E+03 2.261846E+02 3.7060172E+03		
1.76440033E+07 2.182458E+05 1.127657E+07 2.5535016E+03 1.022140E+01 1.3268859E+01		
3.089705E+01 1.067918E+02 6.3667841E+03 5.8425059E+03 5.1000000E+01 2.3080000E+01		
1.497E-02 1.199E-03 5.14E-03 7.880E-03 4.700E+06 2.073E-03 2.553E-05 1.717E+03 2.428E-03 1.215E-03 2.868E-02		
8.575E-04 3.078E-07 1.184E+01 5.573E+02 1.799E-03 1.374E+04 5.253E-05 1.717E+03 2.428E-03 1.215E-03 2.868E-02		
5568 5568 6760 6760 6760 6760 6760 6760 6760 6760 6760 6400 6400		
1666 2735 3268 3409 3439 3421 3421 3362 3362 3362 3362 5456 5456		
603 780 789 793 793 792 792 789 789 789 789 4358 4358		
618 607 602 600 598 596 596 595 595 595 595 3454 3454		
561 559 557 556 556 555 555 555 555 555 555 2731 2731		
556 554 553 552 552 552 552 552 552 552 552 2178 2178		
WTLOSSRAT15 1.5399E+00LBS/SECANDTOTALWTLOSSIS 3.0206E+00LBSANDNOSERADIS 2.4956E-02FT		1060
OSTARIS 5.822E+03BLT/LB		860
6400 6400 6400 6400 5657 4390 3495 2835 2148 2001 1762 1590 1457		
1351 1266 1196 1138 1088 1044 1007 974 946 922 900 882 866		
852 839 829 819 812 805 800 795 792 780 751 751		
3.7000000E+01 2.8398555E+02 5.1057003E+05 1.9069609E+04 2.5308779E+04 -2.6349855E+01 6.1251836E+00		
6.151454E+02 1.337314E+04 9.432156E+04 3.320664E+01 1.320664E+01 3.2359201E+08		
1.163484E+02 5.3939236E+02 1.5419662E+03 1.1665715E+03 2.3246784E+02 1.5451962E+03		
1.7641169E+07 2.235721HE+05 1.1255206E+07 2.6866667E+03 5.2812833E+00 1.508538E+01		
3.2559215E+01 1.0677391E+02 6.4431403E+03 5.9879891E+05 5.1000000E+01 2.3080000E+01		
1.5111E-02 2.456E+04 5.739E+03 7.620E+03 5.067F+08 2.090E-03 1.332E+04 5.183E-05 2.050E+03		
1.055E-03 3.109E-07 1.135E+01 5.719E+02 2.090E-03 1.332E+04 5.183E-05 2.050E+03		

SPOT	0.	4.048E-03	4.465E-03	4.423E-03	4.270E-03	4.091E-03	3.920E-03	2.274E-03	3.682E-02
	6760	6760	6760	6760	6760	6760	6760	6760	6760
2016	4168	4705	4770	4733	4658	4562	5711	5711	5711
826	859	892	901	901	907	890	4610	4610	4610
625	615	611	609	608	606	605	3692	3692	3692
563	560	559	558	557	557	556	2930	2930	2930
557	555	554	553	553	552	552	2344	2344	2344
							1060	1060	1060
WTLOSSRATE15 1.5041E+00LBS/SECANDTOTALWTLOSS15		4.9283E+00LBSANDNOSERADIS 1.1750E-02FT							
05STAR15 5.1062E+03BTU/LB	6400	6400	6400	6400	5305	3969	3122	2542	2121
1393	1301	1227	1164	1112	1065	1027	993	963	937
864	851	840	830	822	815	809	805	801	799
							760	760	760
3.4000000E+01	2.9676008E+02	5.2234110E-05	1.3227621E+04	1.9739276E+04	-2.6473744E+01	6.0598707E+00			
	6.291260E+02	1.06046158E+01	1.2441058E+01	2.8970519E+02	3.5127562E+08				
1.1647207E+02	5.6103680E+02	1.310477E+05	1.5421329E+05	2.3875120E+02	1.5104770E+04				
1.762240E+07	2.2971740E+05	1.125316E+07	3.256489E+03	5.772799E+01	-1.738941E+1				
1.2529764E+01	-1.0675723E+02	6.3526880E+03	6.1205368E+05	5.1000000E+01	2.3080000E+01				
1.5527E-02	8.0466E-03	7.2251E-03	5.50E+00	5.104E-05	2.423E+03				
1.278E-03	3.317E-07	1.08E+01	5.84E+02	2.416E-03	1.283E+04				
5007	1.926E-03	6.052E-03	6.362E-03	6.189E-03	5.947E-03	5.694E+03			
	6760	6760	6760	6760	6760	6760	6760	6760	6760
2044	5924	6251	6192	6075	5981	5814	5969	5969	5969
861	1018	1078	1086	1081	1070	1056	4653	4653	4653
							1060	1060	1060
565	562	625	623	622	620	619	3915	3915	3915
559	556	561	561	559	558	558	3137	3137	3137
							2509	2509	2509
WTLOSSRATE15 1.7611E+00LBS/SECANDTOTALWTLOSS15		7.0297E+00LBSANDNOSERADIS 2.1767E-03FT							
05STAR15 4.6876E+03BTU/LB	6400	6400	6400	6400	6400	6400	3065	2347	1965
1439	1339	1259	1192	1136	1089	1047	1011	980	953
976	862	651	841	832	825	819	815	808	806
							769	769	769
3.9000000E+01	3.0927702E+02	5.3362208E-05	7.5939767E+03	1.4412572E+04	-2.6602781E+01	5.9381510E+00			
	6.4224437E+02	1.0320972E+04	1.1577005E+05	1.1.021E+01	3.0400057E+02	3.9196982E+08			
1.1661274E+02	5.1241357E+02	1.1241357E+04	3.819364E+05	4.463456E+02	1.121357E+4				
1.7611242E+07	2.3365151E+05	1.1241606E+07	3.709365E+03	4.6635557E+01	-1.9754259E+01				
3.2501501E+01	-1.0674127E+02	5.9964422E+03	6.2634340E+05	5.1000000E+01	2.3080000E+01				
1.525F-02	3.431E-07	1.0627373E-03	7.5631E-03	5.63E+00	5.016E-05	2.829E+03			
5007	4.157E-03	1.025271E+01	5.95E+02	2.771E-03	1.222E+04	8.608E+03	7.139E-03	5.134E-03	8.955E-02
	6760	6760	6760	6760	6760	6760	6760	6760	6760
4242	5785	1725	1642	1473	1344	1287	5085	5085	5085
939	641	642	643	640	637	635	4129	4129	4129
567	564	563	562	561	561	560	3326	3326	3326
560	558	557	556	555	555	555	2659	2659	2659
							1060	1060	1060
WTLOSSRATE15 1.53945E+00LBS/SECANDTOTALWTLOSS15		1.0302E+01LBSANDNOSERADIS 1.4320E-03FT							
05STAR15 4.2251E+03BTU/LB	6400	6400	6400	6400	6400	6400	6400	6400	6400
1587	1409	1302	1225	1163	1112	1069	1031	998	969
888	874	862	852	843	836	829	824	821	818
							VMAS	VMAS	VMAS
TIME	X	Y	VEL	Z	ALT	GAMMA	CO		

	PHI XF LAT	THETA YE LONG	ALPHA Z ^E BETA	BET FO QCIR	PS FN 12	ALPT GFZ IX
4.0000000E+01	3.2142579E+02 6.5550779E+02 1.1671888E+02	5.4434838E+05 1.1675938E+04 5.854095E+02	2.2063965E+03 1.2232342E+05 4.1042428E+05	9.3036353E+03 1.0625397E+01 5.1103690E+07	-2.6738445E+01 3.167333E+02 2.5131792E+02	5.0963068E+00 4.2666005E+08 4.1042128E+02
1.0569E-02 1.00E-04 1.00E-07	1.764169E+07 3.2476108E+02	2.3832279E+05 1.1210598E+07	4.0855423E+03 5.7342915E+03	1.781863E+01 6.3917992E+05	-2.1703E+01 5.000000E+01	-2.1703E+01 2.308000E+01
1.795E-01 3.539E-07 9.658E-06	1.069E-03 1.04E-04 1.03E-02	7.349E-03 6.7349E+06	4.420E-05 3.257E+03	9.589E-03 9.689E-01	9.589E-03 9.689E-01	9.589E-03 1.117E+01
500T 6.317E-03 1.049E-02	1.049E-02 1.049E-02	1.057E-02 1.057E-02	1.017E-02 1.017E-02	9.669E-01 9.669E-01	9.669E-01 9.669E-01	9.669E-01 1.017E+01
6760 6760 6760	6760 6760 6760	6760 6760 6760	6760 6760 6760	6760 6760 6760	6400 6400 6400	6400 6400 6400
6089 6760 6760	6760 6760 6760	6760 6760 6760	6760 6760 6760	6760 6760 6760	6400 6400 6400	6400 6400 6400
1102 2811 2915	2915 2772 2543	2772 2543 2379	2543 2379 2192	2379 2192 5343	5343 5343 5343	5343 5343 5343
652 684 688	684 688 682	688 682 673	682 673 667	673 667 4350	4350 4350 4350	4350 4350 4350
569 567 566	567 566 565	566 565 564	565 564 563	564 563 3571	3571 3571 3571	3571 3571 3571
962 558 558	558 557 557	557 556 556	556 556 556	556 556 2815	2815 2815 2815	2815 2815 2815
1060 1060 1060	1060 1060 1060	1060 1060 1060	1060 1060 1060	1060 1060 1060	1060 1060 1060	1060 1060 1060
WTLOSSRATE1S 1.7126E+00LBS/SEC AND TOTALWTLOSS1S OSTARIS 3.7186E+03HTU/LB			1.2292E+01LBSANDNOSENADIS 8.0814E-03FT			
6400 6400 901	6400 3165 886	6400 1639 874	6400 1449 861	6400 1274 854	6400 1175 846	6400 1059 835
6400 6400 901	6400 3165 886	6400 1639 874	6400 1449 861	6400 1274 854	6400 1175 846	6400 1059 835
5.8635352E+00						
1.0000000E+01	3.331103E+02 6.662230E+02 1.1662229E+02	5.5446108E+05 1.0975483E+04 5.9980328E+02	-2.9036547E+03 5.15240935E+04 5.1427385E+02	4.4612753E+03 5.1628105E+00 2.74261105E+00	-2.6002263E+01 3.162817E+02 2.5760238E+02	5.0555993E+00 5.127385E+02 5.127385E+02
1.764017E+07	2.4276550E+05	1.1220202E+05	1.1220202E+07	4.332234E+03	2.2627824E+01	-2.3666699E+01
3.094E-02 2.791E-04 1.003E-02	6.4345E-03 6.629E+08	5.4491359E+03	6.5129131E+05	5.1000000E+01	5.1000000E+01	2.3080000E+01
500T 9.461E-03 1.0462E+07	9.0254E+00 6.103E+02	1.03E+02 5.533E+03	1.093E+04 6.029E+08	1.0922E+05 3.700E+01	1.206E+02 9.031E-03	1.206E+02
1.223E+02 1.223E+02	1.162E+02 1.162E+02	1.162E+02 1.162E+02	1.134E+02 1.100E+02	1.134E+02 1.100E+02	1.206E+02 9.031E-03	1.206E+02
6760 6760 6760	6760 6760 6760	6760 6760 6760	6760 6760 6760	6760 6760 6760	6400 6400 6400	6400 6400 6400
1791 4230 4232	4230 3996 3996	3996 3688 3688	3688 3415 3415	3415 3241 3241	3241 3060 3060	3060 2878 2878
670 773 779	773 779 776	776 747 747	747 720 720	720 4925 4925	4925 4743 4743	4743 4561 4561
572 572 561	572 571 569	571 569 568	569 567 567	568 567 567	567 5491 5491	5491 5209 5209
564 562 561	562 561 560	560 559 558	558 556 556	556 556 556	556 5378 5378	5378 5196 5196
1060 1060 1060	1060 1060 1060	1060 1060 1060	1060 1060 1060	1060 1060 1060	1060 1060 1060	1060 1060 1060
WTLOSSRATE1S 1.0071E+00LBS/SEC AND TOTALWTLOSS1S OSTARIS 3.2003E+03HTU/LB			1.3827E+01LBSANDNOSENADIS 1.33385E-02FT			
6400 6400 916	6400 3874 900	6400 3866 886	6400 875 875	6400 865 857	6400 845 837	6400 825 819
6400 6400 916	6400 3874 900	6400 3866 886	6400 875 857	6400 845 837	6400 825 819	6400 805 797
5.0123682E+00						
4.1940000E+01	3.4401700E+02 6.803337E+02 1.1703284E+02	5.6373240E+05 1.0246162E+04 6.0593998E+02	-1.6180181E+03 1.2460186E+05 0.0893496E+05	-3.6537869E+00 4.475131E+02 4.431693E+02	-2.7032821E+01 4.475131E+02 4.431693E+02	4.6840057E+00 4.6840057E+00 4.6840057E+00
1.0624770E+07	2.682006E+05	1.0669863E+02	1.121055E+07 5.1851546E+03	4.502548E+03 6.6740303E+05	2.6821338E+01 5.1000000E+01	2.6821338E+01 2.3080000E+01
1.07A1E-03 3.737E+07 8.301E+00 6.157E+02 3.920E+03	1.0205E+04 6.992E+05	1.0205E+04 6.992E+05	1.0205E+04 6.992E+05	1.0205E+04 6.992E+05	1.149E+02 1.149E+02	1.149E+02 1.149E+02
500T 1.07A1E-02 1.106E+02	1.133E+02 1.2A3E+02	1.227E+02 1.2A3E+02	1.227E+02 1.187E+02	1.227E+02 1.187E+02	1.149E+02 1.149E+02	1.149E+02 1.149E+02
6750 6760 6760	6760 6760 6760	6760 6760 6760	6760 6760 6760	6760 6760 6760	6400 6400 6400	6400 6400 6400
6760 6760 6760	6760 6760 6760	6760 6760 6760	6760 6760 6760	6760 6760 6760	6246 6246 6246	6246 6246 6246
2967 9484 5460	5460 5146 4777	4777 4519 4259	4519 4259 5501	4519 4259 5501	4259 4259 5501	4259 4259 5501

716	929	931	901	865	840	816	4631
576	563	582	580	578	576	575	3614
566	565	564	563	562	561	561	3041
							1060
WLOSSRATES R.1076E-01LBS/SEC AND TOTALLOSSIS							860
051ARIS 3.2275E-03HTU/LB							7.463AE-03FT
6400	6400	6400	6400	6400	6400	6400	6400
6400	6400	6400	4220	2481	1739	1436	1268
919	919	902	889	878	869	861	856
							851
							848
							807

REFERENCES

1. Six-Degree-of-Freedom Flight-Path Study Generalized Computer Program, FDL-TDR-64-1, Part I, Vol 1, and Part II, Vol I, AF Flight Dynamics Laboratory, October 1963.
2. Dayton, Allen D., Spinning Unguided Rocket Trajectory Digital Computer Program (SPURT), SWC-TDR-63-11, AF Special Weapons Center, February 1963.
3. Krause, H. G. L., Kubler, M. E., Koelle, H. H., Kaeppeler, H. J., The Free Flight Trajectory of Rockets, with Consideration of the Variation of Gravity with Altitude, the Curvature of the Surface of the Earth and the Influences of the Rotation of the Earth and Air Drag, ASTIA doc. AD-86547, Stuttgart, February 1963.
4. Walter, Everett L., Six Variable Ballistic Model for a Rocket, MM445, White Sands Missile Range, New Mexico, June 1962.
5. Lynch, U. H., Six-Degree of Freedom Program, AFWL-TR-66-155, AF Weapons Laboratory, 1966.
6. Hill, Morrissette, A Six-Degree-of-Freedom Reentry Trajectory Program for Ballistic and Lifting Vehicles, RAD-TM-62-7D, AVCO Corp, September 1963.
7. Moulds, W. J., Young, J. D., Capt, USAF, Aerodynamic Heating and Ablation Computer Program (HEATAB), AFWL-TR-66-105, AF Weapons Laboratory, October 1966.
8. Makerson, Baker, Westrom, "Analysis and Standardization of Astrodynamics Constants," Journal of Astronautical Sciences, Vol III, No. 1, Spring 1961.
9. Baker, R. M. L., Makerson, M. W., An Introduction to Astrodynamics, Academic Press, 1963.
10. Herrick, S., Baker, R. M. L., Hilton, "Gravitational and Related Constants for Accurate Space Navigation," UCLA Astronomical Papers, Vol I, No. 24, 1957.
11. Berman, Arthur I., The Physical Principles of Astronautics, John Wiley & Sons, 1961.
12. Herrick, S., Astrodynamics, D. Van Nostrand Co, Inc, 1961.
13. Thomson, William T., Introduction to Space Dynamics, John Wiley & Sons, 1961.
14. Hildebrand, F. B., Introduction to Numerical Analysis, McGraw-Hill Book Co, Inc, p. 237, 1956.
15. Kaye, J., "Survey of Friction Coefficients, Recovery Factors, and Heat Transfer Coefficients for Supersonic Flow," Journal of Aeronautical Sciences, Vol 21, No. 2, pp. 117-129, 1954.
16. Kreith, Frank, Principles of Heat Transfer, International Book Co, 1953.

REFERENCES (cont'd)

17. Rubesin, M. W., Johnson, H. A., Transcript ASME, 71:383, 1949.
18. Kays, W. M., Convective Heat and Mass Transfer, McGraw-Hill Book Co, Inc, 1966.
19. Eckert, E. R. G., Drake, R. M., Jr., Heat and Mass Transfer, McGraw-Hill Book Co, Inc, 1959.
20. Scavia, S. M., A Study of Hypersonic Ablation, GE R59SD438, General Electric MSV Dept, 1959.
21. Analytical Comparison of Ablative Nozzle Materials, NASA CR-54257, July 1965.
22. Lees, L., "Laminar Heat Transfer over Blunt-Nosed Bodies at Hypersonic Speed," Jet Propulsion, Vol 26, pp. 259-264, 1956.
23. Schlichting, H., Boundary Layer Theory, McGraw-Hill Book Co, Inc, 1960.
24. Hecht, A., Clarification of Transition Criteria, GE RSD, PIR-HTT-8151-202, General Electric MSV Dept, 1963.
25. Kopal, Z., Tables of Supersonic Flow around Cones, MIT Center of Analysis, TR No. 1, 1947.
26. Young, J. D., Capt, USAF, Aungier, R. H., Lt, USAF, Private Communication, March 1968.
27. Cox, R. N., Crabtree, L. F., Elements of Hypersonic Aerodynamics, Academic Press, 1965.
28. Mangler, W., Compressible Boundary Layers on Bodies of Revolution, ATI No. 28063, MAP-VG 83-4, June 1946.
29. Eckert, E., "Engineering Relations for Heat Transfer and Friction in High Velocity Laminar and Turbulent Flow over Surfaces with Constant Pressure and Temperature," ASME Paper No. 55-A-31.
30. Schmidt, J. F., Laminar Skin-Friction and Heat-Transfer Parameters for a Flat Plate at Hypersonic Speeds in Terms of Free-Stream Flow Properties, NASA TN D-8, 1959.
31. Bertram, M. H., Correlation Graphs for Supersonic Flow around Right Circular Cones at Zero Yaw in Air as a Perfect Gas, NASA TN D-2339.
32. Equations, Tables and Charts for Compressible Flow, by the Ames Research Staff, NASA R113^c, 1953.
33. Hoerner, S. F., Fluid-Dynamic Drag, published by author, 1958.
34. Hoak, D. E., Ellison, D. E., USAF Stability and Control Datcom, AF Flight Dynamics Laboratory, November 1965.

REFERENCES (cont'd)

35. Gray, D. J.. Drag and Stability Derivatives of Missile Components According to the Modified Newtonian Theory, AEDC TN-60-61, Arnold Engineering Development Center, November 1960.
36. Aungier, R. H., Lt, USAF, Private Communication, March 1968.

DISTRIBUTION

No. cys

MAJOR AIR COMMANDS

1 AUL (SE)-67-464, Maxwell AFB, Ala 36112
2 SAAMA (SANEAD, Lt John Taylor), Kelly AFB, Tex 78241

AFSC ORGANIZATIONS

1 AFSC STLO (SCTL-17, Capt DeLoache), Naval Ms1 Test Cen, Point Mugu, Calif 93041
1 OAR, Holloman AFB, NM 88330
1 (RRRD)
2 (MDST)
1 (MDRCV, Mr. Martin Menk)

KIRTLAND AFB ORGANIZATIONS

AFSWC, Kirtland AFB, NM 87117
1 (SWEH)
2 (SWT)
AFWL, Kirtland AFB, NM 87117
12 (WLIL)
60 (WLDE)
1 (WLRP, Capt James Suttle)

ARMY ACTIVITIES

2 USA Mob Equip Rsch & Dev Cen (Tech Doc Cen), Ft Belvoir, Va 20260

NAVY ACTIVITIES

1 Comdr, NWC (Code 753), China Lake, Calif 93557
Comdr, NOL, White Oak, Silver Spring, Md 20910
1 (Code 730)
3 (Mr. John L. Lankford, Act Chief, Ms1 Dyn Div)

OTHER DOD ACTIVITIES

1 Comdr, Fld Comd, DASA (FCAG3), Sandia Base, NM 87115
20 DDC (TCA), Cameron Sta, Alexandria, Va 22314

AEC ACTIVITIES

Sandia Corp, Box 5800, Sandia Base, NM 87115
1 (Info Dist Div)
1 (Mr. B. E. Bader, Org 1541-2)

OTHER

3 NASA-LRC (Mr. Robert Wright), Mail Stop 214A, Langley Sta, Hampton, Va 23365

DISTRIBUTION (cont'd)

No. cys

1 Aerospace Corp, San Bernardino Opns (A. M. Naqvi), P. O. Box 1308, San Bernardino, Calif 92402

2 Dikewood Corp (Mr. Ed Brannon), 1009 Bradbury Dr SE, Albuquerque, NM 87106

2 Univ New Mexico (Dr. R. C. Dove), Dept Mech Eng, Albuquerque, NM 87103

2 New Mexico State Univ (Dr. C. Q. Ford), Dept Mech Eng, University Park, NM 88001

1 FMC Corp (Mr. D. G. DiCanio), Def Tech Lab, 333 Brokaw Rd, Box 520, Santa Clara, Calif 95052

1 Martin Marietta Corp, Denver Div (Mr. D. A. Schmitt), Mail No. 0409, Denver, Colo 80201

1 NASA, Manned Spacecraft Cen (Mr. D. M. Curry, ES54), Houston, Tex 77058

1 Lovelace Foundation, Biological Instrumentation (Mr. R. Rietz), 5200 Gibson Blvd SE, Albuquerque, NM 87108

1 Emerson Elec Co (Mr. R. Feldman), 8100 Florissant Ave, St Louis, Mo 63136

1 Def Rsch Corp (Mr. R. Boxer), 6300 Hollister Ave, P. O. Box 3587, Santa Barbara, Calif 92105

1 Opns Rsch Inc (Mr. E. Wendorf), 225 Santa Monica Blvd, Santa Monica, Calif 90401

1 Minneapolis-Honeywell (Mr. G. Jacobs), Minneapolis, Minn 55440

1 Westinghouse Corp, Astro-Nuc Lab (Dr. Paul Dixon), P. O. Box 10864, Pittsburgh, Pa 15236

1 Official Record Copy (W. J. Moulds, WLDE)

This page intentionally left blank.

UNCLASSIFIED

Security Classification

DOCUMENT CONTROL DATA - R & D

(Security classification of title, body of abstract and indexing annotation must be entered when the overall report is classified)

1. ORIGINATING ACTIVITY (Corporate author) Air Force Weapons Laboratory (WLDE) Kirtland Air Force Base, New Mexico 87117		2a. REPORT SECURITY CLASSIFICATION UNCLASSIFIED
		2b. GROUP
3. REPORT TITLE AN INTEGRATED SIX-DEGREE-OF-FREEDOM TRAJECTORY AND AERODYNAMIC HEATING AND ABLATION COMPUTER PROGRAM (STRAB-6)		
4. DESCRIPTIVE NOTES (Type of report and inclusive dates) July 1966-November 1967		
5. AUTHOR(S) (First name, middle initial, last name) W. J. Moulds		
6. REPORT DATE August 1968		7a. TOTAL NO. OF PAGES 162
7b. NO. OF REFS 36		
8. CONTRACT OR GRANT NO.		9a. ORIGINATOR'S REPORT NUMBER(S) AFWL-TR-68-61
b. PROJECT NO. 5791		9b. OTHER REPORT NO(S) (Any other numbers that may be assigned this report)
c. Task No. 579122		
d.		
10. DISTRIBUTION STATEMENT This document is subject to special export controls and each transmittal to foreign governments or foreign nationals may be made only with prior approval of AFWL (WLDE), Kirtland AFB, NM, 87117. Distribution is limited because of the technology discussed in the report.		
11. SUPPLEMENTARY NOTES		12. SPONSORING MILITARY ACTIVITY AFWL (WLDE) Kirtland AFB, NM 87117
13. ABSTRACT (Distribution Limitation Statement No. 2) An integrated computer program (STRAB-6) for the complete analysis of a blunt, conical reentry vehicle as to its trajectory and aerothermal environment upon atmospheric reentry is presented. The trajectory portion of the program calculates the vehicle motions in six-degrees-of-freedom, while the thermal portion calculates the aerodynamic heating and ablation of the vehicle. The earth model is an oblate, rotating spheroid whose parameters and gravitational potential are described herein. The equations of motion, the method of integration, thermal model and input forms for the program are discussed. The thermal model examined in this report assumes thick skin solution where the skin is of any composite structure made of discrete layers of material whose properties may vary from layer to layer. Also, the heatshield is comprised of one, two, or more different ablative materials. STRAB-6 computes nose-blunting and includes this effect in the aerodynamics. STRAB-6 is written in FORTRAN IV for the CDC 6600 computer.		

UNCLASSIFIED
Security Classification

14 KEY WORDS	LINK A		LINK B		LINK C	
	ROLE	WT	ROLE	WT	ROLE	WT
Six-degrees of freedom Equations of motion Euler angles Moment of momentum Runge-Kutta Aerodynamic heating Ablation Heat transfer Boundary layer Hypersonic Reentry vehicles						